ADDIS ABEBA UNIVERSITY

SCHOOL OF GRADUATE STUDIES

SCHOOL OF EARTH SCIENCES

GEOLOGICAL AND GEOCHEMICAL STUDIES OF FLOOD BASALTS (AIBA AND ASHENGE BASALTS) IN MAYCHEW AREA, TIGRAY, NORTHERN ETHIOPIA: IMPLICATION FOR THEIR PETROGENESIS.

BY

HAYELOM MENGESHA ARBESIE

ADVISOR: PROFESSOR DEREJE AYALEW

THESIS WORK IS SUBMITTED TO SCHOOL OF GRADUATE STUDIES ADDIS ABABA UNIVERSITY, SCHOOL OF EARTH SCIENCE FOR THE PARTIAL FULFILLMENTOF DEGREE OF MASTERS OF SCIENCES IN GEOLOGICAL SCIENCES (GEOCHEMISTRY).

27th June, 2018

ADDIS ABABA, ETHIOPIA

ADDIS ABEBA UNIVERSITY
SCHOOL OF GRADUATE STUDIES
SCHOOL OF EARTH SCIENCES

GEOLOGICAL AND GEOCHEMICAL STUDIES OF FLOOD BASALTS (AIBA AND ASHENGE BASALTS) IN MAYCHEW AREA, TIGRAY, NORTHERN ETHIOPIA: IMPLICATION FOR THEIR PETROGENESIS.

BY

HAYELOM MENGESHA ARBESIE

ADVISOR: PROFESSOR DEREJE AYALEW

THESIS WORK IS SUBMITTED TO SCHOOL OF GRADUATE STUDIES ADDIS ABABA UNIVERSITY, SCHOOL OF EARTH SCIENCE FOR THE PARTIAL FULFILLMENTOF DEGREE OF MASTERS OF SCIENCES IN GEOLOGICAL SCIENCES (GEOCHEMISTRY).

27th June, 2018

ADDIS ABABA, ETHIOPIA

ADDIS ABEBA UNIVERSITY
SCHOOL OF GRADUATE STUDIES
SCHOOL OF EARTH SCIENCES

GEOLOGICAL AND GEOCHEMICAL STUDIES OF FLOOD BASALTS (AIBA AND ASHENGE BASALTS) IN MAYCHEW AREA, TIGRAY, NORTHERN ETHIOPIA: IMPLICATION FOR THEIR PETROGENESIS.

BY

HAYELOM MENGESHA ARBESIE

Approved by Examining Committee

Dr. Balemwal Atnafu _____	____/___/____	
Chairman School of Earth Science	Signature	Date
Professor Dereje Ayalew _____	___/____/____	
Advisor	Signature	Date
_____	_____	___/____/__
Examiner	Signature	Date
_____	_____	___/___/___
Examiner	Signature	Date

27th June, 2018

ADDIS ABABA, ETHIOPIA

Declaration of Originality

I hereby declare that the thesis entitled "Geological and Geochemical studies of flood basalts (Ashenge and Aiba basalts) in Maychew area, Tigray, northern Ethiopia: Implication for their petrogenesis**"** is my original work prepared for the partial fulfillment of the Degree of Master of Science in Geochemistry, School of Earth Sciences, Addis Ababa University during the year of 2017/2018 under the supervision of Professor Dereje Ayalew. I further declare that this work is not presented and published anywhere else, and all the used sources are well referenced and acknowledged.

	Signature	**Date**
Hayelom Mengesha Arbesie	_____	_____

I hereby declare this is his original work as part of his Master of Science in Geological Sciences (Geochemistry).

	Signature	**Date**
Professor Dereje Ayalew	_____	_____

Abstract

The study area, Maychew, is located in the northern eastern corner of the northwestern Ethiopian plateau. Petrological, petrographic, and geochemical (trace and major elements) data are presented and integrated for Maychew flood basalts to characterize the geochemistry and constrain petrogenetic processes involved in the evolution of these flood basalts. According to these data two types of basaltic groups have been identified; tilted basaltic units (Ashenge basalts) and horizontal to sub horizontal basaltic units (Aiba basalts).The studied samples have low Mg numbers (Mg#:37.99-58.92, excluding sample T2S8 and T4O18) and low compatible element contents such as Ni and Cr suggesting that these lavas have undergone fractionation en route to the surface. Moreover Ce/Pb, La/Nb, and La/Ta ratios, which are sensitive to crustal contamination, of the studied samples indicates that crustal contamination is more pronounced on samples of Aiba basalt than Ashenge basalts. Further, the investigated samples from study area exhibit trace element ratios such as Zr/Nb (3.77-10.88), Ba/La (5.75-13.55), La/Nb (0.76-1.89) and Ba/Nb (4.65-18.07), which overlap substantially the field of OIB. This suggests that these lavas are derived from mantle sources that are similar to OIB-type sources or contain high proportion of OIB-type sources at least on the basis of trace element ratios. Moreover, a plot of two highly incompatible trace elements, thought to be insensitive to fractional crystallization and partial melting, indicates that both of the basaltic groups were originated from a common mantle source. However, the observed distinct trends of these basaltic groups on such plots, and on some major and trace element variation diagrams could be related to variation in degree of crustal contamination and/ or fractional crystallization, rather than source heterogeneity. Hence, the two basaltic groups are originated from a common OIB like mantle source following different paths of petrogenetic processes; crustal contamination and/or fractional crystallization.

Key words: Ethiopian plateau, fractional crystallization, crustal contamination, mantle source, petrogenetic processes, OIB

Acknowledgment

Adigrat University is acknowledged for providing me the opportunity to start my postgraduate program in Addis Ababa University. I am also thankful to Addis Ababa University, School of Earth Science for its complete support from the beginning to the end of this research work.

My deepest gratitude goes to my advisor Professor Dereje Ayalew for his follow up, invaluable advices, constructive comment and suggestion, encouragement, discussion and limitless support at various times throughout the entire thesis. Further, I would like to thank him for his support in suggesting and providing valuable reference materials, and his friendly approach throughout my research work.

My gratitude also goes to my friends and colleagues like Mr. Abay Sharew, Mr.Hagos Hiluf, Mr. Misgan Molla, Mr. Samuel Getachew, Mr.Yemane Kelemework and Mr.Belete Baychekin for their technical and material support during this work.

The contribution from my family is greatly acknowledged especially my father Mengesha Arbesie for his moral support and friendly approach.

Last but not least, the community of Maychew town and its surrounding are greatly acknowledged for their kind and memorable help during the field work.

Table of Contents

List of Figures

List of Tables

List of Acronyms

- Ab	Albite
- An	Anorthite
- ALS	Australian Laboratory Science
- Ap	Apatite
- a.s.l	above mean sea level
- CFB	Continental flood basalt
- CFV	Continental flood volcanism
-CIPW	Cross, Iddings, Pirrson and Washington
- Cpx	Clinopyroxene
- DEM	Digital elevation model
- Di	Diopside
-EARS	East African Rift System
- Fig.	Figure
- GCD Kit tool	Geochemical data kit tool
- GPS	Global Positioning System
-HFSE	High field strength elements
-Hm	Hematite
-HREEs	Heavy rare earth elements
-HT1	High-Ti1
-HT2	High-Ti2
-Hy	Hypersthene
ICP-AES	Inductively Coupled Plasma Atomic Emission Spectrometry
ICP-MS	Inductively Coupled Plasma Mass spectrometry 81
-Inddin	Iddingsite
-Il	Ilmenite
-LILEs	Large Ion lithophile elements
-LOI	Loss on Ignition
-LREE	Light rare earth elements
-LT	Low-Ti

-MER	Main Ethiopian rift
-MORB	Mid-oceanic ridge basalt
-OIB	Oceanic island basalt
-Ol	Olivine
-Opa	Opaque
-Opx	Orthopyroxene
-Or	Orthoclase
-Plag	Plagioclase
-PPL	Plane Polarized Light
- ppm	parts per million
-Pxn	Pyroxene
-Q	Quartz
-REE	Rare Earth Element
-TAS	Total alkali silica
-Tn	Titanite
-UTM	Universal Transvers Mercator
-Vol.%	Volumetric percentage
-WEP	Western Ethiopian plateau
- XPL	Cross polarized light

CHAPTER ONE

INTRODUCTION

1.1.Background

The research project is conducted at Maychew area, which is located in the northern eastern corner of the northwestern Ethiopian plateau, with the aim of understanding the petrogenetic evolution of Aiba and Ashenge flood basalts from their geological and geochemical (major and trace element) characteristics. Further, in this study, detailed stratigraphic section and geological map will also be constructed.

Ethiopian flood basalt province, with a total area of as presently 600,000 km^2, and not less than 750,000 km^2before erosion (Mohr and Zanettin, 1988, Mohr,1983),embraces the Afar triple-rift junction, where the African Rift System meets the Red Sea and Gulf of Aden sea-floor spreading zones (Pik et al., 1998; Corti, 2009; Dereje Ayalew and Gezahegne Yirgu, 2003). Further, at present the Ethiopian flood volcanism have a total volume of about ~350000 km^3 (Mohr, 1983).The flood volcanism is predominantly composed of basaltic lavas together with rhyolitic ignimbrites and pyroclastic-fall deposits, and less common basaltic pyroclastic rocks and rhyolitic lavas (Dereje Ayalew et al., 2002; Kieffer et al., 2004; Ukstins et al., 2002;Natali et al.,2011,2013).The main part of the province crops out in Ethiopia, whereas the rest is located on the eastern side of the Red Sea, in Yemen (Pik et al., 1998).Compilations of 40Ar/39Ar data show that flood basalts and associated rhyolites were erupted across about 1000 km diameter region between 31 and 29 Ma (Dereje Ayalew et al. 2002; Dereje Ayalew & Gezahegne Yirgu, 2003; Baker et al., 1996; Coulié et al., 2003; Hofmann et al., 1997; Rochette et al., 1998; Ukstins et al., 2002), roughly coeval with the initiation of NE-directed extension in the southern Red Sea (Wolfenden et al., 2005) and the Gulf of Aden (Watchorn et al.,1998, as cited in Dereje Ayalew et al., 2006). Furthermore, most studies attribute Ethiopia-Yemen flood basalt activity to impact of the Afar plume head beneath the Ethiopian plateau (Baker et al., 1996; Pik et al., 1999; Kieffer et al., 2004; Dereje Ayalew et al., 2002; Beccaluva et al., 2009).

In northern Ethiopia, the Oligocene pre-rift flood basalts are believed to contain melts formed within an upwelling mantle plume and, in some cases, also from the overlying continental crust (Pik et al., 1998, 1999; Kieffer et al., 2004). Based on trace element and Ti concentrations the north-western Ethiopian flood basalts have been classified into three

distinct geochemical groups (Pik et al., 1998, 1999): low-Ti basalts (LT), high-Ti1 (HT1) basalts and high-Ti2 (HT2) basalts (Fig.2.2).

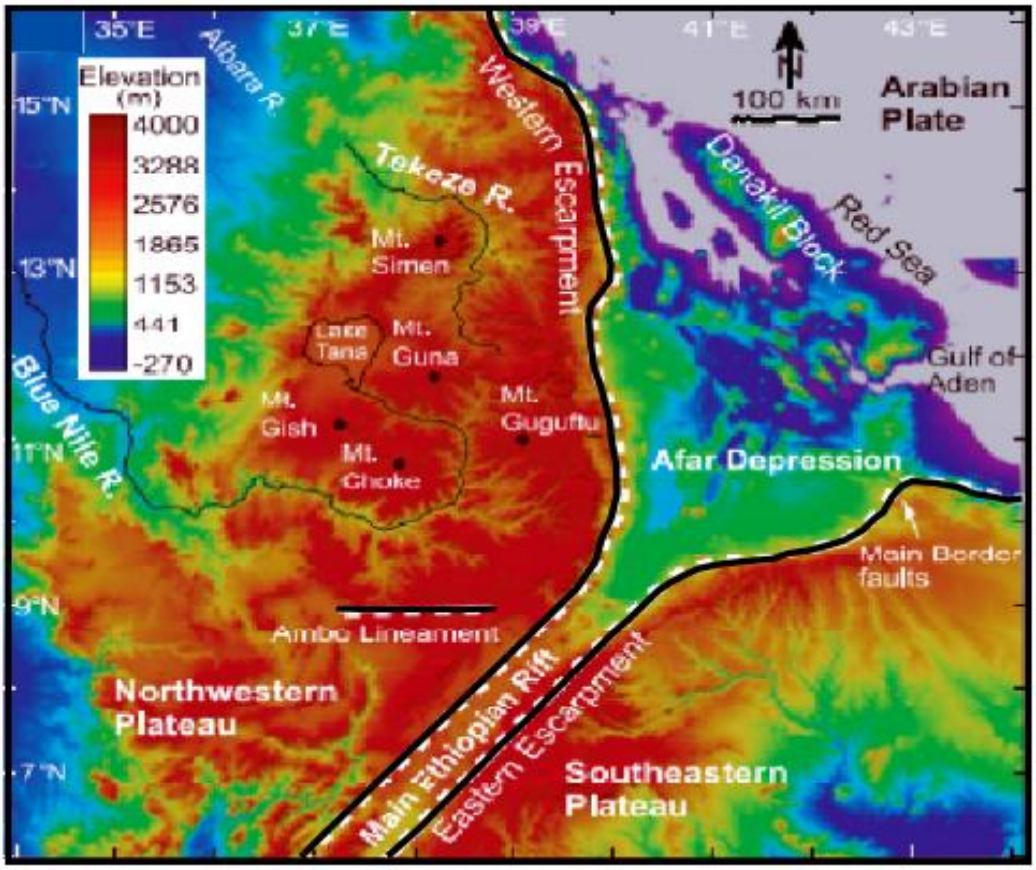

Fig.1.1: Digital elevation model map of the Ethiopian plateau (after Gani et al., 2007). Note the distribution of the flood basalt volcanics along with their bounding Eastern and western escarpment.

1.2.General description of the study area

1.2.1. Location

The study area is located about 660 km north of Addis Ababa in the northern part of the country within Southern Tigray Zone of the Tigray Regional State. Geographically it is bounded between the UTM coordinates of 0555000-0563000E and 1411000-1418000N (Fig.1.2). The area coverage of the study area is about 56 Km^2 with an average elevation of approximately2400m a.s.l.

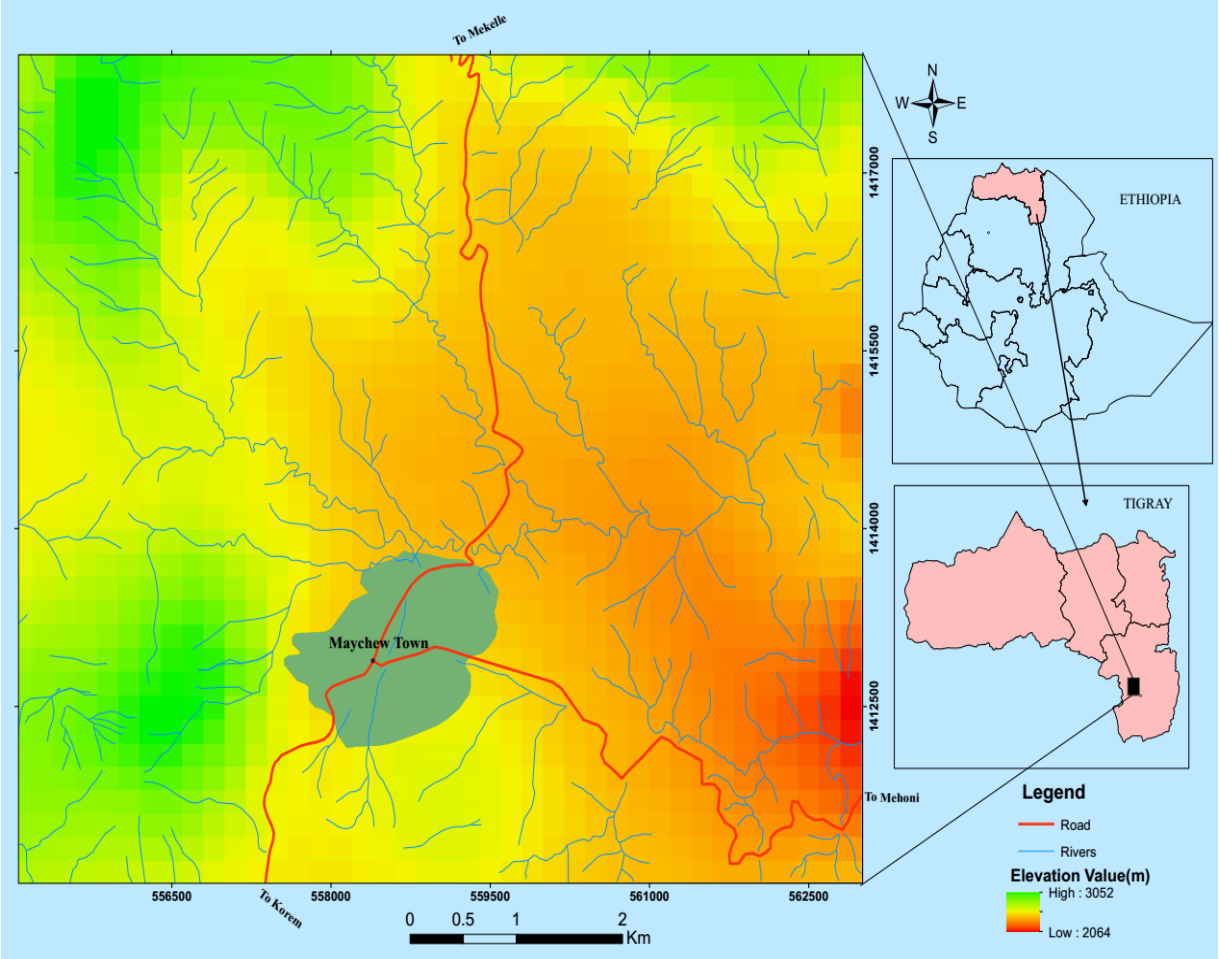

Fig.1.2: Location and Digital Elevation Model (DEM) map of the study area.

1.2.2. Accessibility

The study area is accessed by asphalt road which is running from Addis Ababa through Alamata, Maychew to Mekelle, and there is also a gravel road which runs from Maychew to Mehoni. However, the major part of the study area, for the field work, is accessed by local footpaths that connect the surrounding villages to the Maychew town.

1.2.3. Drainage pattern

The study area is dominantly characterized by dendritic type of drainage pattern (Fig.1.2). Most of the streams such as Tekelehaymanot, Chelekleka, and Katin rivers are located in the western and northwestern part of the study area and flows towards Mehoni marginal graben, which is located on the eastern side of Maychew town. Further, in these parts of the study area (western and northwestern) the streams are densely distributed than the rest of the study area.

1.2.4. Physiography

The study area is characterized by different topographic features such as ridges, hills and flat terrains.The northeastern, northwestern and western parts of the study area are mainly characterized by their ridge and hill forming topographic features whereas the central (including Maychew town) and eastern parts of the study area have relatively flat topographic features. The study area has maximum and minimum elevation of about 3100m and 1950m a.s.l. respectively.

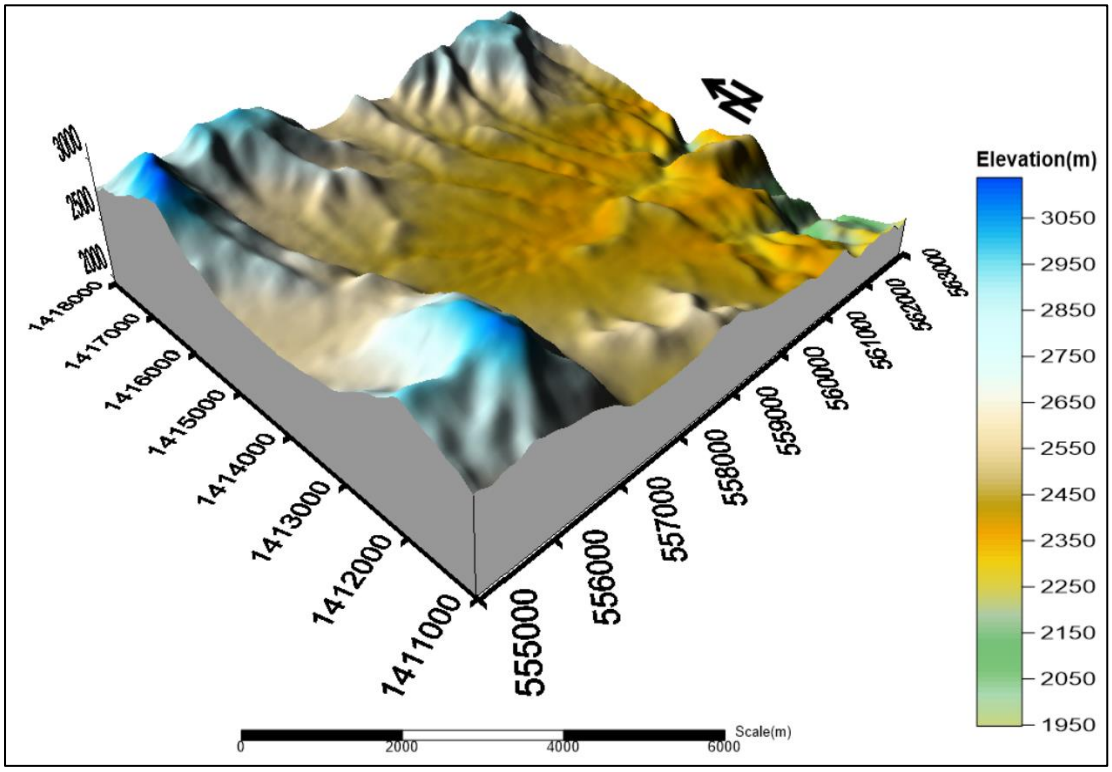

Fig.1.3: Physiographic map of the study area.

1.2.5. Climatic condition

According to Ethiopia's agro-ecological setting, Maychew and its surrounding environments are classified under the Weinadega (semi-temperate zone).Further, according to Molla Mekonnen (2016), based on climatic data of 1994 – 2015, the monthly precipitation distribution in Maychew is not uniform throughout the year; however, rainy periods frequently occur in both summer and winter, comparatively with no dry periods throughout the year, the rainfall being heavy in the summer months. The average annual temperature and rainfall of the study area is 16.2^0C and 753 mm respectively (http://en.climate-org/region/1505/?page=2).

1.2.6. Vegetation

The study area is generally characterized by variety of densely distributed vegetation coverage. The vegetation on the north, south eastern and north western parts of the study area are relatively denser than the other parts (central and eastern). The vegetation types found in the study area are mainly Eucalyptus, shrubs, and cactus bushes.

1.3.Statement of the Problem

Most studies on Ethiopian plateau magmatism have been carried out at a regional scale (Pik et al., 1999, 1998; Kieffer et al., 2004; Seife Michael Berhe et al., 1987; Dereje Ayalew et al., 2002, 2006; Dereje Ayalew and Gezahegne Yirgu, 2003; Mohr, 1983; Hoffman et al., 1997; Natali et al., 2011). Although the northwestern plateau compared to the other parts of the Ethiopian plateau is well studied (Pik et al., 1998, 1999; Kieffer et al., 2004; Beccaluva et al., 2009; Natali et al., 2011, 2013), detailed investigations and geological map on single sections of the plateau are scarce. Thus, the present study will produce a detailed investigation (geological and geochemical investigations), geological map (at a scale of 1:25,000) and stratigraphic section of the study area, Maychew, as part of single section of the northwestern plateau. Moreover, there is a clear tectonic difference between the two formations (Aiba and Ashenge formations); Ashenge is tilted whereas Aiba is horizontal to sub horizontal and thus this research work will check weather this tectonic difference is manifested in their geology and/or geochemistry or not.

1.4.Objectives

1.4.1. General Objectives

The main objective of this study is to understand the geological, petrographic and geochemical characteristics of Aiba and Ashenge flood basalts and thus to determine their petrogenetic evolution.

1.4.2. Specific Objectives

The specific objectives of this research work are as follow:

- ✓ To produce detailed geological map of study area at the scale of 1:25,000.
- ✓ To construct detailed stratigraphic section of the study area.
- ✓ To characterize the petrography of the two formations.
- ✓ To compare the two formations in terms of their geology and geochemistry.

- ✓ To understand the petrogenetic relationship between Ashenge and Aiba basalts.
- ✓ To understand the elemental composition of the rocks with the aim of determining the source and genesis of the magma.

1.5. Basic Research questions

The basic research questions are as follows:

- What is the petrogenetic evolution of Ashenge and Aiba flood basalts?
- What is the Geochemical and/or Geological difference and relationship between Aiba and Ashenge basalts?
- What is the source and genesis of the magma responsible for these flood basalts?

1.6. Methodology and Approaches

In order to achieve the stated general and specific objectives of this research, the following methods and/or approaches have been followed.

1.6.1. Pre- field work

Before the actual start of the field work several activities were done. The activities that were carried out before the field work includes revision and collection of previous case studies, technical journals, extracting of relevant information from aerial photograph and satellite image, reviewing and compiling of literatures (published and unpublished reports) related to the study area. Further, available information's like temperature, rain fall data, vegetation coverage, accessibility of the area, topographic and lithological set up of the study area were collected from topographic map, Google Earth, Aerial photo and from other different existing data. In addition to this, before the actual field work, the study area has been delineated using Arc GIS software (10.2) from topographic map of Maychew sheet (Sheet 1239 B1; Scale 1:50,000).

1.6.2. Fieldwork

The main activities conducted during the field work,which was held on from September 13/2017 to September 29/2017 for a total of 16 days, were tracing of traverse lines , measuring and recording of orientation of geological structures, taking of representative and fresh rock samples for further laboratory analysis (petrographic and geochemical analysis),and detailed descriptions of the rock exposures. Furthermore, during the field work

detailed lithological unit logging for each traverse was carried out. Additionally, transformation of several geological information's such as lithological descriptions, lithological contacts, GPS reading and the geological structures to a geological map with scale of 1:25,000 have been carried out.

1.6.3. Post field

1.6.3.1.Petrographic analysis

After the successful completion of the field work, a total of 16 samples which are believed to be the representative of their respective encountered lithological units were selected for thin-section analysis, and their thin-section preparation were conducted in the Ethiopian Geological survey. Moreover, the thin section samples have been examined under Leica petrographic microscope in the laboratory of Addis Ababa University (School of Earth Science) to determine the modal proportion and textural relationship of the selected representative rock samples.

1.6.3.2. Geo-chemical analysis

After the field work, in addition to petrographic analysis, geochemical analysis (trace and major elements) of representative rock samples have been carried out. The sample preparation for geochemical analysis is done under ALS-Addis Ababa, Ethiopia. During sample preparation several activities have been conducted including removal of the weathered part, breaking of the sample into desirable sizes, crushing of the broken sample, milling of the sample down to micron size particles, and in general the samples were cut carefully to avoid all obvious signs of alteration. Finally, based on their degree of alteration and lithological variation, 12 of the least altered representative samples were sent to the Australian Laboratory Science (ALS) to determine the concentration of major and trace elements. Major elements (including loss on ignition) were analyzed by multi element Inductively Coupled Plasma06 (ME- ICP06) ,whereas trace elements were analyzed by Multi Element Mass Sepectrometry81 (ME-MS81).

1.6.3.3. Structural data analysis

All the structural data that have been measured and recorded for different structural elements such as joints, faults and dikes, and the inclined lava flow layers were plotted and analyzed using a GeoRose software with the aim of determining the overall orientation of these structural elements.

1.7.Significance of the Research

The detailed petrological and geochemical investigations of Maychew flood basalts will provide a scientific basis for understanding the tectonic and petrogenetic evolution of the area. In addition, the results and the findings of this research work will provide detailed information of these flood basalts such as their petrological, geochemical, and petrogenetic relationships. Further, the detailed geological map (1:25,000) and stratigraphic section of study area will serve as a basic source of data for understanding the geological history (tectonic and petrogenetic evolution) of the study area, even for the northwestern plateau.

1.8. Review of Previous works

Since the work of Blanford (1869,1870), who have classified the Ethiopia plateau into lower tilted Ashenge group and upper horizontal Meqdela group, several regional studies were carried out on northwestern Ethiopian plateau which includes the current study area, Maychew. According to Beccaluva et al.(2009)northern Ethiopian continental flood basalts(CFBs),which includes the current study area, preserve a record of magmas generated from the center to the flanks of a plume head, currently corresponding to the 'Afar hotspot'. Further, the Oligocene pre-rift flood basalts in northern Ethiopia are believed to contain melts formed within an upwelling mantle plume and, in some cases, also from the overlying continental crust (Pik et al., 1999; Kieffer et al., 2004). Moreover, according to Dereje Ayalew and Gezahegne Yirgu (2003), the Oligocene volcanic products of northern Ethiopian plateau show a strongly bimodal distribution of basalts and rhyolites, although the province is predominantly basaltic. Most of the basalts and associated felsic rocks were apparently erupted in a short time interval (<5 Ma) with the greatest eruption rates occurring from 31 to 28 Ma (Hoffman et al., 1997; Pik et al., 1998; 1999).

Further, Zanettin et al. (1978b, as cited in Seife Michael Berhe et al., 1987) have recognized two main stages of volcanism in NW Ethiopian Plateau separated by a long period of volcanic quiescence. The first stage (Oligocene, >45 Ma) of this volcanism is characterized by its alkaline to tholeiitic basalts. The second stage (Oligocene to Miocene, 34 to 13 Ma) started with widespread fissural activity of transitional basalts (Aiba Formation) and concluded with a central alkaline activity (Termaber Formation).

Moreover, Pik et al. (1998, 1999) have latter classified the northwestern Ethiopian flood basalts into three distinct geochemical groups based on trace element and Ti concentrations: low-Ti basalts (LT), high-Ti1 (HT1) basalts and high-Ti2 (HT2) basalts. These groups are spatially controlled rather than temporal control; the entire low-Ti (LT) basalt groups are located in the northern part of the plateau whereas all the high-Ti basalts (HT1 and HT2) groups are exposed in the eastern and southern parts of the plateau. In addition, the new major and trace element analyses of the northern Ethiopian plateau confirms also the existence of three main spatially controlled magma types (Beccaluva et al., 2009).According to Beccaluva et al. (2009) Low-Ti tholeiites (LT), in the NW, are quantitatively predominant (150,000 km^3); High-Ti lavas (HT1) predominate southeastwards; ultratitaniferous transitional basalts and picrites (HT2) are concentrated in the Lalibela area, closer to the center of the Afar triangle.

Furthermore, Melese Tadesse et al. (2011) have also carried out a regional wise (1:250,000) geochemical and geological studies on Maychew sheet including the current study area, Maychew. According to these results, Tertiary volcanic rocks of Maychew area have been classified following the previous regional classification names like Ashenge, Aiba, Alaje and Termaber formations. In addition, Kurkura Kabeto (2010) have investigated the volcanic rocks of the Maychew, including the current study area, and identified six sequences of lavas from bottom to top: basanite, alkaline basalts, transitional ankaramite, silica rich tholeiitic to transitional sequence, mafic-felsic volcanism, and tholeiitic to transitional basalt.

CHAPTER TWO

REGIONAL GEOLOGY

2.1. Introduction

The Cenozoic Ethiopian continental flood basalt province is located at the junction of three rifts: two oceanic rifts, Red Sea and Gulf of Aden, and the East African continental rift (Pik et al., 1998; Corti, 2009; Dereje Ayalew and Gezahegne Yirgu.2003), and they are the youngest example of a major continental volcanic plateau (Kieffer et al., 2004; Dereje Ayalew et al., 1999; Dereje Ayalew and Gezahegne Yirgu 2003; George et al., 1998). Continental flood volcanism in Ethiopia and Yemen is presumed to be associated with the Afar plume (Ukstins et al., 2002; Dereje Ayalew et al., 2002) and the initial role of the mantle plume changes spatially within the Ethiopian province (Dereje Ayalew et al., 1999).

Earliest volcanism in the East African rift system (EARS) occurred in southwestern Ethiopia, southeastern Sudan, and northern Kenya at 40-45 Ma (Davidson & Rex, 1980; Ebinger et al., 1993; George et al., 1998). Soon after, between 31 and 22 Ma, volcanism was widespread throughout Ethiopia, Eritrea and Yemen where flood basalts and associated felsic pyroclastic rocks were erupted (Baker et al., 1996; Hofmann et al., 1997; Kieffer et al., 2004; Pik et al., 1998, 1999; Dereje Ayalew, 2011).Immediately after the peak of volcanic activity related to the flood basalt emplacement, a number of large shield volcanoes developed from 30 Ma to about 10 Ma on the surface of the volcanic plateau (Kieffer et al., 2004).The development of the EARS (the formation of magmatic provinces, plateau uplift, crustal thinning and rifting) is attributed to one or several Paleogene mantle plumes (George et al., 1998; Ebinger and Sleep, 1998). Although all available evidence indicates that estimations of the extent, magnitude and timing of uplift needs revision (Seife Michael Berhe et al., 1987), rifting and volcanism have been considered in relation to domal uplifts in East Africa (Gass, 1970).

Ethiopia, since the Cenozoic, was affected by a widespread volcanic activity related to the geodynamic evolution of the Afar triple junction (Tommasini et al., 2005).The earliest volcanism in Ethiopia is restricted to two areas: in SW Ethiopia, where the Akobo basalts give ages as old as 49.4Ma (Davidson & Rex, 1980), and in NW Ethiopia where the Ashenge basalts underlie the Aiba basalts which are dated at 34 to 30 Ma (Seife Michael Berhe et al., 1987).According to Peccerillo et al. (2003) volcanism in Ethiopia, which is thought to be bimodal with respect to SiO_2content (Dereje Ayalew et al., 2006; Peccerillo et al., 2003),

built up a thick succession of lavas and pyroclastic rocks, typically 500-1500 m thick, which covers an area of about 6 *10^5 km^2, and at present forms the western and eastern uplifted plateau and the Ethiopian rift and Afar. Further, the evolution of volcanic activity in Ethiopia consists of three main stages (Peccerillo et al., 2003). During the first stage (about 50-10 Ma), the Ethiopian plateau was constructed by eruptions of flood tholeiitic to transitional basalt lava flows, and interbedded mildly alkaline trachytic and rhyolitic ignimbrites (Mohr & Zanettin, 1988). A second stage of activity occurred around 10-5 Ma and constructed several shield volcanoes made of transitional to Na-alkaline basalts and minor trachytes (Peccerillo et al., 1979). The final stage is Pliocene to Present and is more directly related to formation of the Ethiopian rift and Afar.

2.2. Continental Flood Basalts

Continental flood volcanism (CFV) represents massive outpourings of basaltic lava flows and, in some cases, rhyolitic lavas and pyroclastic rocks (Baker et al.,1996; Dereje Ayalew et al., 2002; Kieffer et al., 2004; Ukstins et al., 2002), often with volumes in excess of 1 X $l0^6$ km^3(Rochette et al., 1998).The continental flood basalt (CFB) province and associated continental break-up are thought to be related to the upwelling of mantle plume impinged on the base of the lithosphere (Storey,1995; Rooney et al.,2007). Nearly all CFB provinces contain significant volumes (up to 20% of the total volcanics) of acidic eruptive, usually in the upper part of the sequence capping the basalts (Dereje Ayalew, 2011).

In addition, the volcanic suites in nearly all continental flood basalt provinces have a bimodal basalt–rhyolite nature with a distinct lack of intermediate compositions (Dereje Ayalew and Gezahegne Yirgu, 2003; Dereje Ayalew, 2011).According to Pik et al. (1999) most of the lavas from main CFB provinces (Parana ´, Deccan, Siberia, Karoo, etc.) have isotopic and trace element signatures that are not typical of OIB, suggesting that they are probably not derived directly from the deep mantle. Instead, in most continental-flood-basalt (CFB) provinces, the magmatism includes variable contributions of melts derived from both lithospheric and convecting mantle sources, and also readily-fusible crust (Baker et al., 1996; Hawkesworth et al., 1999).

Further, Dereje Ayalew et al. (2006) have noted that the initiation of continental flood basalt (CFB) magmatism is spatially and temporally related to continental break-up, which results in the formation of oceanic crust, at least within the past 200 Ma. However, the relationships

between the timing of CFB formation and rifting leading to ocean-floor formation are complex, and can vary in time and space (Courtillot et al., 1999; Hawkesworth et al., 1999). Hence, magmatism can predate continental extension by several million years (e.g. Ethiopia-Yemen), magmatism and break-up can be synchronous (e.g. Parana-Etendeka, North Atlantic Tertiary volcanic province/ Greenland-UK), or magmatism can postdate break-up by several million years (e.g. Australia- India).

Moreover, CFBs are generally not primary magmas but evolve through differentiation of mantle equilibrated, more MgO-rich, parental magmas by fractional crystallization with or without concomitant crustal contamination (Cox, 1980; Farnetani et al., 1996). Most continental flood basalt provinces (CFBs) are associated with low volume alkaline rocks (e.g., Paraná- Etendeka, Ewart et al., 1998 as cited in Dereje Ayalew et al., 2006; Ethiopia, Kieffer et al., 2004).Map 2.1 shows the distribution of major continental flood basalt provinces in the world. Further, the ages and dimensions of these provinces are also given in Table 2.1.

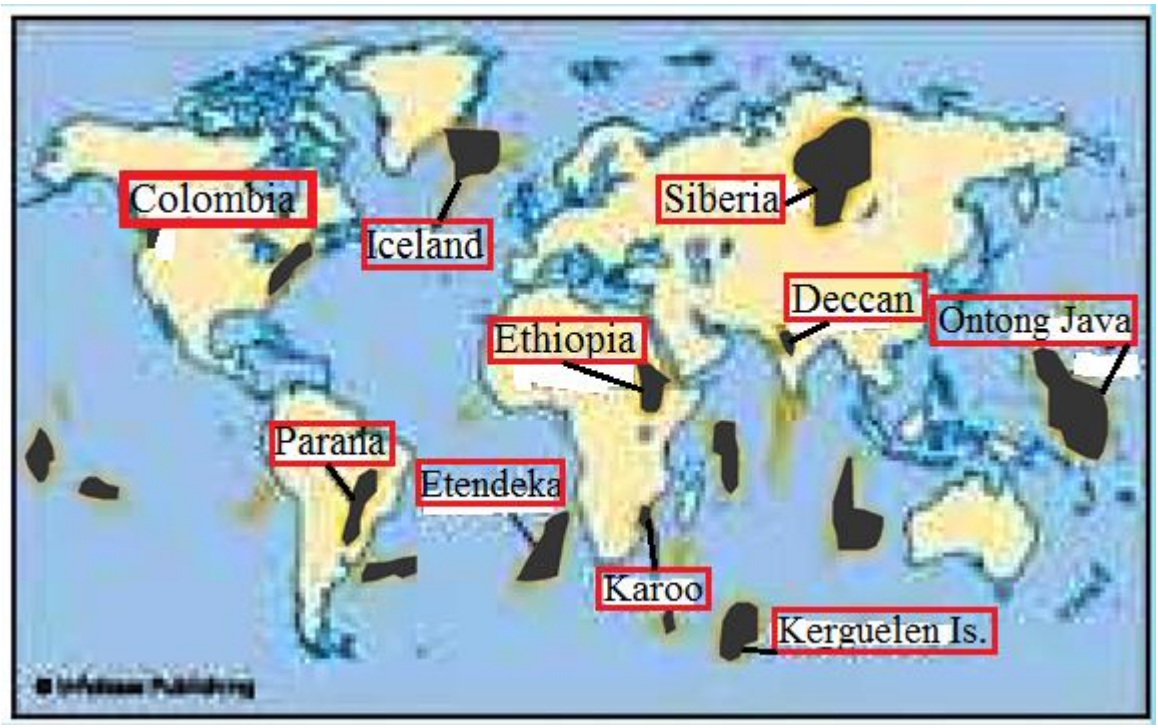

Fig.2.1: Flood basalt distribution in the world (https://www.climate-policy-watcher.org/plate-tectonics/large-igneous-province-flood-basalt-a.html)

Table 2.1.Ages and Dimensions of Major Continental Flood Basalt Provinces.

No	Flood basalt	Location	Age(Ma)	Area(Km^2)	Thickness(m)
1	Snake River Plain	Indaho,USA	16-present	$0.5x10^5$	Up to 1200
2	Columbia River	WA,ID,OR,USA	16-6	$2\ x10^5$	>1500
3	Ethiopia	Ethiopia	31-29	$6\ x10^5$	Up to 3000
4	Deccan Traps	India	65-50	$>5\ x10^5$	>3000
5	Parana Plateau	Brazil	149-119	$12\ x10^5$	1800
6	Karoo	South Africa	206-216	$>1.4\ x10^5$	9000
7	Siberian Traps	Russia	245-216	$>15\ x10^5$	3500
8	Keweenaw	Lake Superior,USA	1200-1050	$>1\ x10^5$	12000

Data sources: The data sources for 1, 2,4,5,6, 7 and 8 are from Frost and Frost (2014). However, the data sources for Ethiopian flood basalts are from Hofmann et al., 1997(age), Mohr and Zanettin, 1988(area), Dereje Ayalew and Gibson, 2009 (thickness).

2.3. Ethiopian Continental Flood Basalts

The Ethiopian continental flood basalt (CFB) province is one of the youngest (30 Myr) large igneous provinces (Dereje Ayalew and Gezahegne Yirgu, 2003; Kieffer et al., 2004;Pik et al.,2003), and associated with continental break-up and ocean basin formation (Dereje Ayalew et al., 1999;Baker et a., 1996).Further, this flood basalt province is located near the Afar triple junction (Dereje Ayalew et al., 2002;Mohr and Zanettin, 1988;Pik et.,1998;1999).The main part of the province crops out in Ethiopia, whereas the rest is located on the eastern side of the Red Sea, in Yemen (Pik et al., 1998). The trap volcanics cover an area at least $6* 10^5$ km^2 (western and eastern plateaus), and the total volume is estimated to be at least $3.5* 10^5$ km^3 (Mohr, 1983; Mohr and Zanettin, 1988) and probably higher than $1.2 *10^6 km^3$, according to Rochette et al. (1998). The thickness of the lava pile varies greatly, reaching up to 2000 m in northwestern Ethiopia and thinning to 500 m towards both north and south (Furman, 2007).

Moreover, the flood volcanism is predominantly composed of basaltic lavas together with rhyolitic ignimbrites and pyroclastic-fall deposits, and less common basaltic pyroclastic rocks and rhyolitic lavas (Dereje Ayalew et al., 2002; 2011; Kieffer et al., 2004; Peccerillo et al., 2007). According to Kieffer et al. (2004) the mineralogical and chemical composition of the Oligocene Ethiopian flood basalt is comparatively uniform and most rocks are aphyric to

sparsely phyric, and contain phenocrysts of plagioclase and clinopyroxene with minor or without olivine. Further, Ethiopian continental flood basalts have tholeiitic to transitional chemical composition (Pik, et al., 1998, Mohr, 1983; Mohr & Zanettin, 1988). Moreover, intermediate lavas are lacking and the volcanism is of a bimodal basalt–rhyolite type (Mohr & Zanettin 1988; Dereje Ayalew, 2011), a feature common to most continental flood basalt provinces (e.g. Karoo and Parana´). Furthermore, the Ethiopian Plateau lavas are characterized by a clear zonal arrangement with Low-Ti tholeiites (LT) to the west, High-Ti tholeiites (HT1) to the east and very High-Ti transitional basalts and picrites (HT2, TiO_2 4–6.5 wt. %) close to the afar triple junction (Beccaluva et al., 2009; Kieffer et al., 2004; Pik et al., 1998, 1999).

Most of these basalts and associated felsic rocks were apparently erupted in a rather short time interval (<5 Ma) with the greatest eruption rates occurring from 31 to 28 Ma (Hoffman et al., 1997; Pik et al., 1998; Ukstins et al., 2002; Coulié et al., 2003). This strong eruption was concomitant with the onset of continental rifting in the Red Sea–Gulf of Aden systems by 29 Ma (Wolfenden et al., 2005), but predates the main rifting phases associated to the development of the MER (Corti, 2009). According to Mohr and Zanettin(1988) the eruptive process for the Ethiopian continental flood basalt (CFB) province was particularly active during mid-Tertiary, and was renewed in Afar some 5 My ago. In addition, Mohr and Zanettin(1988) have noted that the Eruption rates on the Ethiopian plateaus, averaged over the 43 My of activity, have been significantly less than in other flood basalt provinces, perhaps ultimately reflecting a slower rate of lithospheric thinning. This slow eruption rate in Ethiopia is consistent with the unusually long period over which this volcanic province has been active,43 My, compared with only a few million years for the rapidly constructed Columbia River and Deccan Plateau piles (Hooper, 1982; Cox and Hawkesworth, 1985 as cited in Mohr and Zanettin, 1988).

The Ethiopian flood basalts have been attributed to melting associated with the activity of one (Afar plume) or two (Afar and East African or Kenyan plumes) mantle plumes impinging the base of the continental lithosphere (Rogers et al., 2000; Ebinger and Sleep, 1998; George et al., 1998; Pik et al., 2006). In addition, it has been suggested that the flood basalts of Ethiopia may result from multiple plume stems rising from a single, broad and deep-seated mantle upwelling rising from the lower mantle (the African super plume; Furman et al., 2006). Additionally, Kieffer et al. (2004) have noted that the heterogeneity of the flood basalts that

built the Ethiopian plateau supports a magma genesis from a broad region of mantle upwelling, heterogeneous in terms of both temperature and composition. Further, the Oligocene Ethiopian traps present He isotopic ratios characteristic of a deep mantle contribution (Marty et al., 1996), showing that the early development of the Afar plume (Stewart and Rogers, 1996) is responsible for the eruptions of Ethiopian CFB. However, in the Ethiopian province, the contribution of mantle plume to magmatism appears to vary geographically; lithosphere and mantle plume derived magmas are thought to be concomitant in the north (Pik et al., 1998), while in the south lithosphere derived magmas occur in the earlier flood basalts and mantle plume contribution increases with time (Stewart and Rogers, 1996).

Furthermore, Kieffer et al. (2004) have noted that Ethiopian Oligocene flood volcanism is overlain by low-angle shield volcanoes that are magmatically similar to the underlying flood basalts, i.e. tholeiitic shields overlie tholeiitic flood basalts and alkaline shields overlie alkaline flood basalts. The deposition of these prominent central volcanoes above the fissure-fed flood basalts, together with a distinct magmatic composition within the province and an incorporation of high amount of felsic lavas and pyroclastic products, distinguishes the Ethiopian volcanic province from other typical flood basalt provinces (e.g., Parana, Deccan; Kieffer et al.,2004), which are characterized by thick homogeneous series, continuous, sub-horizontal flows of oceanic-type basalts without overlying shield volcanoes (Corti, 2009).

The main Ethiopian rift (MER), which started to develop during Miocene time (Davidson and Rex, 1980; Gidey WoldeGabriel et al., 1990; Tadiows Chernet et al., 1998), dissects the Ethiopian dome, which is made of Precambrian crystalline basement, Mesozoic marine and continental sediments and Tertiary –Quaternary volcanic rocks (Merla et al., 1979).Similarly Wolfenden et al. (2004) suggested that the northern Main Ethiopian Rift (NMER),developed about 11 Ma, dissected the Ethiopian Plateau into northwest and southeast sections (Fig.2.2).The Ethiopian plateau rocks rest either directly over the Neoproterozoic crystalline basement or over the Mesozoic sedimentary sequences (Peccerillo et al., 2003, 2007; Pik et al., 1999).Furthermore, volcanic fields in Ethiopia and Yemen were adjacent about 30 Ma ago and have subsequently been separated by the opening of the Red Sea and the Gulf of Aden (Dereje Ayalew and Gezahegne Yirgu, 2003).

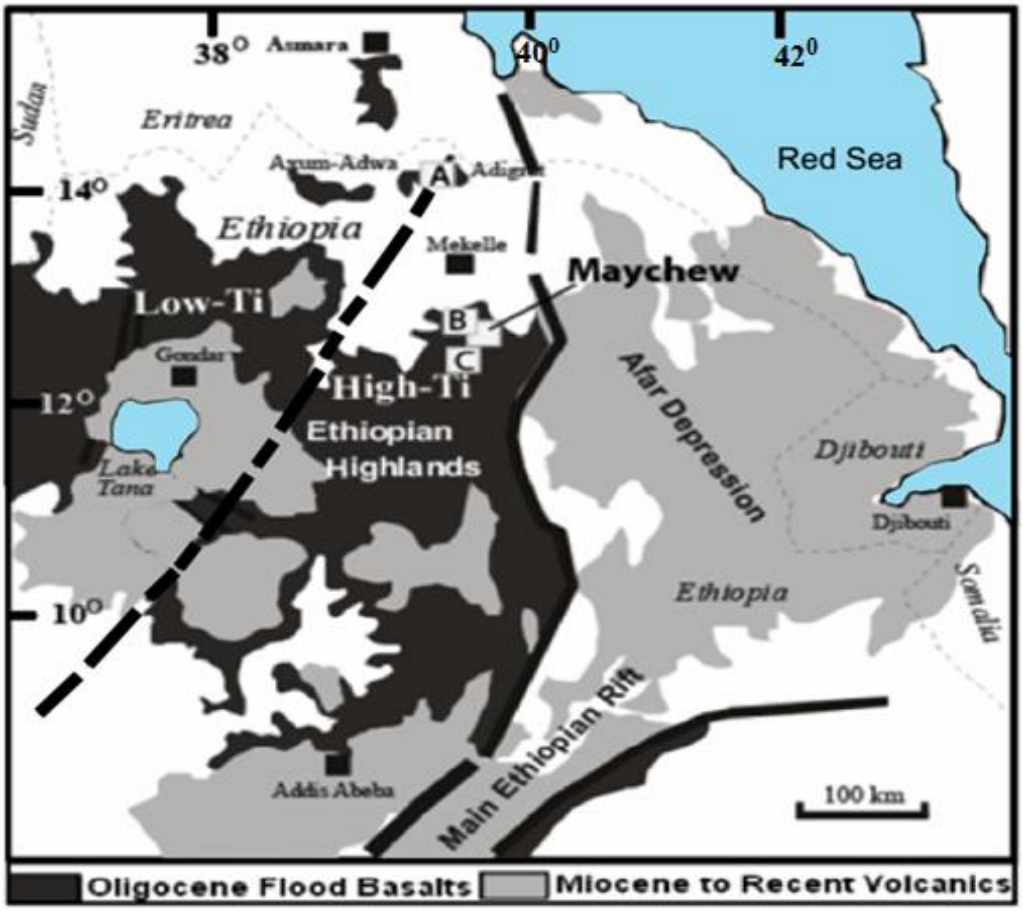

Fig.2.2: Location map of NW Ethiopian Plateau, Afar Rift and Main Ethiopian Rift (after Kuster et al., 2005). The approximate broken line separates the low-Ti and High-Ti flood Basalt province (Pik et al., 1998).

2.4. Northwestern Ethiopian Plateau

The northwestern Ethiopian Plateau, with a mean elevation of 2.5 km, is located on the western flank of the tectonically active Main Ethiopian Rift and the Afar Depression (Gani et al., 2007). According to Mohr and Zanettin (1988) the flood volcanic succession in the WEP includes basaltic lava flows, basaltic tuffs, as well as a considerable volume of rhyolitic, trachytic and phonolitic products. Moreover, the Oligocene northern Ethiopian Plateau (and its Yemeni counterpart) is characterized at the top by large volumes of rhyolitic volcanics partly interlayered with plateau basalts (31–28 Ma, Dereje Ayalew et al., 2002, 2006; Rochette et al., 1998; Ukstins et al., 2002; Dereje Ayalew and Gezahegne Yirgu, 2003).

Based on their geochemistry, the Northern Ethiopian plateau basalts are classified into three magma types (Pik et al., 1998; Beccaluva et al., 2009; Fig.2.2): Low-Ti tholeiites (LT) distributed in the northwestern areas; high-Ti1 lavas (HT1) in the eastern areas and

ultratitaniferous transitional basalt and picrites of the high-Ti2 (HT2) series, which are concentrated in the Lalibela area close to the Afar depression. Further, those authors (Pik et al.,1998; Beccaluva et al., 2009) and Pik et al.(1999) have stated that the LT and HT1 basalts display compositional ranges similar to those of the low and high-Ti groups from other main CFB provinces(e.g. Parana, Deccan, Karoo, and Siberia). However, the HT2 group exhibits extreme OIB-like compositions. This unusual geochemical signature suggests the involvement of deep mantle in the genesis of the HT2 magmas. Moreover, most of the HT1 basalts were emplaced at the end of the flood basalt episode, between 29.4 and 26.4 Ma whereas the two main magma types, LT and HT2, have been extruded contemporaneously in different areas of the plateau between 31 and 29.5 Ma. Furthermore, the textures and mineral compositions of the basalts are very homogeneous within each magma group but significantly different from one to the other. In addition, on the northwestern Ethiopian Plateau, the extreme LT and HT2 geochemical signatures are the most common in the lavas. On the other hand, in southern Ethiopia and Yemen, basaltic traps display the same characteristics as the intermediate HT1 group.

Most of the huge volume of basalts in this region of Ethiopia were extruded over a short period of time (1–2 my) around 30 Ma (Hofmann et al., 1997). Soon after the northwestern Ethiopian flood basalt deposition, a number of large central/shield volcanoes developed sporadically from 23 Ma to about 10 Ma on the surface of the flood basalts (Kieffer et al., 2004). Furthermore, Pik et al. (1998) have stated that the Oligocene basalts on the northwestern Ethiopian Plateau are overlain by less voluminous Miocene lavas, erupted from large central vent volcanoes whereas in southern Ethiopia, where youngest volcanic activity is represented by Miocene basalts and ignimbrites, the Eocene–Oligocene basalts are rare and the volcanic sequence is dominated by thick Eocene–Miocene acidic lavas and ignimbrites.

Moreover, nearly coeval CFB volcanism is recorded in the Yemen conjugate margin covering an area of approximately 80 000 km^2 (Baker et al., 1996; Ukstins et al., 2002).In addition, Bosworth and Stockli (2016) have noted that the CFV of southwest Yemen share many similarities with those of northern Ethiopia. However, the presence of basanite and phonolite flows underlines the generally more alkaline character of the Yemen flood pile, compared with the contemporaneous lavas of the northern Ethiopian Plateau.

The northern Ethiopian Plateau, which mainly consists of tholeiitic to transitional basaltic lavas (Mohr & Zanettin, 1988), represents the huge volcanic event related to the Afar plume (Natali et al., 2011; Beccaluva et al., 2009, Dereje Ayalew et al., 2002,). Similarly, Dereje Ayalew and Gibson(2009) stated that the large volume and widespread distribution of these basalts together with contemporaneous topographic uplift suggests that their genesis may be linked to the impact of the 'starting-head' of the mantle plume, which is believed to be currently located beneath the Afar region (Marty et al., 1996).Additionally, Beccaluva et al. (2009) have stated that the northern Ethiopian continental flood basalts (CFBs) with an original volume of about 250 000 $km^3$and an eruption rate of the order of 0.2-0.3 km^3/year, preserve a record of magmas generated from the center to the flanks of a plume head, currently corresponding to the 'Afar hotspot'(Fig.2.3).Furthermore, the basalts in the northern Ethiopian Plateau cover an area of 210 000 km^2 with a lava pile up to 2000 m thick in the central-eastern part, thinning to less than 500 m toward the northern and southern boundaries (Beccaluva et al., 2009).

There are certain features which distinguish the magmatic centers of NW Ethiopia and SW Ethiopia. According to Merla et al. (1979) the NW Ethiopian Plateau has a higher proportion of silicic volcanics within the Flood Basalts. Moreover, the NW Ethiopian Plateau is notable for the frequent occurrence of major volcanic edifices overlying the Flood Basalts some of which reach as much as 100 km in diameter (Dainelli, 1943, as cited in Seife Michael Berhe et al., 1987). Large volcanic centers are rare within the SW Plateau. There also appear to be more phonolitic lavas in the shield volcanics of SW Ethiopia than have so far been reported in Northern and Central E Ethiopia (Seife Michael Berhe et al., 1987). The absence of Mesozoic sediments between the basement and the volcanics is another distinctive feature of the SW Ethiopian Plateau (Seife Michael Berhe et al., 1987).

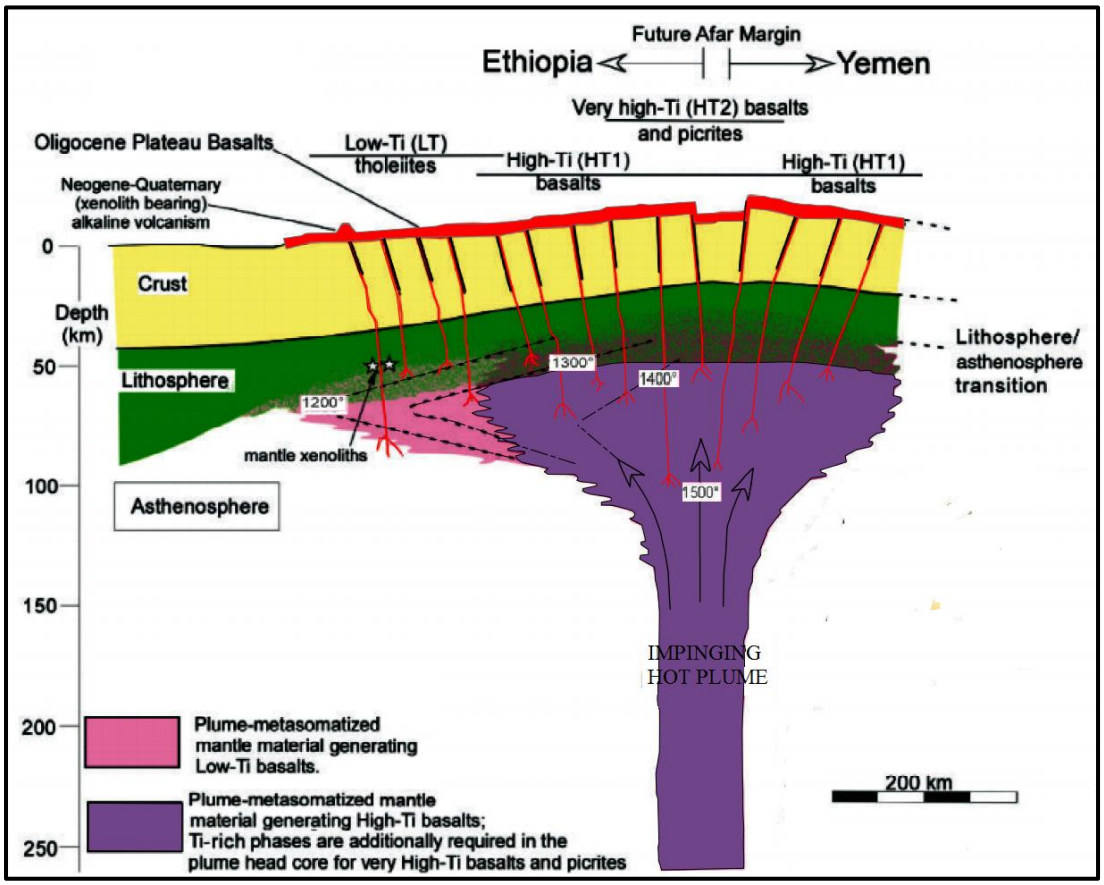

Fig.2.3: Schematic cartoon depicting the Afar plume impinging on the Afro-Arabian lithosphere and the generation of Oligocene Northern Ethiopia–Yemen Continental Flood Basalts (After Beccaluva et al., 2009).

2.5. Stratigraphy of Northwestern Ethiopian Plateau

Since the original classification of northeastern part of the Ethiopian plateau into a lower tilted Ashenge Group and upper horizontal Magdala Group (Blanford, 1869; 1870), several works have been carried out to understand the stratigraphic section of the Ethiopian flood basalts. According to Seife Michael Berhe et al. (1987) the Oligocene volcanism of the northwestern Ethiopian plateau were divided into three stages: the Ashenge (Pre Oligocene), Aiba (34 to 30 Ma) and Alaje (30 to 26 Ma), based on lithology, age and chemical characteristics. In addition, Merla et al. (1979) and Mohr and Zanettin (1988) have classified northern Ethiopian plateau into Ashenge, Aiba, Alaje and Termaber formations, from oldest to youngest. Other authors like Mohr, 1983; Mengesha Tefera et al., 1996 have also supported this regional classification. Thus, the regional classification name of Ethiopian plateaus, northwestern plateau, is summarized as follows from the oldest to youngest formation.

2.5.1. Ashenge Formation

Ashenge Formation, which represents the earliest fissural flood basalt volcanism on the northwestern plateau, is predominantly consists of mildly alkaline basalts with interbeded pyroclast and rare rhyolites ,and commonly injected by dolerite sills and dykes (Mengesha Tefera et al., 1996).Further, Ashenge lavas are generally quartz-hypersthene or hypersthene – olivine normative (with " hypersthene " dominating in both types), and include both transitional and tholeiitic basalts (Mohr & Zanettin, 1988).

According to Merla et al. (1979) Ashenge basalts have variable thickness: From 600 m to 800 m along the escarpment and in the northern portion of the plateau, to zero meters between Debre Markos and Addis Ababa. Further, the basalt flows of Ashenge formation are several hundreds of meters to a kilometer thick of strongly weathered, fractured, tilted basalts which lie below the major pre- Oligocene unconformity (Zanettin et al., 1980, as cited in Mengesha Tefera et al., 1996). Moreover, according to Mohr & Zanettin (1988), in the Alaje-Aiba-Maychew region a steeply south- or southeasterly-dipping basalt lava sequence underlies the rest of the volcanic pile with strong unconformity, which was the basis of Blanford (1869, 1870) subdivision of the flood basalt pile into, a lower Ashenge Group, and upper Magdala Group.

Moreover, over large areas of the NW Ethiopian Plateau the Ashenge Formation is unconformably overlain by the Amba Aiba Basalts but it rest conformably on the Mesozoic arenaceous sediments and locally on the basement (probably by fault)(Merla et al. 1979). In addition, Seife Michael Berhe et al. (1987) have noted that Ashenge Formation of NW Ethiopia does not extend further south to the Abbay (Blue Nile) Basin, as no unconformity similar to that observed between the Ashenge and Aiba Formations in NW Ethiopia occurs within the thin lava pile. Moreover, Ashenge formation has been affected by a compressional episode, which resulted in the tilting and folding of the basalts prior to eruption of the Aiba basalts (Merla &Minucci, 1938, as cited in Seife Michael Berhe et al., 1987).

2.5.2. Aiba Formation

Aiba basalts, which unconformably overlay the Ashenge Formation, represent the second major pulse of fissural basalt volcanism on the northwestern Ethiopian plateau (Mengesha Tefera et al., 1996; Merla et al., 1979). According to Mohr & Zanettin (1988), Aiba Formation (32-25 my) is typically composed entirely of massive flood basalt flows, with or without intervening agglomerate beds. Furthermore, the flows with a thickness of between 15 and 50 m (in extreme cases ponding to 100 m) extend sub horizontally for at least tens and possibly a hundred or more kilometers, and are generally composed of dense, dark, fine-grained olivine basalt, commonly columnar. Moreover, its upper limit with the Alaje Formation is defined by the base of the earliest silicic horizon. Aiba basalts/lavas, which are almost all uniformly quartz-normative transitional basalts (Mohr & Zanettin, 1988), show a distinctive tholeiitic nature with transitions to mildly alkaline varieties (Mengesha Tefera et al., 1996).

2.5.3. Alaje Formation

Alaje Formation with an age range of 32-15 Ma (Mohr & Zanettin, 1988) mainly consists of aphyric flood basalts associated with rhyolites (ignimbrites) and subordinate trachytes (Mengesha Tefera et al., 1996).Alaje basalts are chemically and mineralogically very similar to Aiba basalts, but overall are slightly less silica-saturated (Mohr, 1983). Furthermore, Mengesha Tefera et al. (1996) have noted that the migration of Alaje type volcanism from north to south is indicated by the occurrence of the older volcanics of this formation on the northern part of the northwestern plateau. In addition, those authors have noted that on the northwestern Ethiopian plateau, Alaje Formation which contains basalts of transitional to tholeiitic nature, rests conformably on Aiba basalts but in some places (e.g. Kassem Gorge, Mugher Canyon and in most outcrops on the southeastern plateau) it rests directly on the Mesozoic sediments. Further, in the type area (at Amba Alaje), Aiba basalts are overlain directly and conformably by silicic (trachyte/rhyolite) ignimbrites, which maintains a similar thickness over kilometers or, where preserved, even tens of kilometers lateral extent (Mohr & Zanettin ,1988).

2.5.4 .Termaber Formation

Termaber Formation, which has an age between 30-13 my (Mohr & Zanettin, 1988), represents Oligocene to Miocene basaltic shield volcanism on the northwestern and southeastern plateaus (Mengesha Tefera et al., 1996).According to Mohr & Zanettin (1988) the mafic lavas comprising the Termaber Formation form large, low angle shields up to tens of kilometers in diameter, although smaller and steeper edifices also occur. According to Mohr and Wood (1976) the alkaline basalts of the Termaber Formation comprise about forty shield-like piles on the Ethiopian and Harar Plateaus. Among these shields considerable physical, lithological and chemical variety is exhibited. Furthermore, on the northwestern plateau the Termaber shield volcanoes become progressively younger from north to south (Mengesha Tefera et al., 1996), and also these authors have described that the central type Termaber formation basaltic volcanism was followed by fissural eruptions particularly along the escarpments of northwestern and southeastern plateaus.

Summarized radiometric data reveal that Alaje and Termaber-type volcanism largely overlapped in time in the north, and for this reason Mohr & Zanettin (1988) divided Termaber Formation into an Early Miocene Termaber Guassa and a Middle Miocene Meghezez Formation. Accordingly, the name Termaber Guassa Formation is used for the shield volcanoes of northern Ethiopian plateau with an absolute age range of 26 to 16 Ma whereas Termaber Meghezez Formation is used for the younger shield volcanoes with an absolute age range of 16 to 13 in the southern part of northwestern plateau and southeastern plateau. Moreover, shield basalts of the Termaber Guassa and Termaber Meghezez formations typically are alkaline and ne-normative (Mohr & Zanettin, 1988).

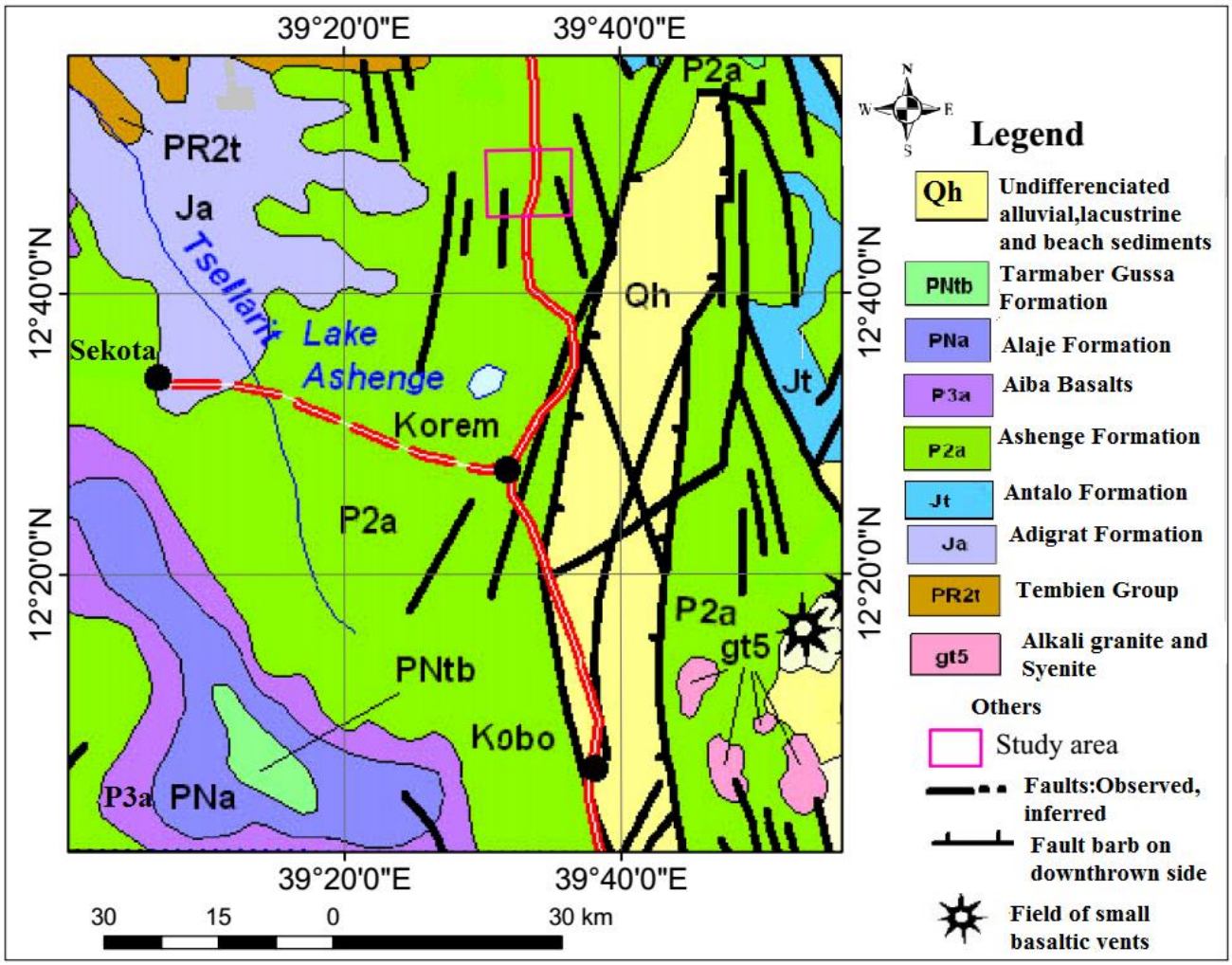

Fig.2.4: Geological map of Maychew area and its surroundings (Modified from Mengesha Tefera et al., 1990). Note the distribution of Ashenge, Aiba, Alaje and Tarmaber Formations.

CHAPTER THREE

GEOLOGY OF THE STUDY AREA

3.1. Introduction

The study area, which is part of northwestern Ethiopian plateau, is mainly constituted by basaltic rocks with some pyroclastic materials (unwelded tuff unit). Primary name of lithological units were given during the field work based on textural and mineralogical compositions. Broadly, from field observations, the basaltic units exposed in the study area are classified into tilted, and horizontal to sub horizontal basaltic units. These two major basaltic rock units are separated by unconformity, which is commonly marked by thin layers of paleosols. The local classification name of northern Ethiopia plateau; Ashenge, Aiba and Alaje formations (e.g. Merla et al., 1979; Mohr & Zanettin, 1988), is directly adopted for the present study. Ashenge formation (tilted basaltic units), which covers much of the study area, is represented mainly by pyroxene-olivine phyric and pyroxene phyric basalts whereas Aiba formation (horizontal to sub horizontal basaltic units) is represented almost all by massive and cliff forming aphyric basaltic unit. Although the focus of this study is on Ashenge and Aiba formations; Alaje formation, which is represented by Olivine phyric basalt and unwelded tuff unit, is also included on the geological map of the study area. Furthermore, there are also unmappable units intercalated with pyroxene-olivine phyric basalts of Ashenge formation such as agglomeratic basalt, unwelded tuff unit, vesicular and plagioclase phyric basalts. The different lithological units representing the geology of the study area at a scale of 1:25,000 are shown in Fig.3.1. Besides, the study area is associated with different geological structures (Mainly with Ashenge basalts) such as joints, faults, dikes, veins. Furthermore lineaments, which are traced from drainage patterns along with satellite image and aerial photographs, are distributed in the study area having different orientations such as north-northeast, northwest, and west-northwest to east-west (Fig.3.1) Structural data of the inclined lava flows and the associated geological structures have been collected and analyzed to illustrate and evaluate mean orientations of the various structural components. The structural measurements of the tilted lava flows and the geological structures are provided in Appendix V. Generally, the detailed field description for the lithological units and their associated geological structure is given as follows:

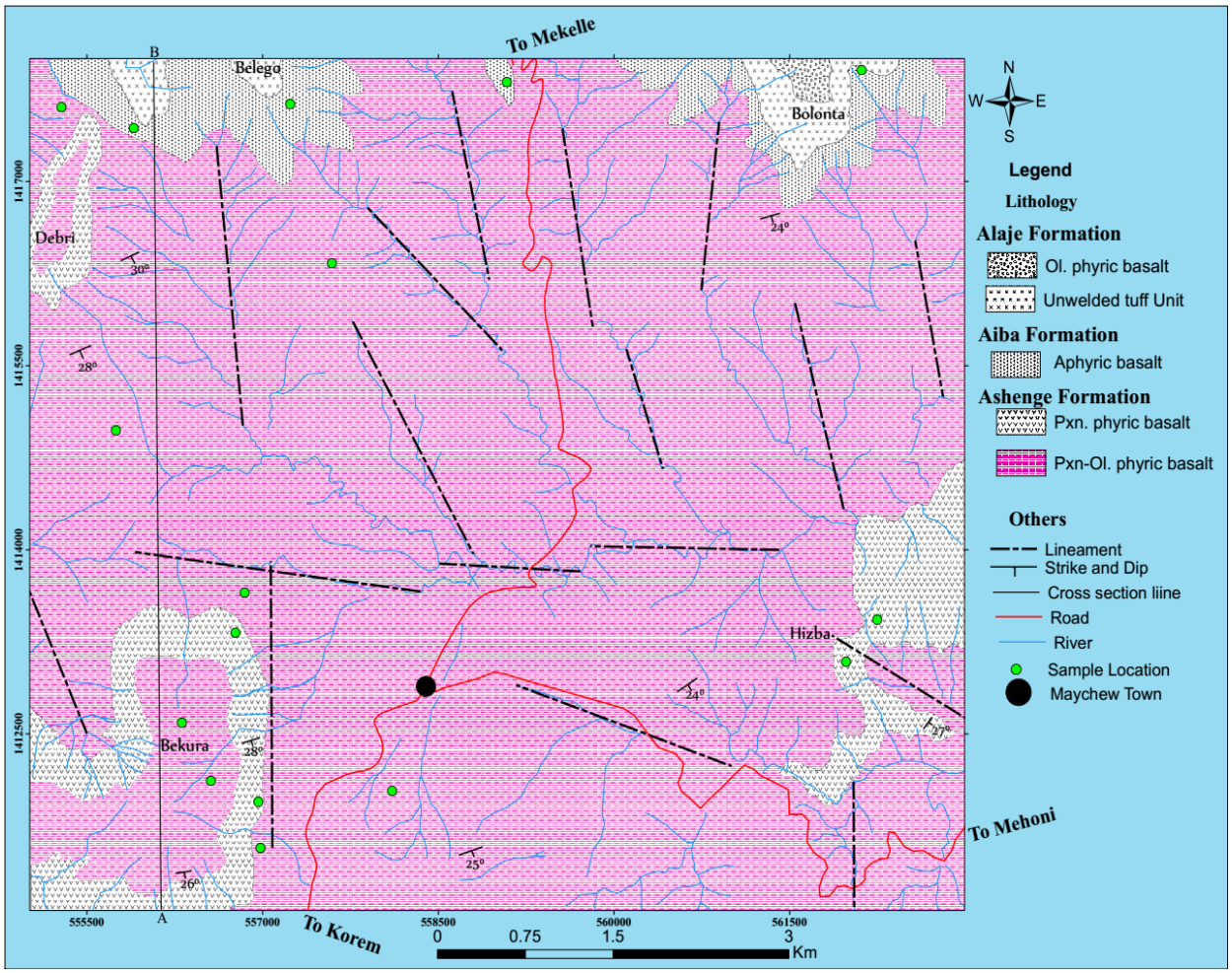

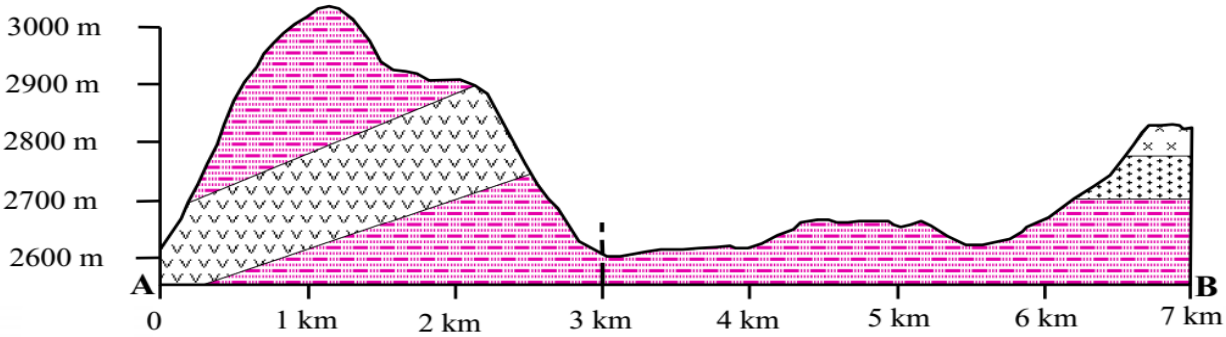

Fig.3.1: Geological map and cross section of the study area. Abbreviations (Ol. and Pxn.) are as in list of Acronym.

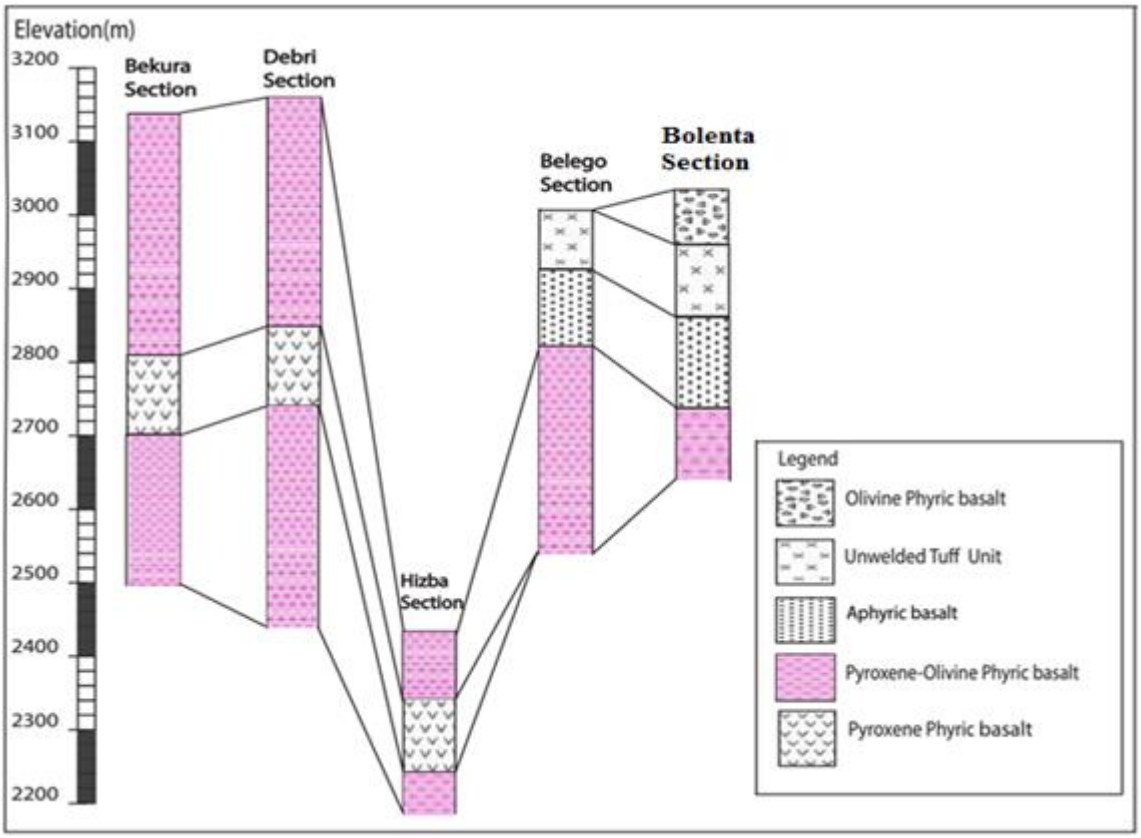

Fig.3.2: Composite Lithostratigraphic section of the study area.

3.2. Ashenge Formation

This basaltic group, which covers much of the study area, is characterized by its porphyritic texture with dominant clinopyroxene, little olivine and very little plagioclase phenocrysts, later confirmed through petrographic analysis (see chapter four). In the study area, Ashenge basalts are dominantly composed of basalt with varying proportions of aphyric basalt, vesicular basalt, and porphyritic basalt. The exposures of Ashenge Formation, which have majorly light black fresh color and light gray weathered color, are strongly weathered, intensely fractured, jointed and cut by dikes. Because of this tilted and faulted/jointed nature of the lava flows, it is very difficult to trace the lateral extent and estimate the possible maximum thickness of this basaltic formation. Moreover, the contact between this formation with the overlaying Aiba Formation is marked by the presence of paleosols (Fig. 3.5).This paleosol unit has an average thickness of 1m, and its top part has highly compacted/consolidated nature relative to its lower part, which has friable nature.

Although Ashenge Formation commonly occurs as a series of stacked flows of 1-3 m thick separated commonly by 20cm to 50 cm thick paleosol horizons (Fig.3.4) and 3-8 m thick patchy basaltic agglomerate, it occurs as a series of massive to blocky bodies of 20-30 m thick layers.

This Formation, in most part of the study area, is characterized by its tilted nature with an average orientation of N72^{0}E/26/SE (Fig.3.3).Furthermore it is affected by both systematic and non-systematic sets of joints having an average joint spacing from10 cm to 20cm. From stereonet projection (Fig.4.7) these joints have an average orientation of N5-10^{0}W/61/NE (Appendix IV for dip amount).Moreover this rock unit is also dissected by highly compacted olivine phyric basaltic dike having an average thickness of 1m along with their average orientation of N25-30^{0}W/58/SE (Fig.4.7) .Similarly Quartz vein structures, which are filled by Zeolite and agate minerals, are also associated with this rock unit with an average orientation of N20^{0}E/55/NW. Furthermore there are normal faults associated with this rock unit with an orientation of E-W/50/N (Fig.4.6).

In the study area Ashenge Formation is mainly represented by two mapable units: Pyroxene-olivine phyric basalt and Pyroxene phyric basalts.

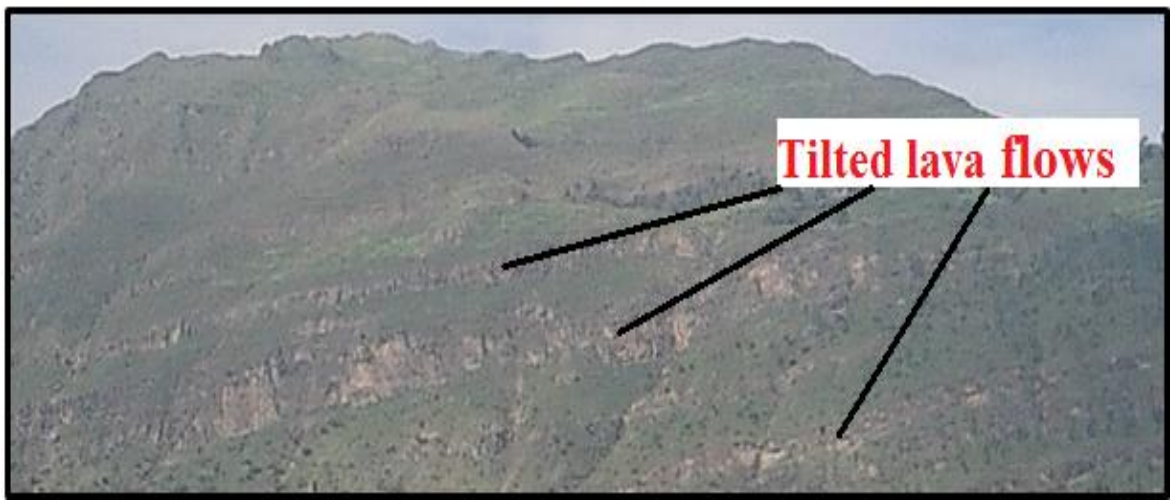

Fig.3.3: Panoramic View of Ashenge formation showing its tilted lava flow layers. The photo is taken from western side of Maychew town around Bekura Ridge (0557325E:1413056N)

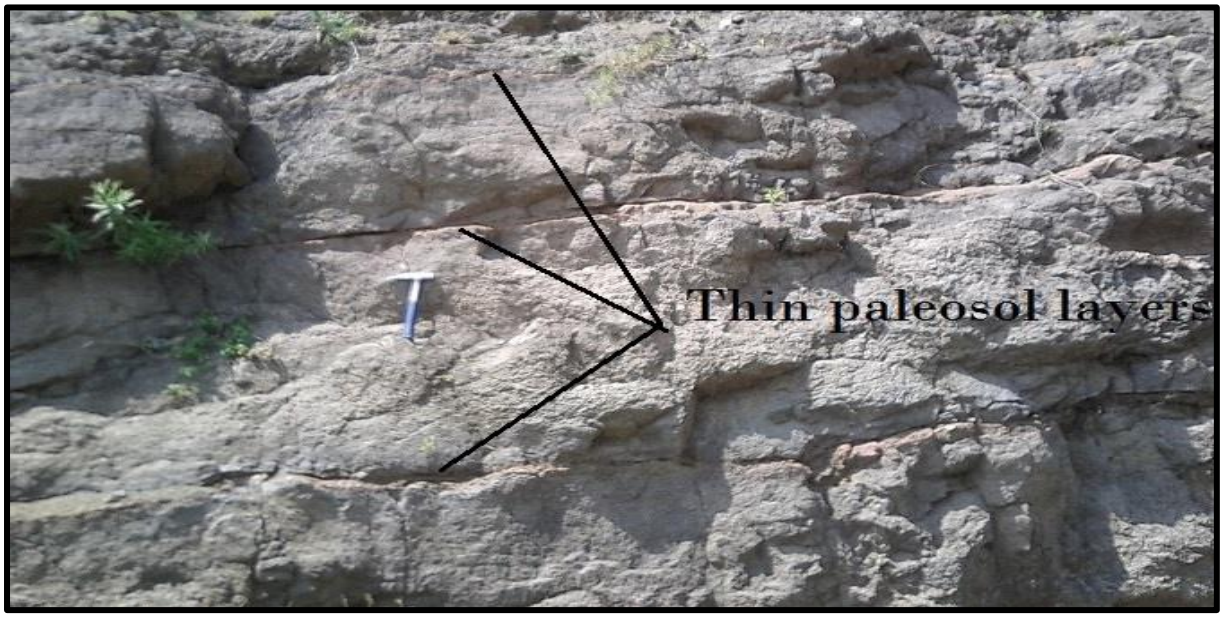

Fig.3.4: Field photograph of series of stacked flows of Ashenge formation separated by 10-20cm thick paleosols (0556906E:1412738). The average thickness of these lava flows is about 1m. Further, these stacked series of lavas are dipping towards southeast.

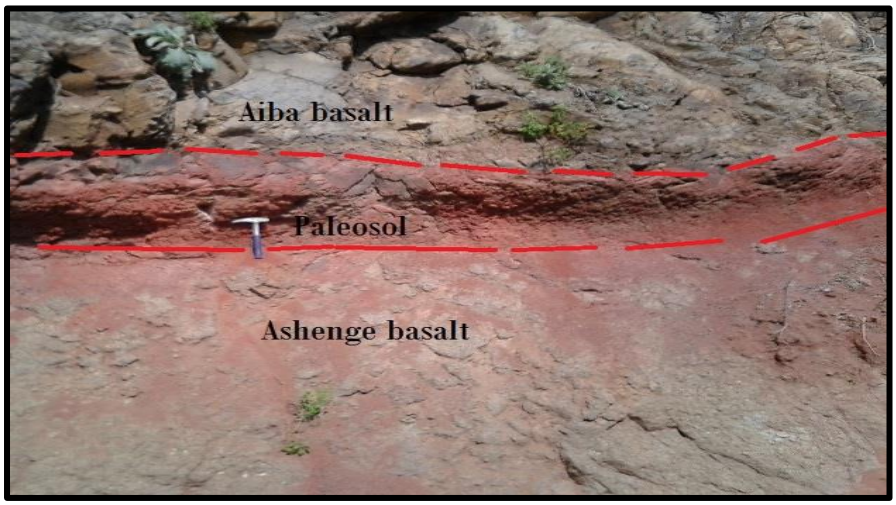

Fig.3.5: Field photograph of paleosol separating the two basaltic groups (0559085E:1417867N).The top part of this paleosol unit, which indicates a time gap between the two basaltic formations, have highly compacted/consolidated nature relative to its lower part, which has friable nature.

3.2.1. Pyroxene-Olivine phyric basalt

This rock unit, which commonly occurs as ridge forming and partly as flat laying topography, is the major rock unit that represents Ashenge formation in the study area. Moreover, it is characterized by its porphyritic texture with phenocrysts of clinopyroxene, olivine and few plagioclases; consistent with the petrographic examination of the analyzed samples (chapter

four). In the major parts of the study area it is dominated by phenocrysts of pyroxene followed by olivine and then very few plagioclase. Further, this rock unit rarely consists of some rounded to sub rounded vesicles, which are wholly to partly filled by dull appearance secondary minerals (possibly quartz).In addition, this rock unit has light black fresh color and light grey weathered color, and is highly affected by weathering. However, the degree of weathering of this rock unit ranges from deeply weathered (majorly in the Eastern part of the study area; e.g. around Hizba Maryam, Tegule and along the gravel road from Maychew to Mehoni) to weakly/moderately weathered (in the western and northern part of the study area; e.g. in Bokura ridge, Tsehafti Maryam). Exfoliation weathering is the common type of weathering in the study area which predominantly affects this rock unit. Further, this rock unit is characterized by its tilted nature with an average orientation of $N72^{0}E/28/SE$ (Appendix V and Fig.4.7).

Moreover, intercalated with this rock unit there are different unmappable units such as agglomeratic basalt, vesicular basalt, plagioclase phyric basalt and unwelded tuff unit (See their photographs along with their description below).

Fig.3.6: Field photograph of Pyroxene-Olivine phyric basalt. Note its typical exfoliation weathering (0563066E: 1416734N).

3.2.1.1. Agglomeratic basalt

This rock unit is exposed in scattered (patchy) form and found mainly in Bekura ridge, Debri ridge, and in very small amount at around Hizba Maryam. Moreover, this rock unit is characterized by its pink to gray fresh color and light gray weathered color, and the presence of coarse rounded to sub rounded clasts with a size of about 10cm to 50cm (Fig.3.7).The clasts, which are dominantly dark colored, are hard/consolidated and pyroxene dominated. Besides, the rock hosting the clasts are dominantly reddish colored and pyroxene dominated. Mineralogically, this unit is principally composed of pyroxene and olivine. Like the mappable units of Ashenge formation, e.g. pyroxene-olivine phyric basalt, it is also characterized by its tilted nature with an orientation of $N60^0E/30/SE$.

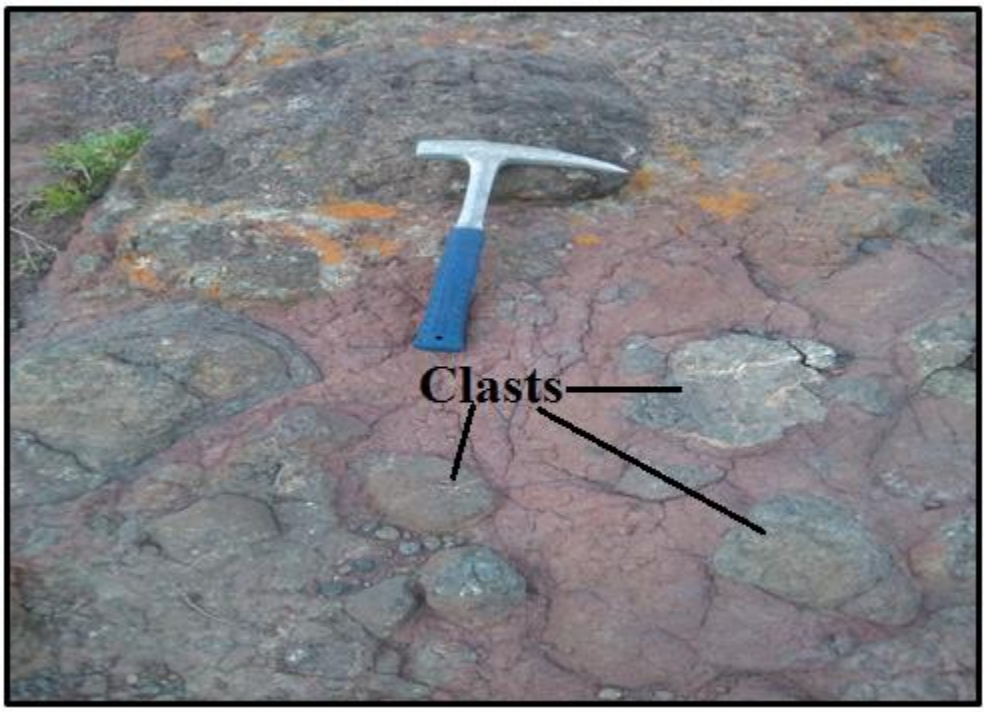

Fig.3.7: Field photograph of Agglomeratic basalt. Note coarse rounded to sub rounded shape clasts with a size of 1cm to 50cm (0557723E: 1415796N).

3.2.1.2. Vesicular basalt

This rock unit with an average thickness of about 10 m is mainly exposed around the northern, western, and south western part of the study area. In most parts of the study area this rock unit is characterized by its light brownish fresh color and gray weathered color, and it is composed of pyroxene with some olivine minerals. Furthermore, although it has dominantly a vesicular texture, in places amygdaloidal texture is also common (Fig.3.8), where the vesicles are filled by calcite and some green minerals (possibly malachite and

chalcedony). The shape of the vesicles ranges from spherical to elongate. Moreover, in the study area (e.g. in Belego Michael and Bolonta Giorgis), this rock unit is found near the top of pyroxene- olivine phyric basalt, marking the contact with the overlying basaltic unit (aphyric basalt of Aiba formation).

Fig.3.8: Field photograph of Vesicular basalt. Note its dominantly vesicular texture and partly amygdaloidal texture, and note also the green dot staining's (possibly malachite or chalcedony) (0562821E:1417327N).

3.2.1.3. Plagioclase phyric basalt

This rock unit is also found intercalated with pyroxene-olivine phyric basalt. Like vesicular basalt, in most part of the study area, it is found marking the contact between pyroxene-olivine phyric basalt and aphyric basalt of Aiba formation. It has porphyritic texture with dominant phenocrysts of plagioclase, and is characterized by its highly weathered and friable nature. Most of the plagioclase phenocrysts are elongated and randomly oriented (Fig.3.9)

Fig.3.9: Field photograph of Plagioclase phyric basalt. Note the white to gray elongated crystals of plagioclase (0557172E:1417098N).

3.2.1.4. Unwelded Tuff unit

This unit with an average thickness of 1m is found intercalated with pyroxene phyric basalt of Ashenge formation in Bekura Ridge. Furthermore, this unit is petrologically(field description) similar to the tuff unit of Alaje formation that overlain Aiba formation(e.g. around Belego Mikael and Bolonta Giorgis), which is characterized by its gray to brown fresh color and light gray weathered color, and its friable and unconsolidated nature, pyroclastic texture. In addition, this rock unit contains k feldspars, quartz and lithic fragments. However, unlike the tuff unit that overlain Aiba basalt, which has horizontal to sub horizontal alignment, it is tilted with an orientation of N46E/20^0/SE. Moreover, it is affected by closely spaced (about 10cm) systematic joints which have an orientation of N20W/55/SE.

Fig.4: Field photograph of unwelded tuff unit. Note the sub rounded to angular lithic fragments of this unit (0556986E: 1411951N).

3.2.2. Pyroxene phyric basalt

This basaltic unit is the second mapable unit of Ashenge formation in the study area, following pyroxene- olivine phyric basalt. It is majorly exposed around Bekura Ridge, Debri Ridge and Hizaba Ridge (Fig.3.1).Moreover, petrologically this rock unit resembles to aphyric basalt of Aiba Formation, which has aphyric texture, compact/massive and hard nature, cliff former topography. However, Pyroxene phyric basalt is characterized by its tilted nature unlike the horizontal to sub horizontal pattern of Aiba Formation. Like the other units of Ashenge Formation this rock unit is also characterized by its tilted, jointed and faulted nature. The mean orientation of this tilted lava flow layer and the associated joints is N67^{0}E/26/SE, N40W/61/NE respectively (Appendix V). In the field, this rock unit is characterized by its porphyritic texture with phenocrysts of dominantly pyroxene .However, petrographic examination (chapter four) indicates the presence of olivine and few plagioclase phenocrysts in addition to the dominant pyroxene phenocrysts. Further, this rock unit is also affected by an East -West striking and north dipping normal fault (Fig.4.6).

Fig.4.1: Field photograph of Pyroxene phyric basalt. Note its characteristics massive and consolidated nature, and note also the systematic joints which are intersected at about 90^0(0556772E:1413342N).

3.3. Aiba Formation

3.3.1. Aphyric basalt

This basaltic unit, which occurs between an elevation of around 2800m and 2900m, attains a maximum thickness of about 80m.In the study area; this rock unit is the only mappable unit that represents Aiba Formation. Furthermore, this unit comprises many horizontally stratified massive basaltic flows of 1-5 m thickness. Unlike the lava flows of Ashenge Formation, which are highly tilted and laterally limited, lava flows of Aiba Formation(aphyric basalt) are traceable and extend for at least tens or more kilometers. Moreover, the characteristics features of this unit are its black fresh color and light gray weathered color, aphyric texture, compact/massive and hard nature, cliff former topography. In the northern and western parts of the study area (around Bolonta Giorgis and Belego Michael) this rock unit is unconformably underlain by pyroxene-olivine phyric basaltic unit of Ashenge formation, and conformably overlain by unwelded tuff unit of Alaje Formation. The lower part of aphyric basalt is marked by laterally continuous reddish color and thin (about 1m thick) paleosol layers. Further, associated with this rock unit there are systematic joints which have an

average joint spacing of from 50cm to 1.5m, and the average orientation of these joints is $N50^0$ E/65/SE (Appendix V).

Fig.4.2: Panoramic view of Aiba Formation showing it's horizontally to sub horizontally layered lava flows. The photo is taken from western side of Kola Bolonta Abagabir (0562270E:1417482N).

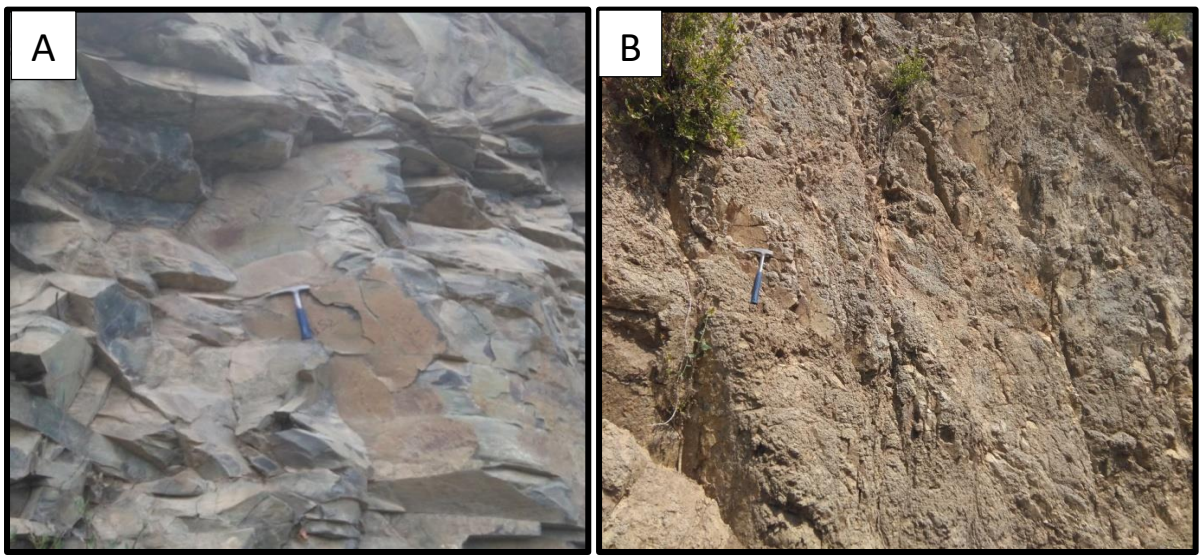

Fig. 4.3: Field photograph of aphyric basalt and the joint associated with it. (A) Aphyric basalt showing its hard/consolidated and massive nature (0562114E:1417907N). (B) Widely spaced (about 1m) systematic joints with an orientation of $N65^0W/68^0$/NE are affecting aphyric basalt (0558987E:1418651N).

3.4. Alaje Formation

3.4.1. Unwelded Tuff unit

In the study area, this unit is found around Bolonta Giorgis and Belego Michael. Further, it is found overlying the aphyric basalt of Aiba Formation. Petrologically (Field descriptions), this rock unit is generally similar to that of unwelded tuff unit that is found intercalated with Ashenge Formation (See section 3.2.1.4.). However, this unit has a horizontal to sub horizontal pattern nature rather than the tilted nature of Ashenge Formation. Further, like that of the other units of the study area, this rock unit is also affected by joints and faults which have an average orientation of generally $N20^0E/56/SE$ and $N37^0E$ /60/SE respectively.

Fig.4.4: Field photograph of unwelded tuff unit with its characteristic unconsolidated and friable nature. Note also the systematic joints affecting it (0561650E:1417549N).

3.4.2. Olivine Phyric basalt

This unit is found, in the study area, around Bolonta Giorgis (Fig.3.1).Stratigraphycally, olivine phyric basaltic unit is found overlaying the unwelded tuff unit of Alaje Formation. Further, this unit is characterized by its highly porphyritic texture with the dominant phenocrysts of olivine. In study area, this rock unit appears to have affected by exfoliation weathering like that of pyroxene-olivine phyric basalt of Ashenge Formation, and thus have a boulder forming appearance. In addition, this unit is found generally as gentle forming topography which could be related to its highly weathered and eroded nature.

Fig.4.5: Field photograph of Olivine phyric basalt. Note the Exfoliation weathering and the boulder forming appearance of this unit (0561670E:1417926N).

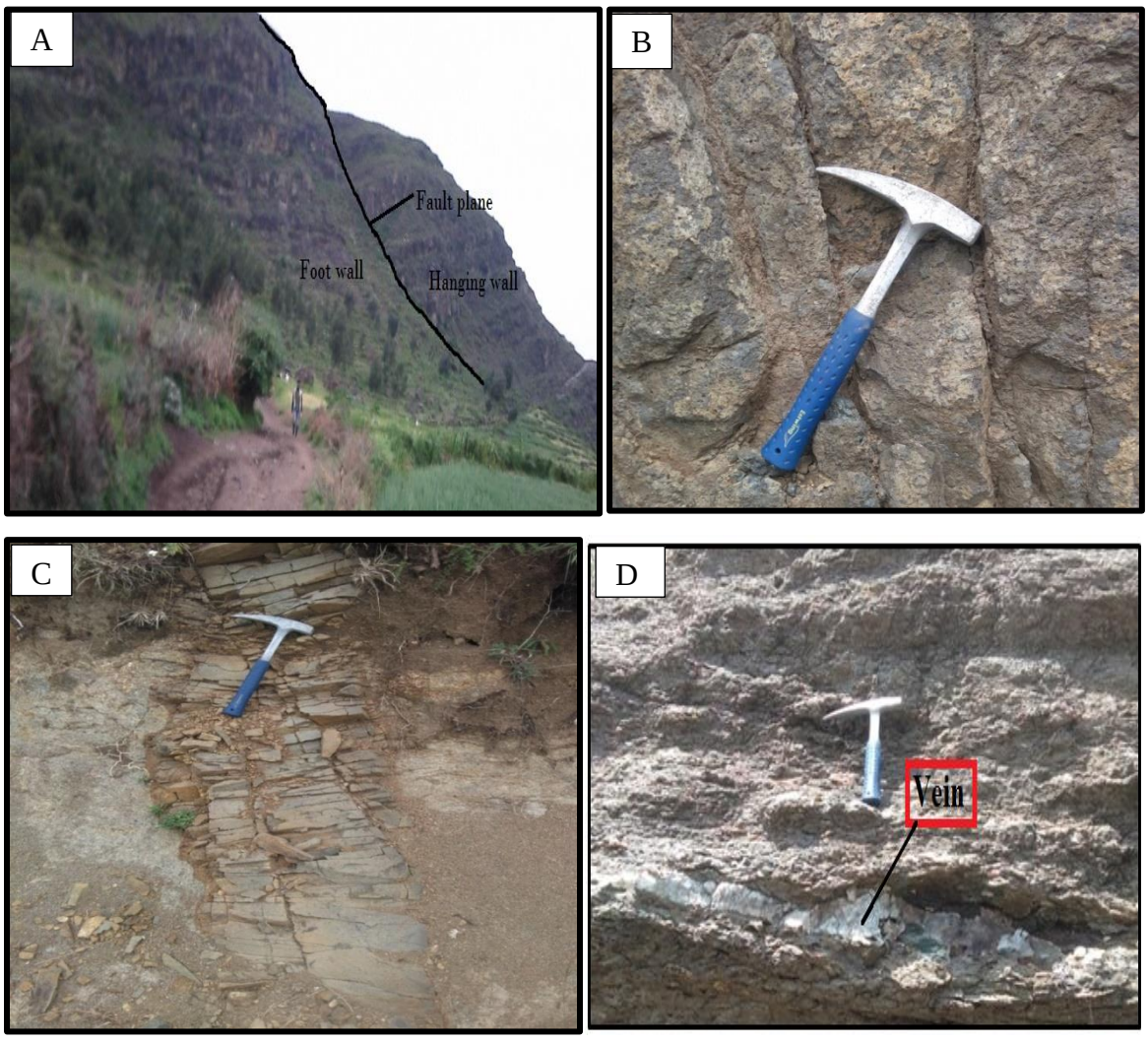

Fig.4.6: Field photograph of geological structures associated with Ashenge formation (A) East west striking and North-dipping (55°) normal fault on the pyroxene phyric basalt of Ashenge formation. The Photo is taken from western side of Maychew town, Bekura Ridge (0557588E, 139869N). (B) Closely spaced systematic joints (25cm-50cm) with an average strike direction of N22^{0}W are affecting the pyroxene–olivine phyric basalt (0555749E:1415102N). (C)N30^{0}W striking basaltic dike cutting the pyroxene-olivine phyric basalt (557588E, 139869N).The dike has aphyric texture and compacted nature, and attains a thickness of about 1 m. (D) Quartz vein associated with pyroxene-olivine phyric basalt of Ashenge formation with an orientation of N20E/40/NW (0559471E:1415303N).

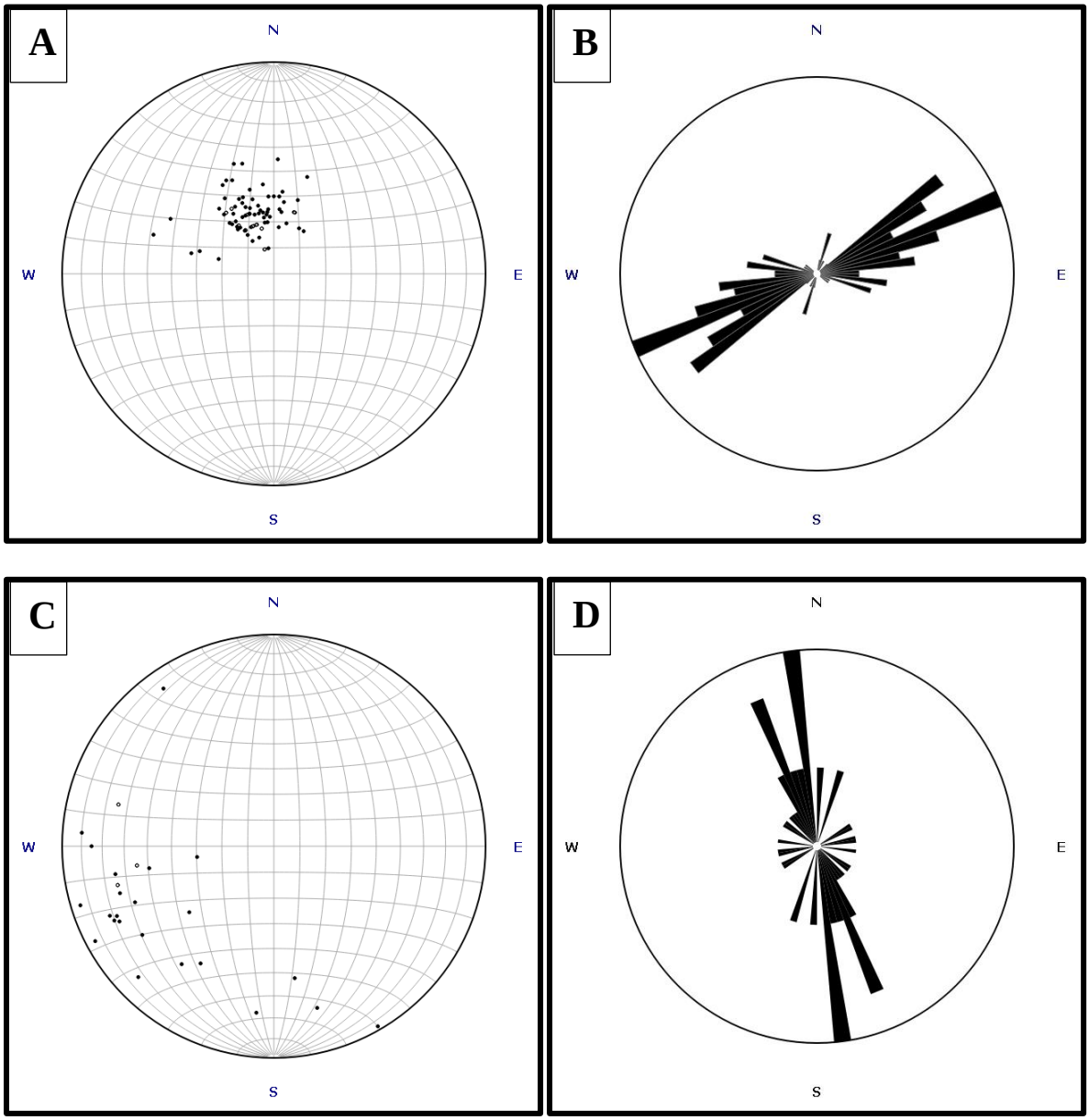

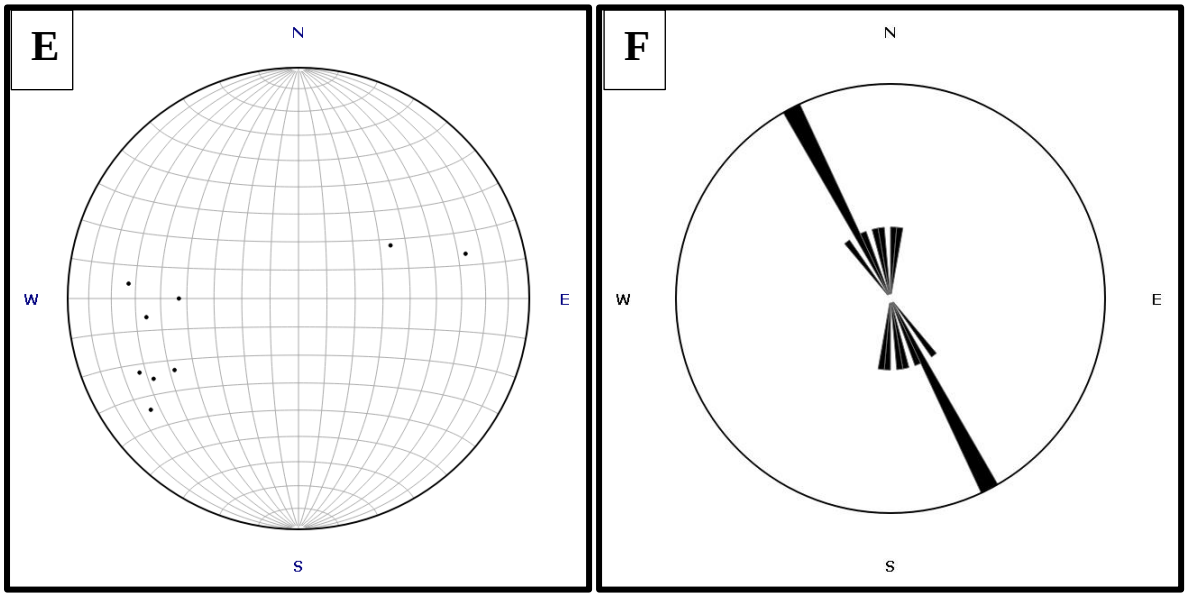

Fig.4.7: Stereonet plots of the tilted lava flows, joints and dikes. (A) Equal area plots of the tilted lava flows (for both Pyroxene - olivine phyric and pyroxene phyric basalts). Poles to the tilted lava flows are generally clustered on the NW quadrant of the stereonet with some scattered plots. This indicates that the tilted beds (lava flows) are dipping towards SE. (B) Rose diagram of the tilted lava flows: The longest wedge of the rose diagram represents N65^0-70^{0}E and this value indicates that the mean value of the strike direction of the tilted beds of Ashenge formation. (C)Equal area plot of the joints showing the scatter distribution of the poles majorly on the SW quadrant of the stereonet and this could be as the result of the existence of different sets of joints dipping towards NE. (D) Rose diagram plot showing two sets of joints where one set of the joint system is represented by an average strike direction of N5^0-10^{0}W whereas the second joint set have an average strike direction of N20^0 - 25^{0}W. (E) Equal area stereonet plot of the dikes. The poles to dikes are clustered on the SW quadrant with few scatters and this shows that the dikes are dipping towards NE. (F) Rose diagram of the dikes: The longest wedge of the rose diagram represents N25^0-30^{0}W, which indicates mean value of the strike direction of the associated dikes.

CHAPTER FOUR

PETROGRAPHIC STUDY OF THE STUDY AREA

4.1. Introduction

To further characterize the petrogenetic history of the two basaltic units in the study area, 16 thin sections from representative rock samples have been prepared and examined. Out of this thin section 12 are from Ashenge formation (pyroxene-olivine phyric basalt and pyroxene phyric basalt) whereas the rest (4) are from Aiba basalts. The studied samples are selected based on their stratigraphic position and/or field description. The observed textures of most samples include porphyritic, glomerophyric, sub-ophitic, seriate and rarely poikilitic. Aiba basalts (aphyric basalt) are generally characterized by their aphyric to sparsly porphyritic texture with phenocrysts of dominantly plagioclase. However, the lava flows of Ashenge Formation (pyroxene phyric and pyroxene-olivine phyric basalts) are characterized by their highly porphyritic textures with phenocrysts of clinopyroxene, plagioclase and olivine embedded in a fine-grained matrix of plagioclase, opaque minerals and to a lesser extent clinopyroxene and olivine. Plagioclase crystals in some flows (aphyric basalt) generally exhibit trachytic textures, but in the majority of samples (pyroxene phyric and pyroxene-olivine phyric basalt) the crystals are randomly aligned. Phenocrysts proportion of the studied samples range from 0–5 vol. % (aphyric basalt) through 25 vol. % (pyroxene phyric basalt) to 35-40 vol. % (pyroxene-olivine phyric basalt). Most of the phenocrysts in both Ashenge and Aiba basalts are euhedral in shape whereas the interstitial materials are anhedral. Detailed petrographic description for each basaltic unit/formation is given below:

4.2. Ashenge Formation

Petrographically, it is characterized by its porphyritic texture with a phenocrysts of principally clinopyroxene, little olivine and plagioclase. The proportion of the phenocrysts is about 30-35 % by volume. The groundmass is dominated by plagioclase with considerable amount of clinopyroxene and olivine and few opaque minerals. Furthermore, euhedral clinopyroxene, olivine and plagioclase phenocrysts, up to 5 mm diameter, are abundant 15–25 vol %(Fig.4.1). However, there is also subhedral/anhedral phenocrysts of these minerals associated with this basaltic formation. The samples from this formation are mostly glomerophyric (plagioclase/clinopyroxene, plagioclase plus clinopyroxene and/or olivine), and some rarely aphyric. The presence of colorless to pale green fibrous minerals with

moderate birefringence as an amygdule (possibly zeolite), reddish brown high birefringence mineral (iddingsite, altered olivine), partly to wholly altered clinopyroxene crystals, zeolite and quartz filled vein (Fig.4.1) indicates that this basaltic unit have undergone an alteration process, consistent with its lithological description. The detailed petrographic description for each lithological unit of this formation is given below:

4.2.1. Pyroxene-Olivine phyric basalt

Petrographically, this rock unit is characterized by its highly porphyritic texture with phenocrysts of clinopyroxene, olivine and plagioclase set in intergranular and intersertal textured groundmass of the same mineral assemblage as the phenocrysts with some oxides. From the studied samples the proportion of the phenocrysts ranges from 35-40 vol %. The modal composition of this rock unit is dominated by clinopyroxene, followed by olivine and plagioclase. Furthermore, very few scattered opaque minerals also present both in the groundmass and phenocrysts assemblage. Besides, the phenocrysts, in some samples, shows seriated texture i.e. they shows a wide range of grain size from fine grained (1mm) up to coarse grained (5mm). Most of the phenocrysts, particularly clinopyroxene and olivine, are found showing compositional zoning.

In places, olivine phenocrysts show hexagonal euhedral shape with irregular cracks and slight iddingsite alteration along the cracks. Furthermore, scarce iddingsitised olivine phenocrysts are also present in these basalts. Moreover, clinopyroxene occurs as euhedral, elongated variegated color (dominantly pinkish) phenocrysts which are partially embayed and resorbed. Besides, in places, olivine and clinopyroxene occur together as glomerocysts. Opaque minerals are also included in some clinopyroxene phenocrysts. For a complete petrographic description of the samples, see appendix VI and Fig. 4.1.

4.2.2. Pyroxene phyric basalt

Petrographic examination of this rock unit indicates that, with the exception of one sample (T4S3, which has aphyric texture), it is porphyritic texture with phenocrysts of principally clinopyroxene, olivine and very few opaque minerals. Although the proportion of phenocrysts for pyroxene phyric basalt (about 25 vol %) is less than that of pyroxene-olivine phyric basalt (about 35-40 vol %), it is much higher than aphyric basalt of Aiba Formation (0-10 vol. %). Like phenocrysts of pyroxene-olivine phyric basalts, the phenocrysts of pyroxene phyric basalts are glomeophyric, and are mostly euhedral to subhedral in shape. Pyroxene phyric basalt is different from pyroxene-olivine phyric basalt in that it lacks plagioclase phenocrysts, which exists in pyroxene-olivine phyric basalt both as a phenocrysts and groundmass. Further, the groundmass of pyroxene phyric basalt is much glassy than pyroxene-olivine phyric basalt. Moreover, thin section analysis of this unit shows signs of alteration which is evidenced by the presence of partly and wholly altered clinopyroxene crystals, and zeolite and quartz filled vein (Fig.4.2) Its modal proportion is principally dominated by clinopyroxene with very few olivine and opaque minerals. For a complete petrographic description of the samples, see appendix VI and Fig. 4.1.

4.3. Aiba Formation

4.3.1. Aphyric basalt

From petrographic study, this rock unit is characterized by its aphyric to sparsely porphyritic texture with micro to mega phenocrysts of dominantly plagioclase (8-10 vol %), and very few clinopyroxene (2-5 vol %) and olivine (< 2 vol %). These phenocrysts are set in a pilotaxitic groundmass of predominantly plagioclase microlites, clinopyroxene, Fe-Ti oxides and glass. The interstices between the plagioclase laths in the groundmass are filled by clinopyroxene and partly olivine (i.e. they show intergranular texture).The plagioclase phenocrysts in the phenocryst assemblage are randomly oriented whereas, in places, they show trachytic texture. Further, plagioclase phenocrysts are elongated and euhedral shaped, and show concentric zoning. Like the other units of Ashenge basalts the phenocrysts of aphyric basalt have partly glomerophyric texture but their abundance is very small (up to 4 vol. %).Moreover, the proportion of the phenocrysts ranges from 0 to 5%, of which plagioclase is about 95% and clinopyroxene is about 5%. For a complete petrographic description of the samples, see appendix VI and Fig.4.2.

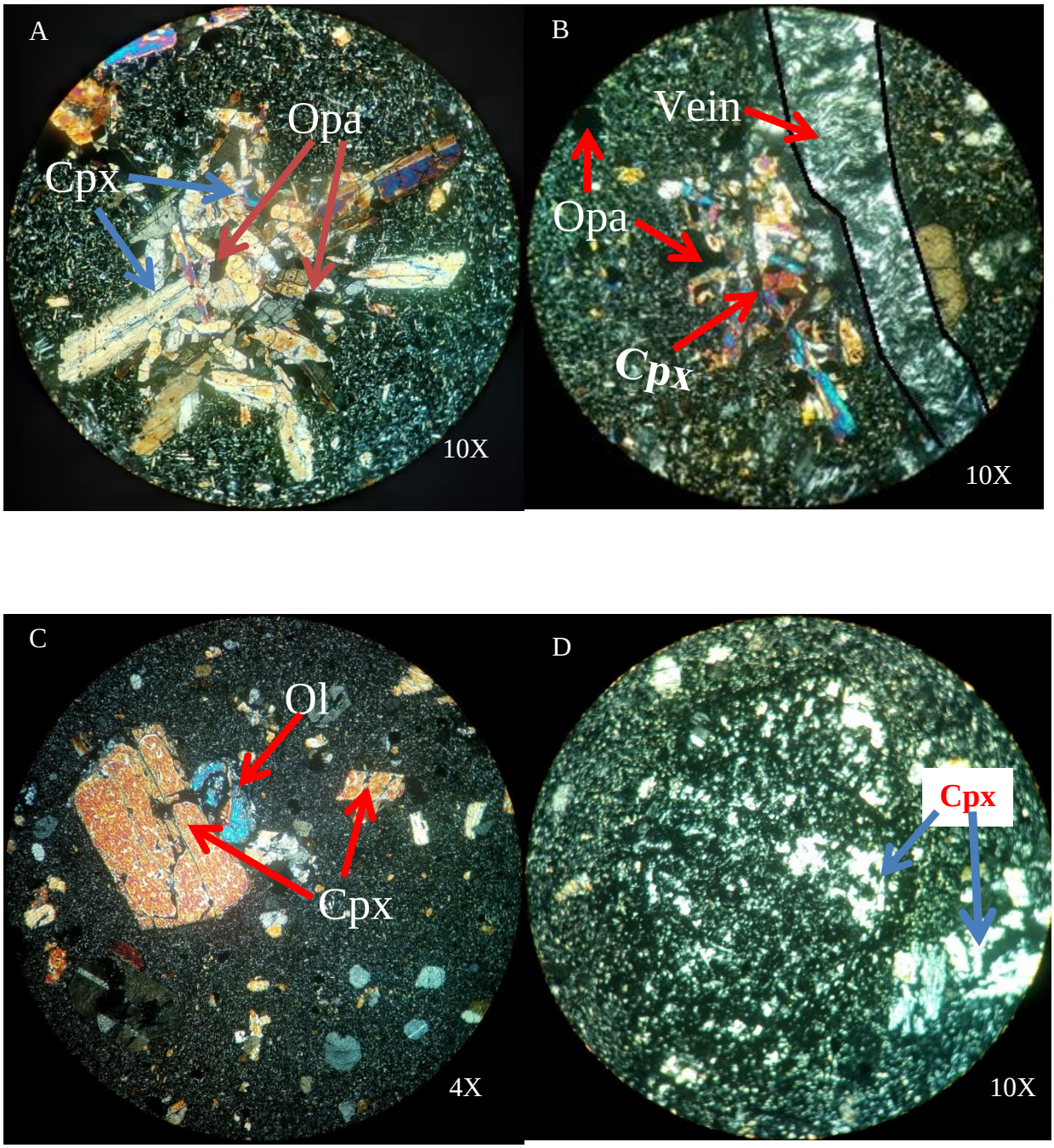
A
Opa
Cpx
10X
B
Vein
Opa
Cpx
10X
C
Ol
Cpx
4X
D
Cpx
10X

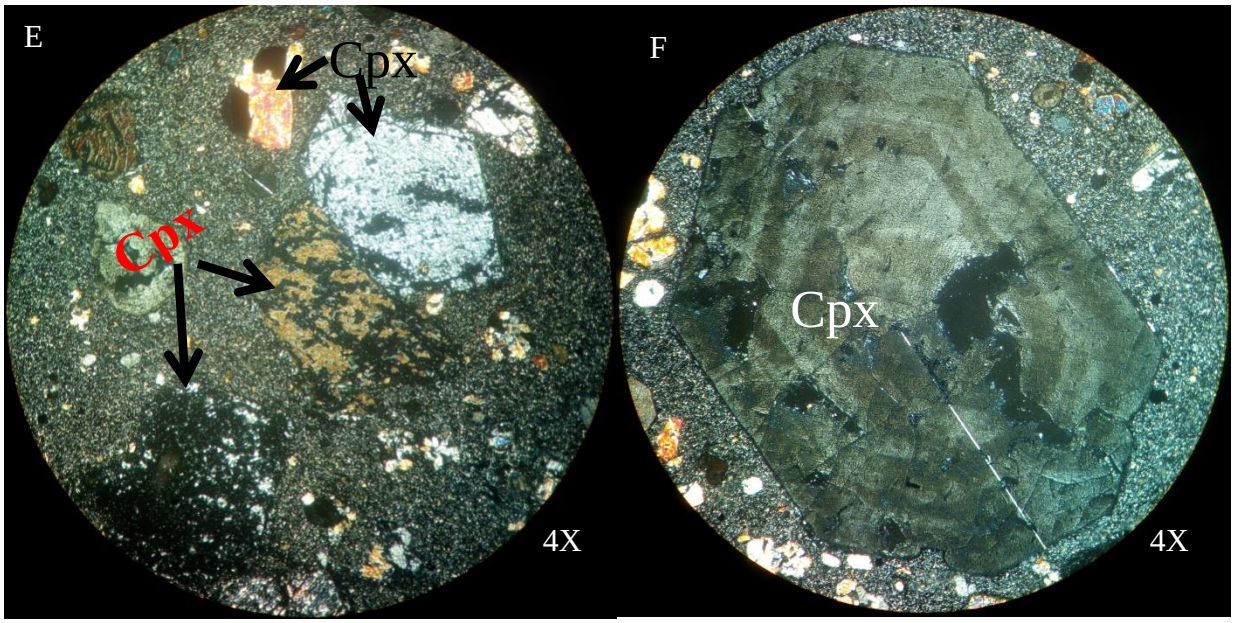
E
Cpx
Cpx
4X
F
Cpx
4X

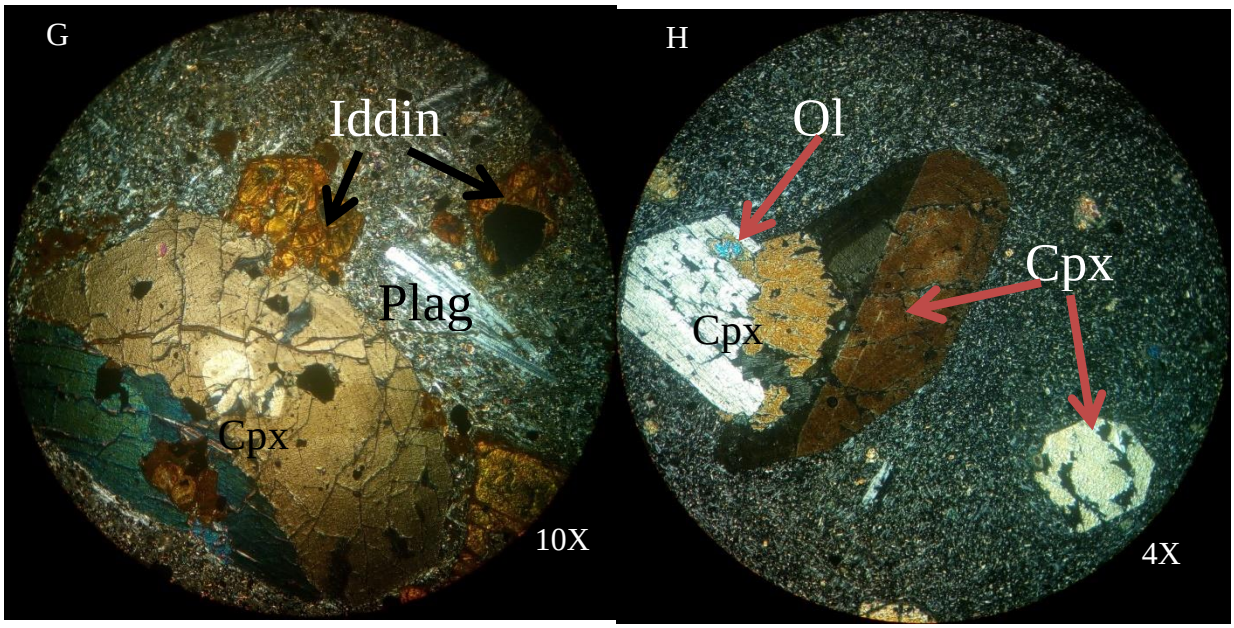
G
Iddin
Plag
Cpx
10X
H
Ol
Cpx
Cpx
4X

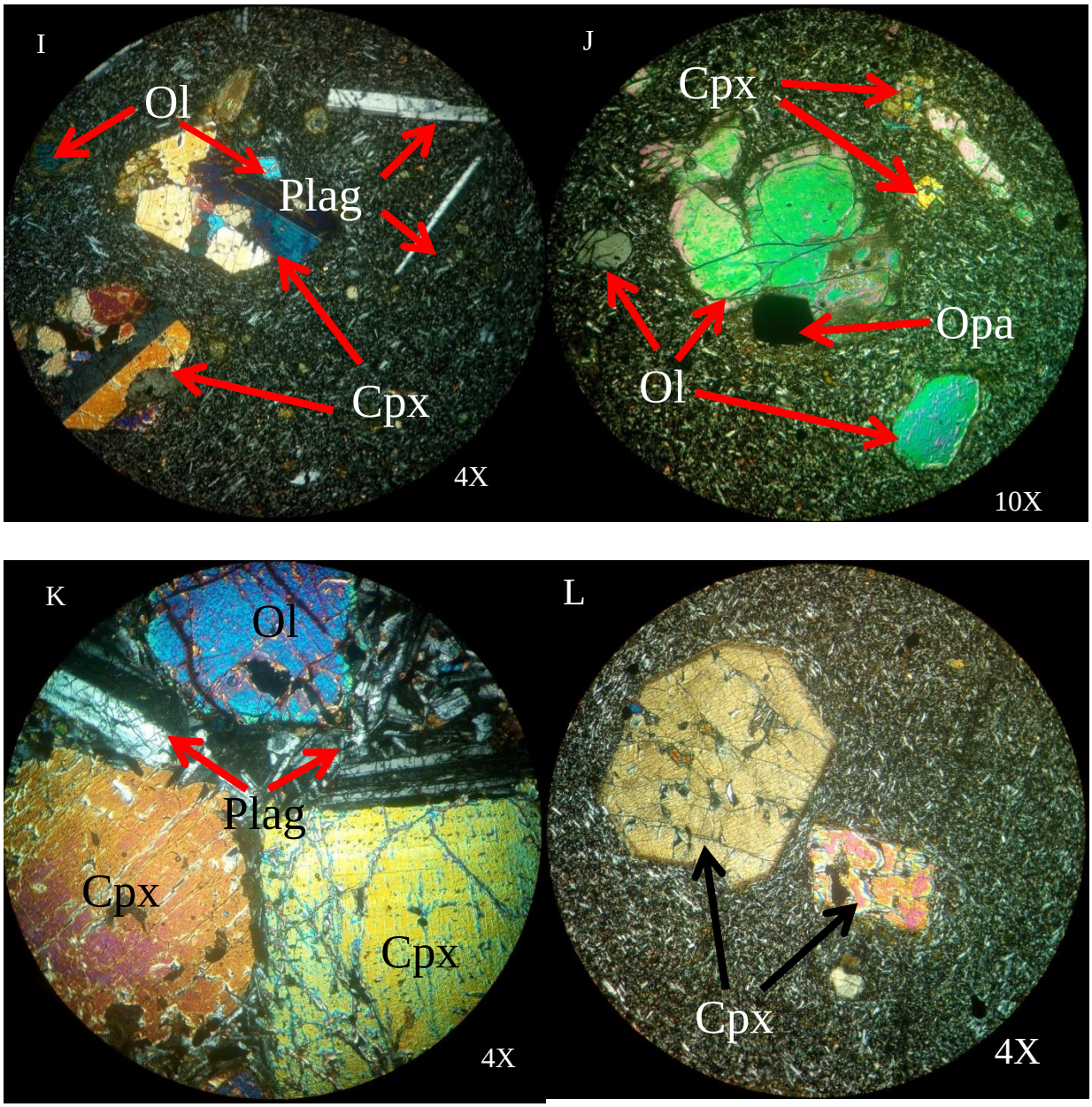

Fig.4.1 (A-L): Microscopic photo-pictures of Ashenge Basalts. (A)Glomerophyric textured phenocrysts of clinopyroxene, olivine and some opaque (probably Fe-Ti oxides) are embedded in a glassy groundmass. (B) Vein which are filled by quartz and zeolite (showing radial pattern) minerals. Note also the clusters of clinopyroxene phenocrysts, and the presence of anhedral shape opaque minerals both in the groundmass and phenocrysts assemblage.(C) Phenocrysts of clinopyroxene (showing brownish color and seriate texture) and olivine minerals are set in cryptocrystalline textured groundmass.(D) pentagonal euhedral shaped altered phenocryst of clinopyroxene is set in intersertal textured plagioclase dominated groundmass. (E) Partly to wholly altered subhedral to euhedral shaped clinopyroxene phenocryst is set in a glassy groundmass. Note also the glomereoporphyritic nature of clinopyroxene phenocryst (on the bottom right side of the thin section photo). (F) Low interference colored euhedral shaped

megacrysts of clinopyroxene is set in microcrystalline -textured groundmass. Note also the vesicles within this crystal (irregular dark appearance under XPL whereas light appearance under PPL). (G) Phenocrysts of clinopyroxene, plagioclase, and iddingsite (reddish brown coloured altered olivine) are embedded in interstitial textured plagioclase dominated groundmass. Note also the resorbed olivine (bottom right of the photograph, dark appearance). (H) Euhedral shaped megacrysts of clinopyroxene are set in brownish colored glassy material rich groundmass. Note also the cumlophyric nature of the phenocrysts, and zoning of clinopyroxene crystal. (I) Sub to euhedral shaped glomerophyric textured clinopyroxene and light gray colored plagioclase laths are embedded in a groundmass of dominantly fine grained plagioclase laths and some reddish brown interstitial glassy material. (J) Phenocrysts of subhedral to euhedral olivine, euhedral clinopyroxene and opaque minerals are embedded in a groundmass of dominantly light gray elongated plagioclase crystals. (K) Megacrysts of clinopyroxene, plagioclase and olivine are set in a medium to coarse grained plagioclase lath dominated by interstitial textured groundmass.(L) Tabular to prismatic euhedral shaped phenocrysts of clinopyroxene is set in a plagioclase dominated microcrystalline groundmass. Note also the flow of plagioclase crystals arround the clinopyroxene phenocryst ***Note that all the photographs taken are under XPL only. Microscopic photo-pictures from A to F are from Pyroxene phyric basalt ,whereas from G to L are from pyroxene-olivine phyric basalts.*** *From all the thin section photos (A to F) note the absence of plagioclase phenocrysts, the glomereoporphyritic nature and alteration of some of the clinopyroxene phenocrysts.*

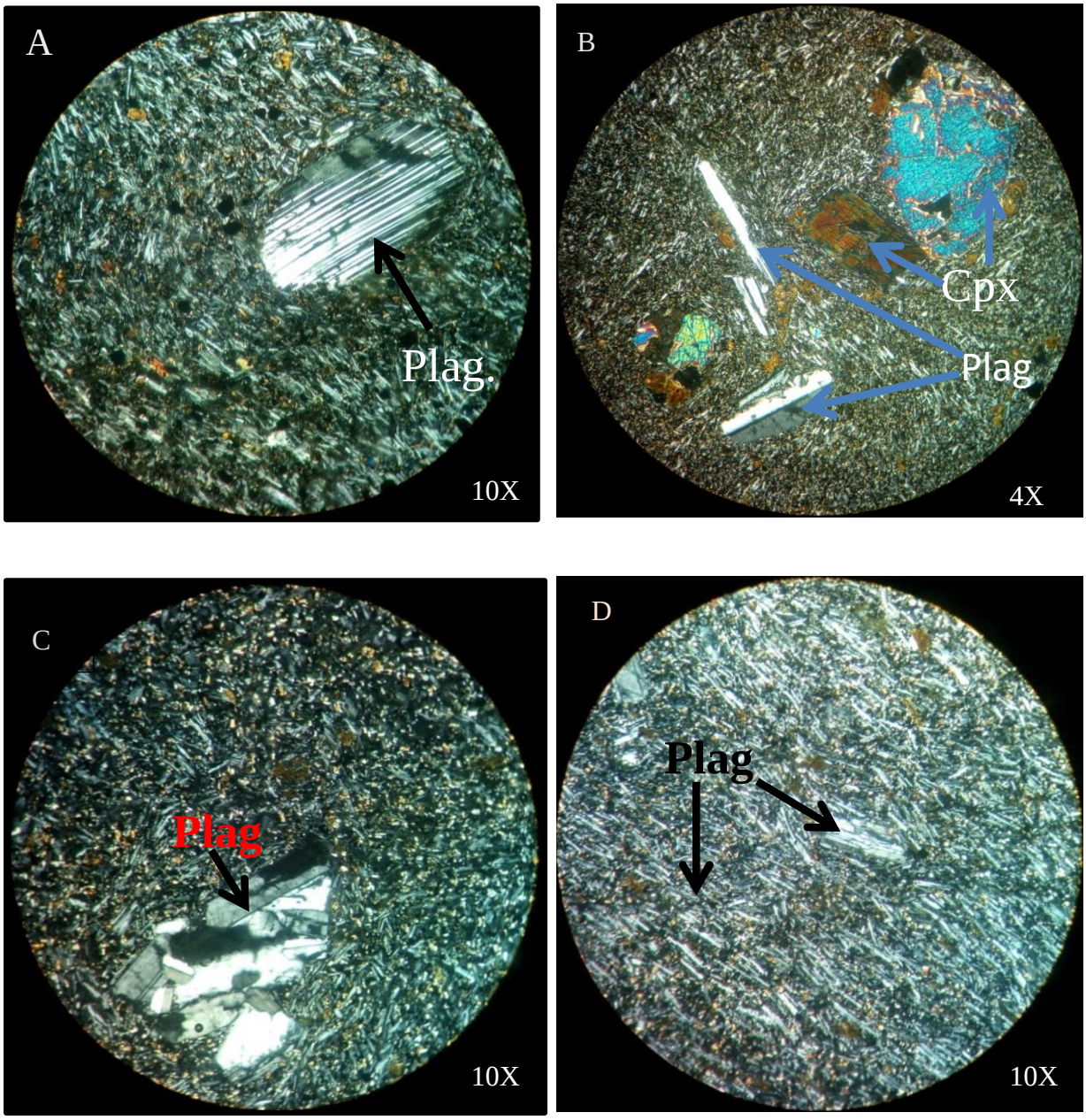
A
Plag.
10X
B
Cpx
Plag
4X
C
Plag
10X
D
Plag
10X

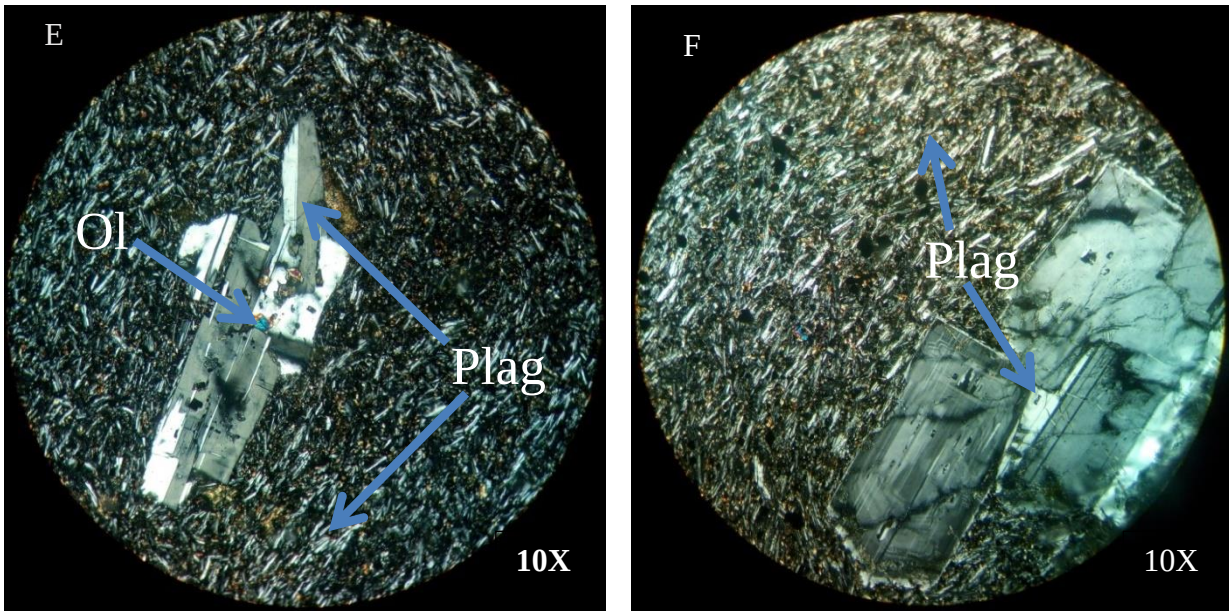

Fig.4.2 (A-F): Microscopic photo-pictures of Aiba Basalts (aphyric basalt). (A) Micro phenocryst of plagioclase crystal showing its diagnostic polysynthethic twining is set in a plagioclase dominated microcrystalline groundmass. Note also the interstitial textured groundmass wherein the interstices between plagioclase laths are filled by olivine and redish brown colored glassy minerals (possibly cpx).Further,note also the plagioclase phenocrysts have euhedral crystal form.(B)Subhedral to euhedral shaped phenocrysts of clinopyroxene,olivine and plagioclase are set in plagioclase plagioclase dominated groundmass.(C) glomerophyric textured phenocrysts of plagioclase are set in intersertal textured groundmass where the interstices between the plagioclase laths are filled by redish brown glassy minerals,and dark colored opaque minerals.(D) This thin section shows trachytic texture where plagioclase laths are arrenged in a well defined manner.(E) Megacryst of elongated plagioclase crystals are embeded in fine grained plagioclase rich groundmass. Further, note the flow of the plagioclase laths of the groundmass suurounding the megacryst of plagioclase. Note also the inclusion of clinopyroxene within megacryst of plagioclase (i.e. poiklitic texture). (F) Phenocryst of euhedral and elongated plagioclase crystals are embeded in intersertal textured plagioclase(light gray elongated minerals) and opaque mierals(anhedral dark minerals;possibly Fe-Ti oxides) dominated groundmass. Note also the cumulophyric nature and concentric zonnig of the plagioclase phenocryst.

CHAPTER FIVE

WHOLE ROCK GEOCHEMISTRY

5.1. Introduction

A total of 12 fresh samples were selected for whole-rock geo-chemical analyses from Maychew flood basalts based on their stratigraphic position and/or field description as well as their petrographic examination. The sample preparation has been carried out under ALS services in Addis Ababa, Ethiopia, particularly; in Nifas silk Sub city, Wereda 09, House No.1659 crushing and milling room. The sealed and packed powdered samples were submitted to the Australian Laboratory Science (ALS), Ireland, in order to determine the concentration of major and trace elements. Major elements and trace elements were analyzed by Inductively Coupled Plasma Atomic Emission Spectrometry (ICP-AES) and Inductively Coupled Plasma Mass spectrometry 81(ICP-MS) respectively. Besides, multi element four acid digestions 81(ME-4ACD81) were used for base metal determinations such as Cr, Co, Ni. In addition, loss on ignition (LOI) at 1000^0 C is determined by an instrument WST-SEQ. The analytical results for both major and trace elements are presented in table 5.1. Accordingly, the analyzed samples have low LOI (loss on ignition) value ranging from 0.69-3.07 and this indicates the samples are fresh and unaltered. However, the LOI values (0.81-3.07) for Ashenge basalts are higher than that of Aiba basalts which have LOI values of ranging between 0.69-1.4. To use the analyzed geochemical data(trace and major elements as well as loss on ignition) for the purpose of this research work, the data have been integrated and exercised through different software packages such as Microsoft excel 2007, petrographic 2 beta(version 1.0.2) and geochemical data kit (GCDKit version 3.2.0). In particular, petrographic 2 beta and GCDKit software have been used to construct classification diagrams (TAS), REE spider plot and multi element variation diagram along with various major and trace element variation diagrams. Further, Microsoft excel 2007 were used to compute the values of some selected trace element ratios. All diagrams, descriptions and interpretation of major elements are according to the recalculated (volatile free basis) results presented in Appendix I.

Table 5.1.Major (wt. %) and trace (ppm) element analyses for Ashenge and Aiba formations, Maychew, Tigray, Northern Ethiopia.

	Aiba formation			Ashenge Formation								
	Aphyric Basalt			Pyroxene-olivine phyric Basalt						Pyroxene phyric Basalt		
Sample	T1S2	T1S3	T6S3	T3S17	T2S8	T3S6	T5S1	T4S13	T7S9	T4S3	T4018	T7
SiO_2	54.5	51.1	49.2	46.8	45.5	46.9	45.4	46	47.3	46.4	45.5	42.8
TiO_2	3	3.27	3.54	4.48	3.78	3.35	3.63	3.56	3.55	3.75	4.31	4.08
Al_2O_3	14.85	14.5	14.4	12	9.24	10.75	10.9	10.7	11.95	14	7.37	10.55
Fe_2O_3	10.45	12.85	13.05	14.3	14.1	13.4	13.6	13.75	13.25	13.45	14.05	16.25
MnO	0.15	0.19	0.19	0.19	0.18	0.18	0.19	0.2	0.16	0.23	0.17	0.26
MgO	3.82	4.99	5.24	6.46	13.15	8.04	9.1	9.86	6.36	4.12	12.85	5.92
CaO	7.4	8.14	9.43	9.46	9.09	10.1	10.55	10.75	8.7	8.26	9.9	12.35
Na_2O	2.99	2.95	2.93	2.45	1.82	2.32	2.06	2.17	2.93	2.99	2.1	1.95
K_2O	1.99	1.08	1.03	1.23	1	1.13	1.1	1.12	1.76	2.47	0.98	1.94
P_2O_5	0.37	0.45	0.45	0.53	0.4	0.45	0.46	0.45	0.59	0.82	0.5	0.79
LOl	0.88	1.4	0.69	1.57	0.81	1.99	2.08	1.97	2.93	1.37	0.97	3.07
Total	100.4	100.92	100.15	99.47	99.07	98.61	99.07	100.53	99.48	97.86	98.7	99.96
CaO/Al_2O_3	0.5	0.56	0.66	0.79	0.98	0.94	0.97	1.01	0.73	0.59	1.34	1.17
Mg#	42.23	43.71	44.54	47.47	65.1	54.55	57.23	58.92	48.98	37.99	64.65	42.15
Sc	21	21	26	25	26	30	31	31	22	17	29	28
V	324	369	373	411	368	381	389	385	357	305	398	512
Cr	30	80	30	210	780	350	480	600	450	<10	1110	20
Co	25	36	41	47	67	51	53	53	52	34	65	57
Ni	6	31	33	130	542	75	86	99	153	5	446	38
Rb	44.1	11.3	15.9	15.7	19.3	21.3	19.2	21.2	34.5	47.1	16.8	40.9
Sr	513	563	587	629	484	648	750	829	724	980	463	1250
Y	31.5	34.3	37	36.2	29.4	27.1	23.9	24.1	28.7	36.6	32.2	28.5
Zr	271	252	286	386	308	312	278	280	364	431	385	384
Nb	24.9	26.5	28.6	45.7	38.4	42.6	44.5	45	64	83.8	41.8	102

Cs	0.51	0.17	0.11	0.06	0.33	0.21	0.22	0.24	0.4	0.3	2.26	0.6
Ba	450	364	273	307	202	315	298	317	544	561	194.5	672
La	33.2	31.5	27.3	39.3	30.7	35.2	35.6	36.4	54.1	69.7	33.8	77.7
Ce	70.8	64.7	62.5	89.9	69.7	78.7	80.8	81.3	116	150	79	157.5
Pr	9.52	9.14	8.94	11.95	9.6	10.7	10.75	10.8	14.65	19.3	11.15	19.4
Nd	41.6	42.9	38.8	55	43.9	47.4	46.4	46.7	63.5	81.2	54	77.9
Sm	8.63	9.33	9.02	11.35	9.51	9.07	9.6	9.3	11.1	14.45	12.35	13.8
Eu	2.34	2.67	2.91	3.52	2.81	3.04	2.75	2.87	3.1	4.36	3.36	3.65
Gd	7.67	8.29	8.82	10	8.43	7.93	7.41	7.46	8.85	11.65	10.55	9.62
Tb	1.1	1.17	1.3	1.45	1.19	1.1	0.98	0.96	1.1	1.49	1.39	1.26
Dy	6.3	6.6	7.73	7.39	6.13	5.8	5.17	5.44	6.08	8.2	7.47	6.3
Ho	1.14	1.31	1.5	1.39	1.15	1.07	0.97	0.93	1.11	1.49	1.23	1.14
Er	3.06	3.05	3.81	3.41	2.74	2.41	2.09	2.2	2.69	3.72	3.02	2.77
Tm	0.45	0.41	0.5	0.46	0.35	0.32	0.29	0.26	0.39	0.51	0.35	0.34
Yb	2.57	2.49	3.04	2.76	2.22	1.89	1.73	1.69	2.2	2.88	2.09	2.03
Lu	0.38	0.35	0.43	0.35	0.3	0.23	0.23	0.2	0.28	0.4	0.28	0.27
Hf	5.9	6	6.7	9	7.5	6.9	7	6.6	8.5	10.2	9.3	9
Ta	1.3	1.3	1.3	2.4	1.7	1.9	1.9	1.7	2.7	4	10.2	5
Pb	7	7	3	11	6	<2	9	<2	13	8	7	6
Th	5.21	4.01	2.5	4.45	3.17	3.42	3.33	3.26	5.23	7.35	3.15	8.76
U	1.19	0.81	0.72	1.48	0.88	0.94	0.98	0.9	1.43	2.41	0.88	1.62
ΣREE	188.8	183.91	176.6	238.2	188.7	204.9	204.77	206.51	285.2	369.4	220.	373.9
(La/Yb)N	8.61	8.43	5.99	9.49	9.22	12.42	13.72	14.36	16.39	16.13	10.78	25.52
(La/Sm)N	2.37	2.08	1.86	2.13	1.99	2.39	2.28	2.41	3	2.97	1.68	3.46
(Gd/Yb)N	2.38	2.65	2.31	2.89	3.03	3.35	3.42	3.52	3.21	3.23	4.02	3.78
(Eu/Yb)N	2.6	3.06	2.73	3.64	3.62	4.6	4.54	4.85	4.03	4.33	4.59	5.14
Eu/Eu*	0.88	0.93	1	1.02	0.96	1.1	1	1.06	0.96	1.03	0.9	0.97

N-denotes that the concentration is normalized to the chondrite abundance. Total iron is as Fe_2O_3. Mg# (Wager and Deer, 1939) = {(MgO/40)/ (MgO/40+ Fe_2O_3/80)}*100

Table 5.2: Incompatible trace element ratios of Ashenge and Aiba flood basalts from Maychew area.

	Aiba formation			Ashenge formation								
	Aphyric Basalt			Pyroxene-olivine phyric Basalt						Pyroxene phyric Basalt		
Sample	T1S2	T1S3	T6S3	T3S17	T2S8	T3S6	T5S1	T4S13	T7S9	T4S3	T4018	T7
Zr/Nb	10.88	9.51	10	8.45	8.02	7.32	6.25	6.22	5.69	5.14	9.21	3.77
Zr/Ce	3.83	3.9	4.56	4.29	4.42	3.96	3.44	3.44	3.14	2.87	4.87	2.44
Hf/La	0.18	0.19	0.25	0.23	0.25	0.2	0.2	0.18	0.16	0.15	0.28	0.12
La/Nb	1.33	1.89	0.96	0.86	0.8	0.83	0.8	0.81	0.85	0.83	0.81	0.76
La/Ta	25.54	24.23	21	16.34	18.06	18.53	18.74	21.41	20.04	17.43	3.31	15.54
Rb/Nb	1.77	0.43	0.56	0.34	0.5	0.5	0.43	0.47	0.54	0.56	0.40	0.40
Th/Ta	4.01	3.09	1.92	1.85	1.86	1.8	1.75	1.92	1.94	1.84	0.31	1.75
Th/Nb	0.21	0.15	0.09	0.1	0.08	0.08	0.08	0.07	0.08	0.09	0.08	0.09
Ce/Pb	10.12	9.24	20.83	8.17	11.62	39.35	8.98	40.65	8.92	18.75	11.29	26.25
Nb/U	20.92	32.72	39.72	30.88	43.64	45.32	45.41	50	44.76	34.78	47.5	62.96
Ba/La	13.55	11.56	10	7.81	6.58	8.95	8.37	8.71	10.06	8.05	5.75	10.06
Ba/Nb	18.07	13.74	9.55	6.72	5.26	7.39	6.7	7.04	8.5	6.7	4.65	6.59
La/Yb	12.92	12.65	8.98	14.24	13.83	18.62	20.58	21.54	24.59	24.20	16.17	38.28
Tb/Yb	0.43	0.47	0.43	0.53	0.54	0.58	0.57	0.57	0.5	0.52	0.67	0.62

5.2. Major Element Geochemistry

Major and trace element data for the Maychew flood basalts is reported in Table 5.1. Although there are some overlaps, both Ashenge and Aiba basalt are characterized by their different major element concentrations and ratios. Aiba basalts, relative to Ashenge basalts, have higher concentration of Al_2O_3, SiO_2 and Na_2O but lower concentration of TiO_2, Fe_2O_3, CaO and P_2O_5.Further,the studied samples have a CaO/Al_2O_3 value ranging from 0.5-1.34,being higher for Ashenge basalts(0.59-1.34) and lower for Aiba basalts(0.5-0.66).Two samples from pyroxene phyric basalt of Ashenge formation (T4O18, T2S8) have anomalously high MgO content; 13.15 wt. % for T2S8 and 12.85 for T4O18.The studied samples, excluding the two anomalously high MgO samples (T4O18, T2S8), have MgO contents ranging from 3.82 to 9.86 wt. % and mg # of between 37.99 and 58.92. In particular, Ashenge basalts, excluding the two samples, have MgO content and mg# ranging from 4.12-

9.86wt. % and 37.99-58.92 respectively. In contrast, Aiba basalts have MgO content and mg# that ranges from 3.82-5.24 and 42.23-44.54 respectively. For comparison, some selected major and trace element data of the three basaltic types (LT, HT1and HT2) from northwestern plateau are presented in appendix III. Accordingly, samples of Ashenge basalts have geochemical characteristics similar to HT2 basalts whereas samples of Aiba basalts have a geochemical affinity similar to HT1 basalts.

On the TAS diagram (Fig.5.1), the studied samples are dominated by basaltic compositions, and are majorly plotted at the boundary between alkaline and sub alkaline/tholeiite field with some scattered plots, indicating their general transitional basalt affinity. In support of this, in the $Na_2O + K_2O$ vs. SiO_2 diagram (Fig.5.2), most of them are plotted in the transitional field of Ethiopian lavas (Peccirillo et al., 1979). However, the two anomalously high MgO samples (T4O18 and T2S8) have an alkaline affinity. Further, based on CIPW norm composition (Appendix II), all samples are quartz and hypersthene normative excluding the two high MgO samples, which are olivine and hypersthene normative, and T7 which is hypersthene normative only. The alkaline affinity of the two anomalously high MgO samples is inconsistent with CIPW norm composition (olivine and hypersthene).

Variations of major elements against MgO (as the index of differentiation) are illustrated in Fig.5.3. Accordingly, CaO exhibit inflected trends in which CaO contents increase up to 9.86 wt. % MgO and then decrease with decreasing MgO. Furthermore, increasing trend of SiO_2, K_2O, Al_2O_3 and Na_2O against decreasing MgO is also observed among the samples of Aiba and Ashenge basalts. Additionally, flat to decreasing concentration of Fe_2O_3 and TiO_2 with decreasing MgO are also characteristic features of Ashenge and Aiba flood basalts. In the Fe_2O_3 versus MgO variation diagram, the slightly flat trend is constituted by samples of Ashenge basalts whereas the strongly positive trend is formed by samples of Aiba basalts. Moreover, on the P_2O_5 vs. MgO variation, two distinct trends are observed; positive trend among samples of Aiba basalts and negative trend among samples of Ashenge basalts. Although the bivariate major element plots (Fig. 5.3) show the lavas display an evolutionary trend, distinct trends (P_2O_5, $TiO_2$and K_2O) are formed by each basaltic group (Ashenge and Aiba basalts).

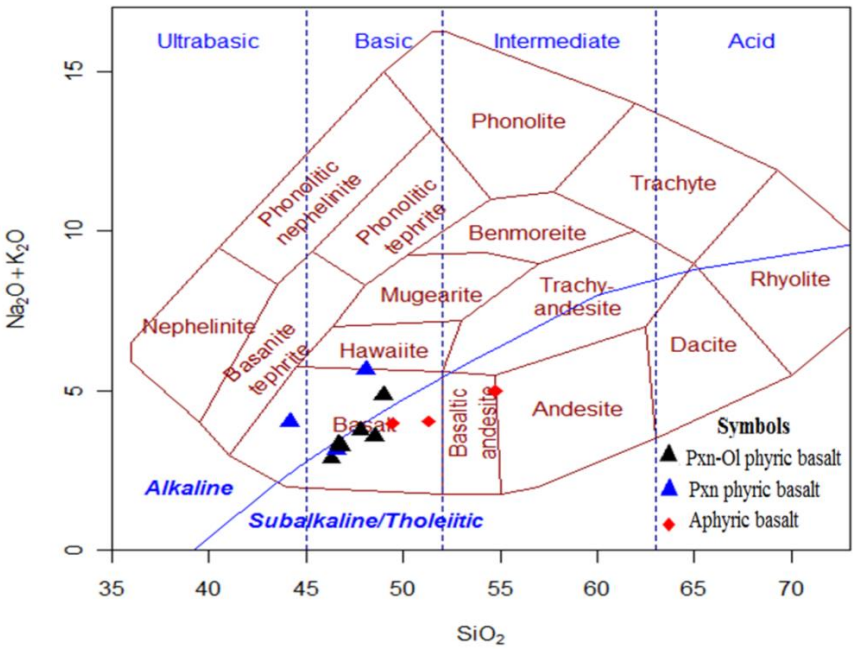

Fig.5.1: TAS classification diagrams of Ashenge and Aiba flood basalts (after Cox et al., 1979).Note their general transitional basalt affinity for most of the samples. Note also the alkaline affinity of the two anomalously high MgO samples from pxn- phyric basalt of Ashenge formation.

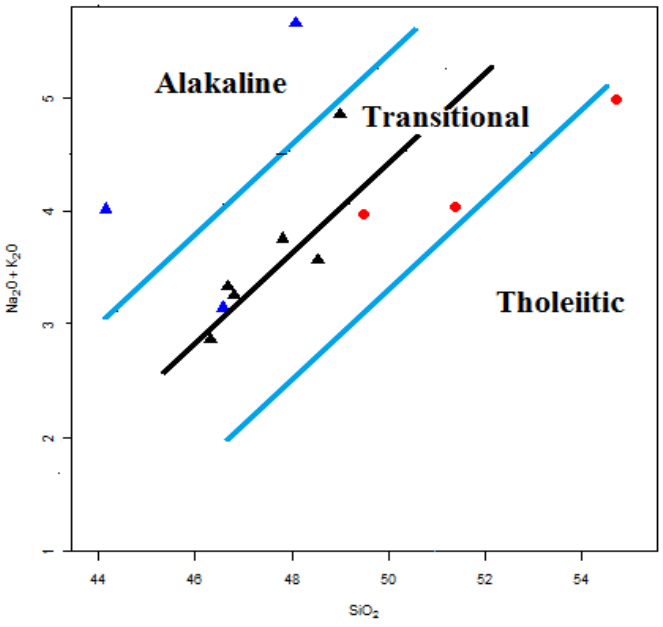

Fig.5.2: (Na_2O+K_2O) versus SiO_2 diagram for Ashenge and Aiba flood basalts. The solid black line represents the boundary between the tholeiitic and alkaline fields of Hawaiian volcanic rocks (Macdonald and Katsura, 1964, as cited in Pik et al., 1998).The solid blue line represents the limits of the Ethiopian transitional basalt field after Peccirillo et al., 1979. Symbols are as in Fig.5.1.

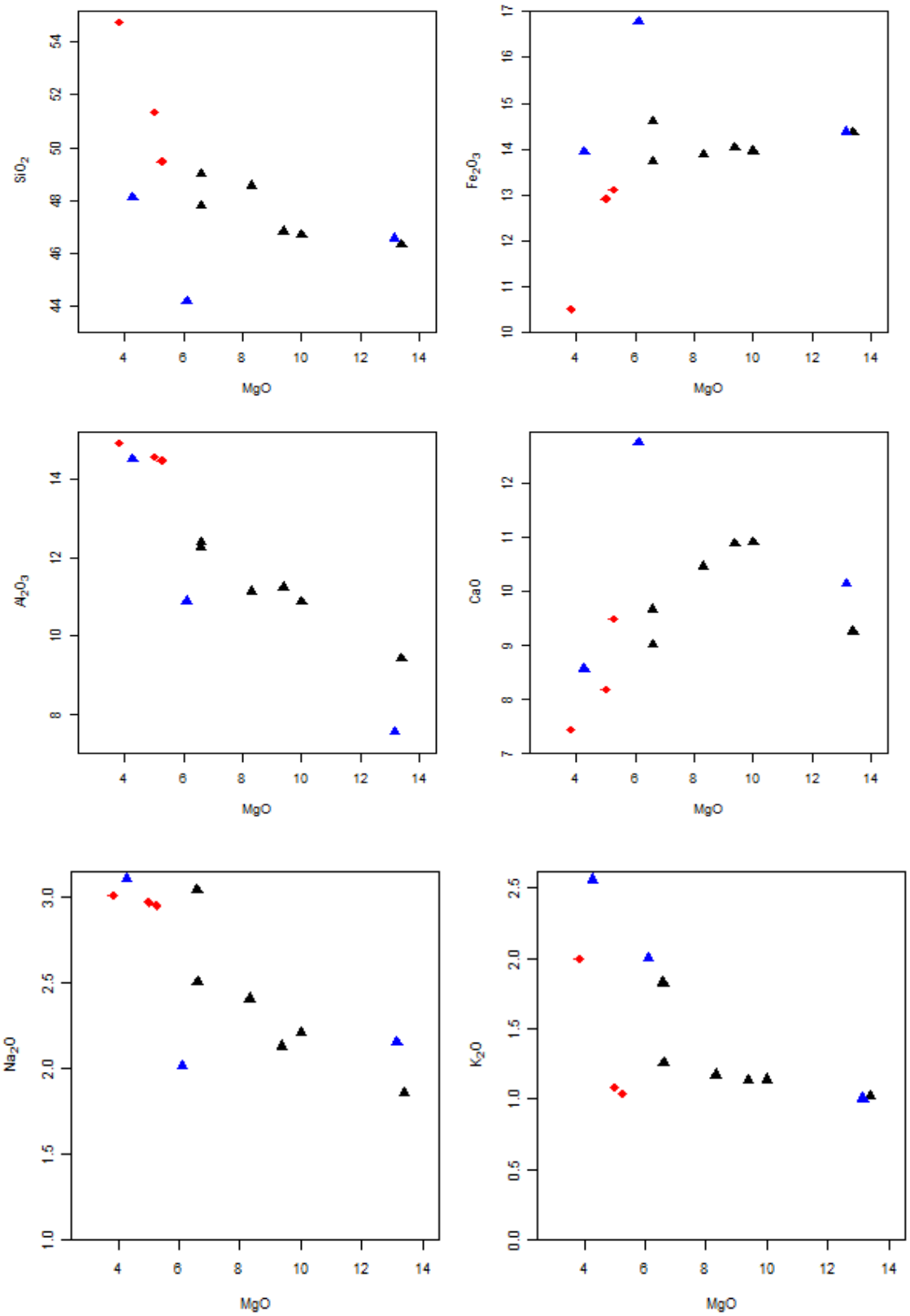
SiO2
MgO
Fe2O3
MgO
Al2O3
MgO
CaO
MgO
Na2O
MgO
K2O
MgO

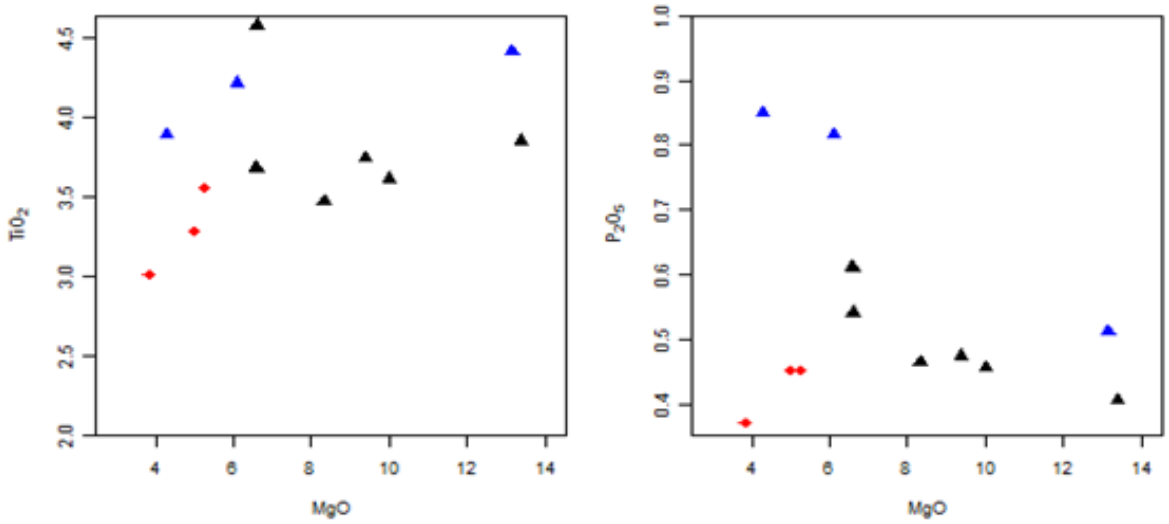

Fig.5.3: Variation diagrams of major element contents as a function of MgO for Ashenge and Aiba flood basalts. Major element data are recalculated to 100% on a water-free basis. Symbols are as in Fig.5.1.

5.3. Trace Element Geochemistry

5.3.1. Trace element variation

The studied samples of Ashenge and Aiba basalts shows, like their major element concentration and plots, a greater variation of both compatible and incompatible trace elements (Table 5.1).However, the variation within each basaltic group is generally very limited or uniform with the exception of the two anomalous samples which have anomalous values of elements like MgO (mg#), Ni, Cr, Co. The basaltic lavas, excluding the two high-MgO samples (T4O18 and T2S8), have compatible trace element contents such as Ni (5-153ppm), Cr (<10-600ppm) and Co (25-57ppm).Particularly, Aiba basalts have a compatible element contents of such as Ni (6-33ppm),Co (25-41ppm) and Cr (30-80) whereas Ashenge basalts, excluding the two samples (T2S8 and T4O18), are characterized by their relatively higher compatible trace element concentrations like Ni (5-153ppm),Co(34-57ppm) and Cr (<10-600ppm).The two anomalous samples; T4O18 and T2S8 ,have a compatible trace element content of Ni(446,542),Cr(1110,780),and Co(65,67) respectively. Further, Ashenge basalts, relative to Aiba basalts, have higher concentration of LILE (Rb, Ba, and Sr) and HFSE (La, Zr, Nb, Ta, U, Pb, and Ce).However, the two anomalously high MgO samples have lower concentration of LILE (e.g. Rb, Ba, and Sr) and HFSE (e.g. La, Zr, Nb, U, and Ce) than the rest of the Ashenge samples but higher than the samples of Aiba basalts. In the plots of Ti/Y versus Nb/Y(Fig.5.6),samples of Aiba basalts fall in the field of HT1 whereas Ashenge samples are plotted with in the field of HT2.This strongly supports the major

element based HT1 and HT2 interpretation of Aiba basalts and Ashenge basalts respectively(section 5.2).

Compatible and incompatible trace-element concentrations of Ashenge and Aiba samples are plotted against MgO (Fig.5.4 and Fig.5.5 respectively). Accordingly, the compatible elements such as Ni, Cr, Co, and Sc show generally a decreasing trend against decreasing MgO. However, the incompatible elements like Th, Ba, La, Ce, Rb and U shows an increasing trends against decreasing MgO for both Ashenge and Aiba basalts. Further, the trends of other incompatible elements like Nb and Sr are not the same for both of the basaltic groups; both Nb and Sr shows increasing trend against decreasing MgO for samples of Ashenge basalts whereas samples of Aiba basalts exhibit decreasing trend of these elements against decreasing MgO. Moreover, distinct trends, like on that of some major element variation diagram (Fig.5.3), are clearly observed on these incompatible trace elements variation diagrams against MgO.

Plots of two highly incompatible trace elements, thought to be insensitive to fractional crystallization and partial melting (Rollison, 1993; Dereje Ayalew et al., 1999; Wilson, 1989), are shown in Fig.5.7. In this figure, plots of A and B (Yb vs.Tm and Yb vs.Y) defined more or less a single and simple correlation line for both samples of Ashenge and Aiba basalts, and these elements have been interpreted to be relatively insensitive to crustal contamination(Wilson,1989).However, plots of highly incompatible trace elements from C-F (Th vs. La,Th vs. Ta,Th vs. Nb, and La vs. Nb) forms distinct trends for each basaltic groups(Ashenge and Aiba basalts),and these elements are highly sensitive to crustal contamination(Hart et al.,1889; Kent et al., 2002). In addition, Ratio- Ratio plots of these highly incompatible and crustal contamination sensitive elements are also shown in Fig.5.8, and show clear distinct trends for each basaltic groups. However, the distinct trends observed in Fig.5.7and 5.8 intersect at about the same point.

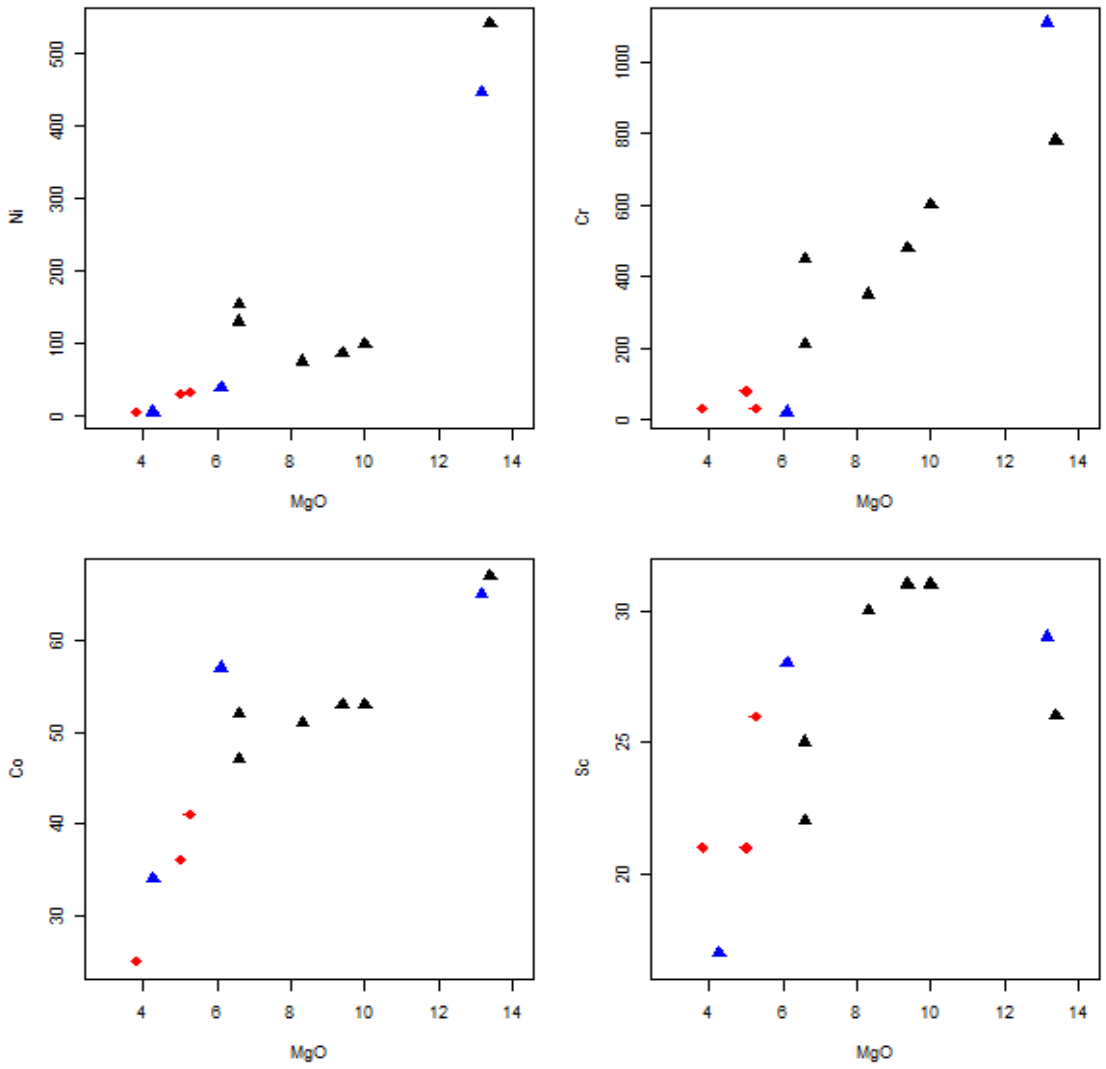

Fig.5.4: Trace element variation diagram showing the variation of compatible elements against MgO as index of differentiation. Symbols are as in Fig.5.1.

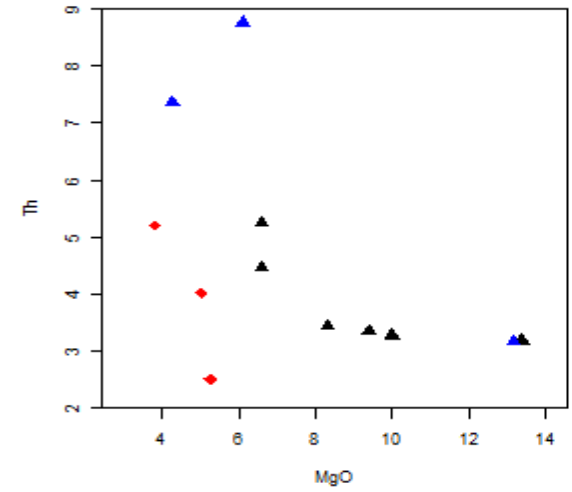
Th
MgO
2
3
4
5
6
7
8
9
4
6
8
10
12
14

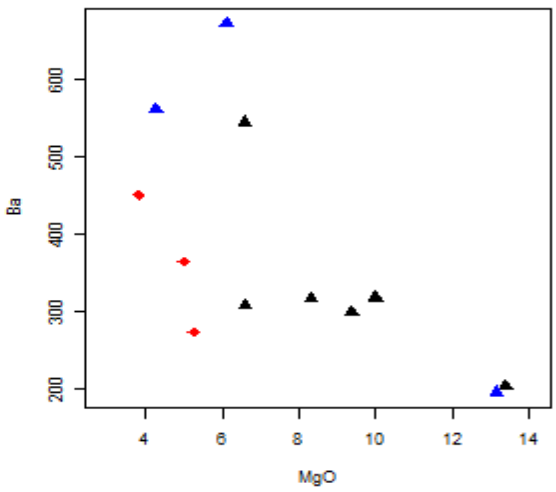
Ba
MgO
200
300
400
500
600
4
6
8
10
12
14

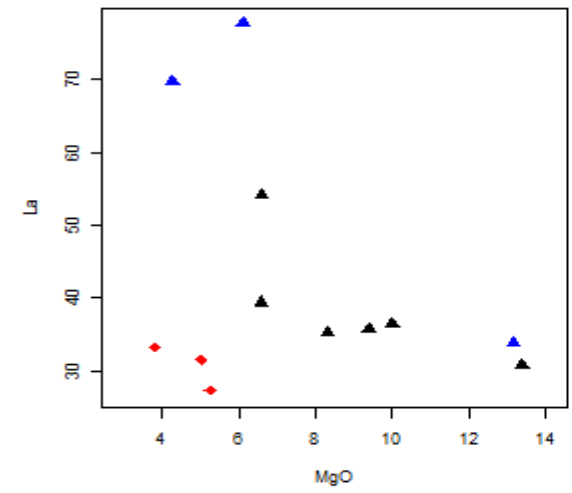
La
MgO
30
40
50
60
70
4
6
8
10
12
14

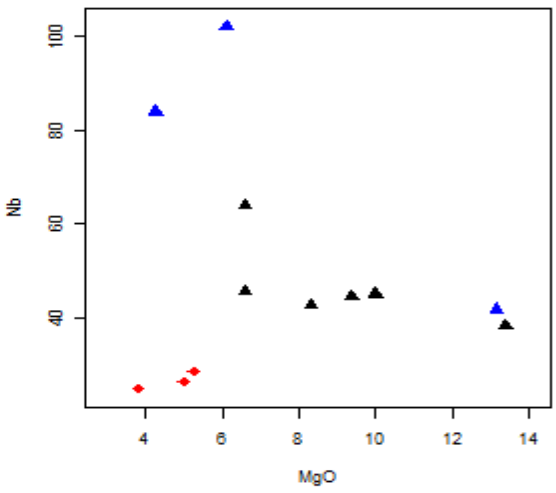
Nb
MgO
40
60
80
100
4
6
8
10
12
14

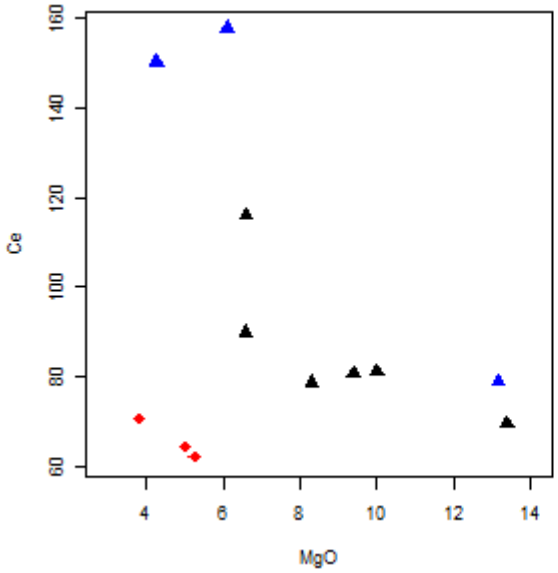
Ce
MgO
60
80
100
120
140
160
4
6
8
10
12
14

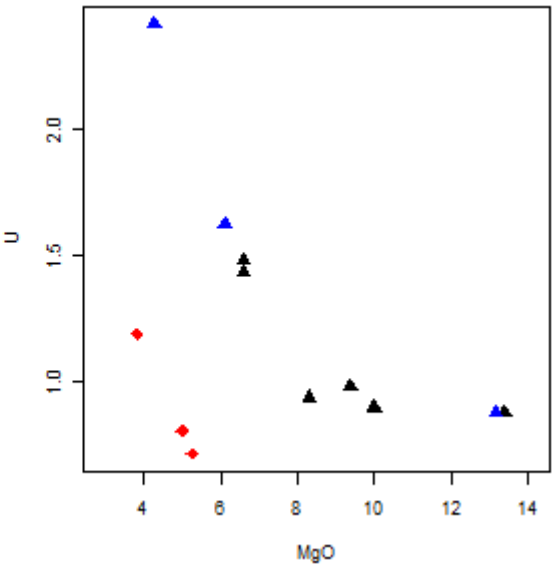
U
MgO
1.0
1.5
2.0
4
6
8
10
12
14

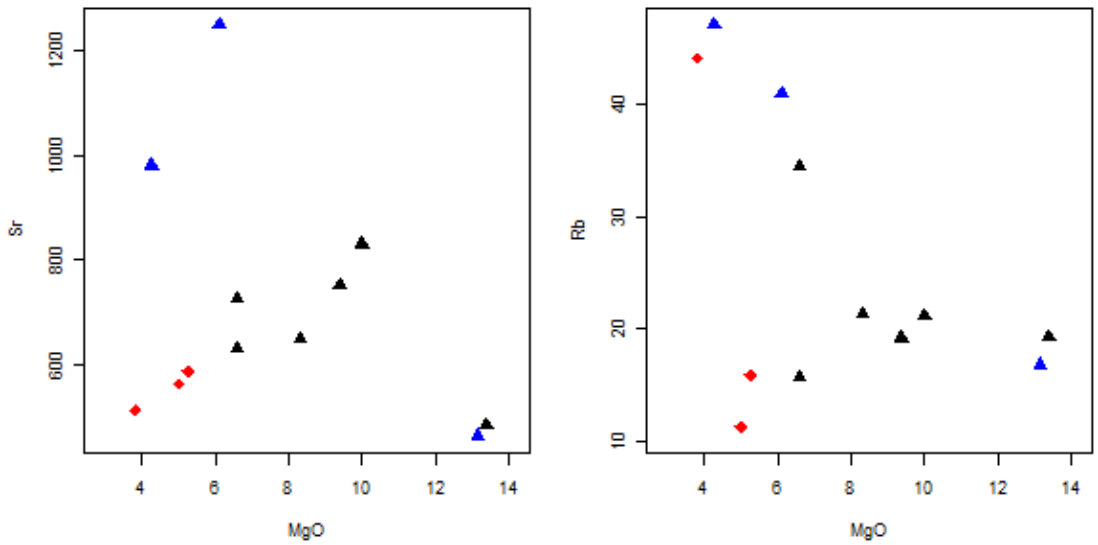

Fig.5.5: Trace element variation diagram showing the variation of incompatible elements against MgO as index of differentiation. Symbols are as in Fig.5.1.

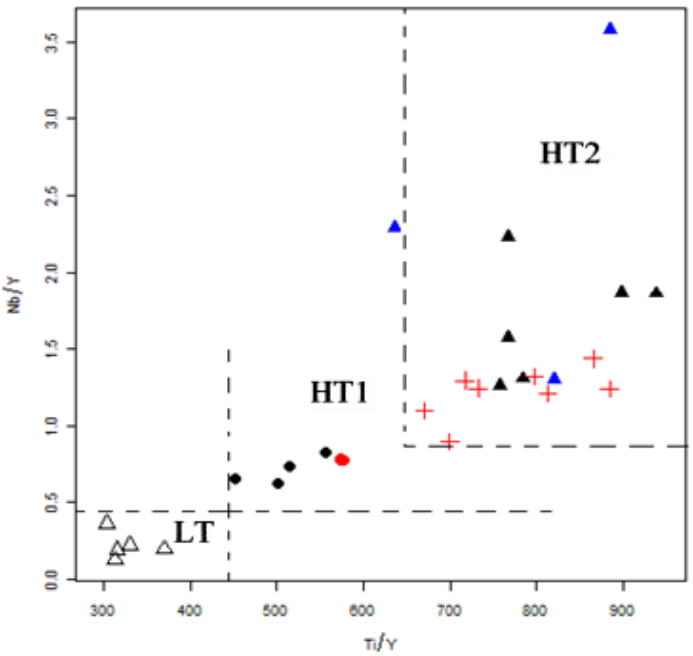

Fig.5.6.:Ti/Y versus Nb/Y diagram for Ashenge and Aiba flood basalts (after Pik et al., 1998).The data from LT (△), HT1 (•) and HT2 (+) are also taken from Pik et al. (1998).The symbols for this study are as in Fig.5.1.

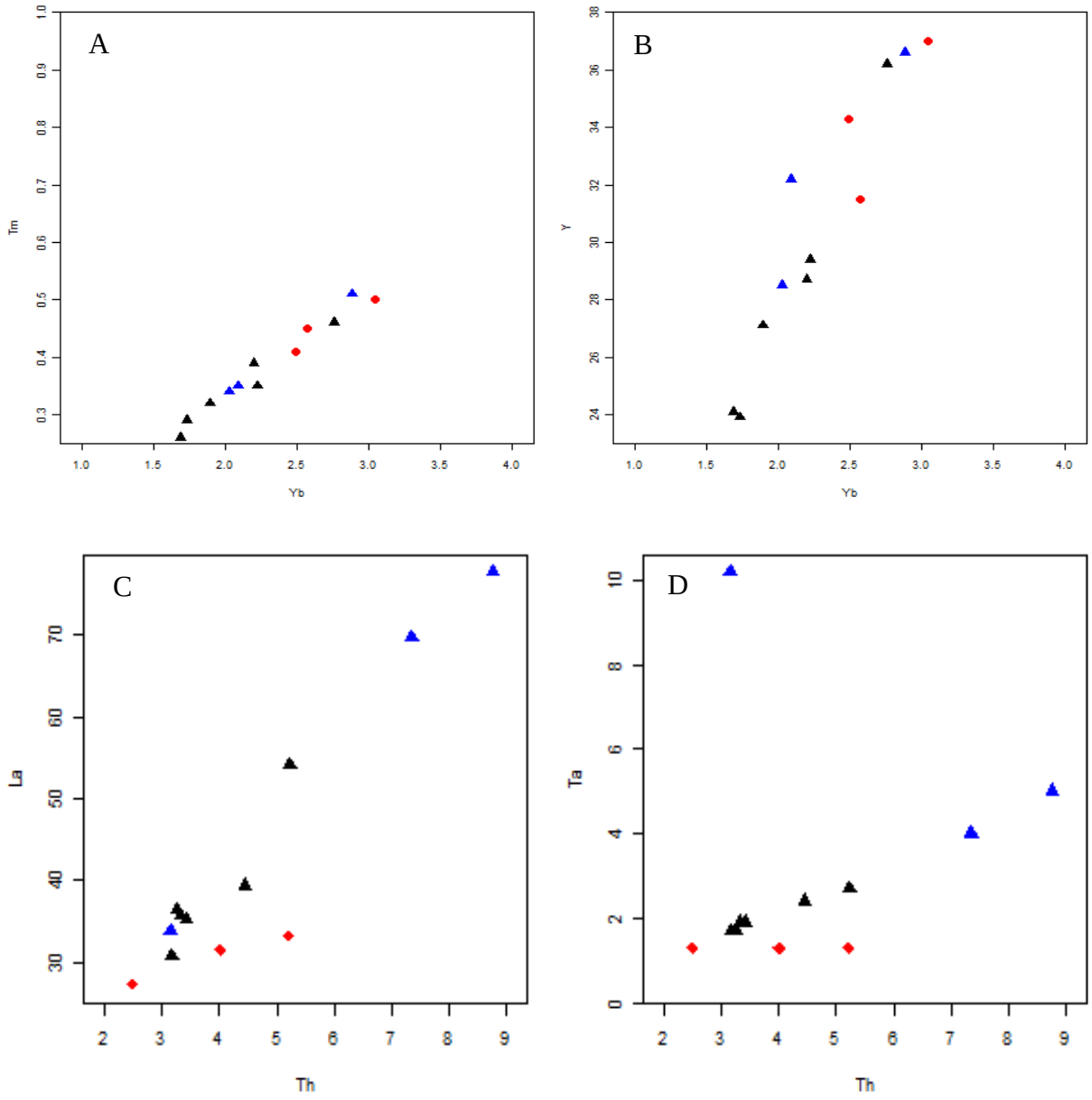
A
Tm
Yb
B
Y
Yb
C
La
Th
D
Ta
Th

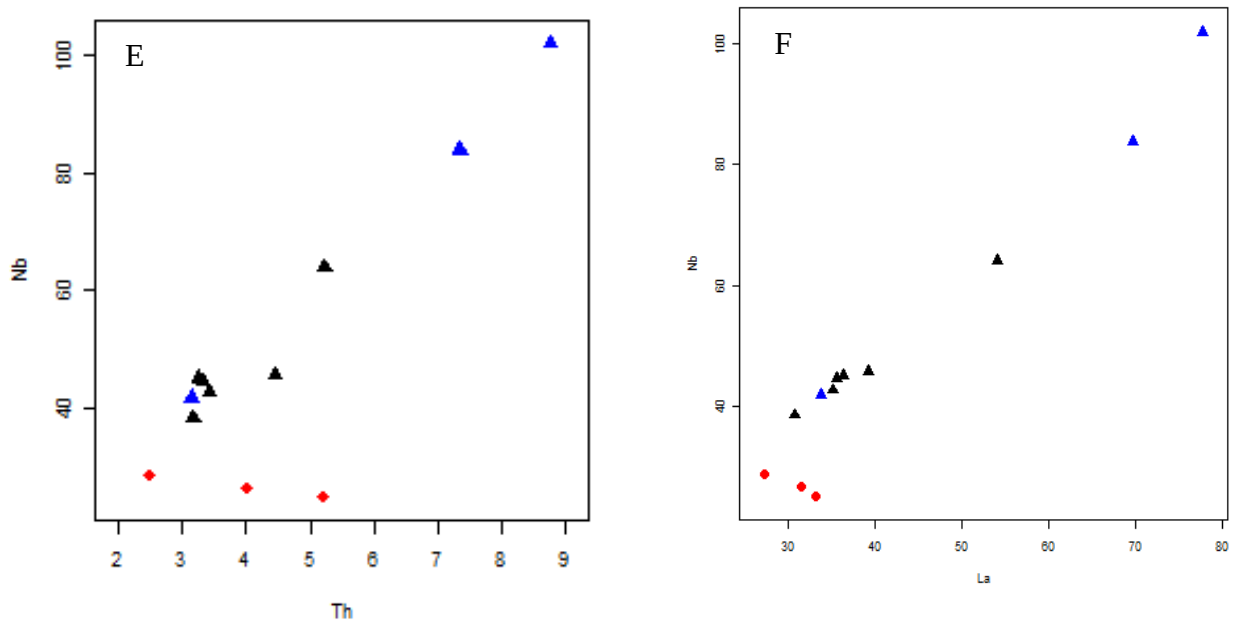

Fig.5.7: Binary plots of highly incompatible trace elements. Note the distinct trends and their intersecting pattern formed by Ashenge and Aiba basalts (C-F). Note also simple correlation line (A and B).Symbols are as in Fig.5.1.

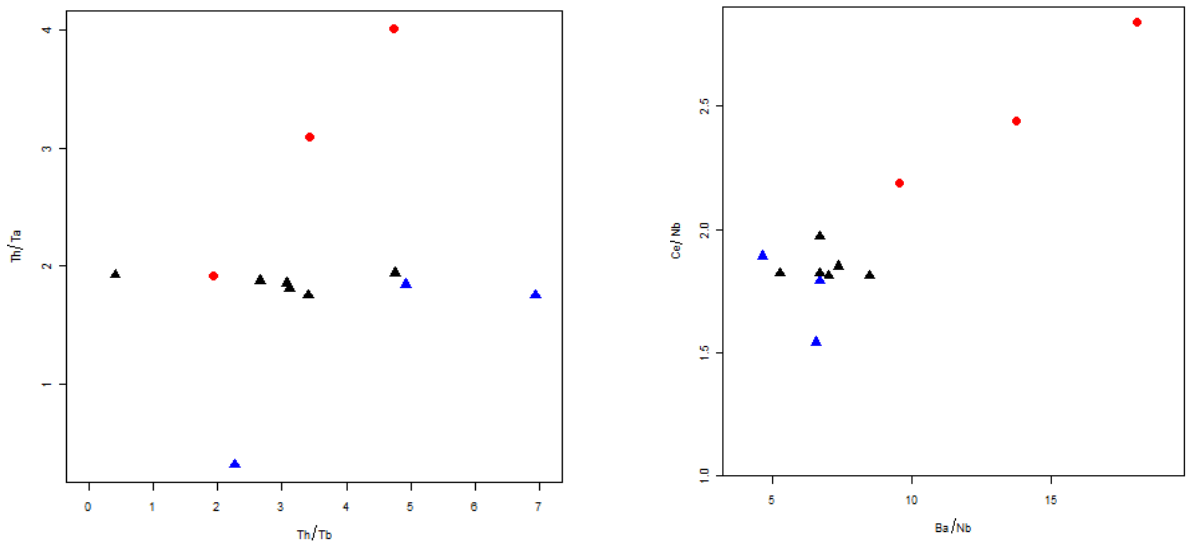

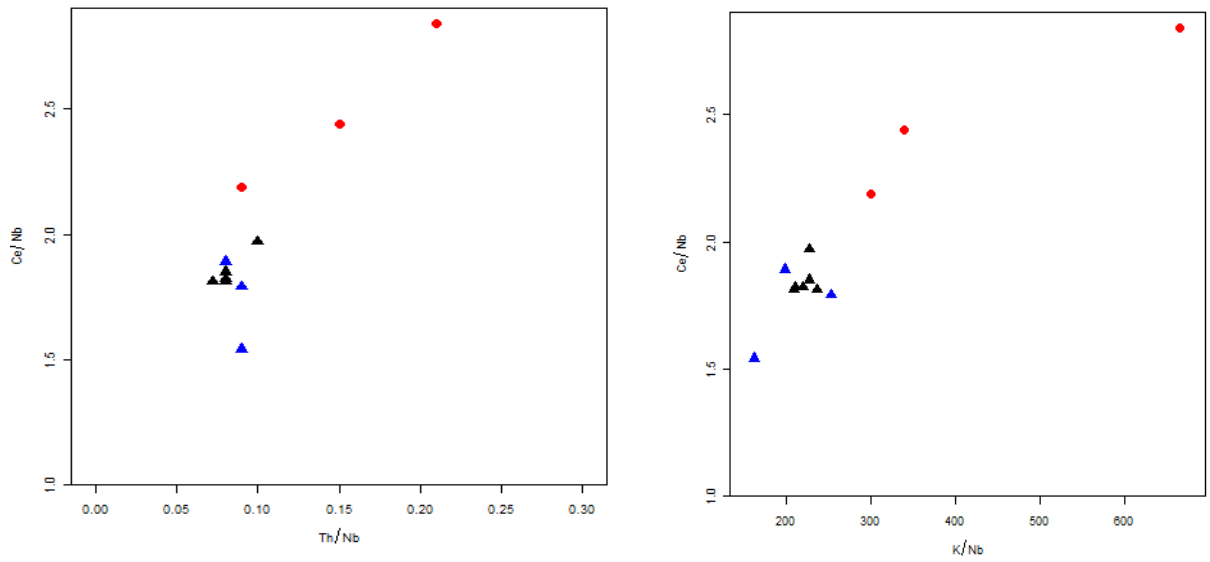

Fig.5.8: Ratio –Ratio plots of selected highly incompatible trace elements. Note also the intersecting pattern of the two trends constituted by each basaltic group. Symbols are as in Fig.5.1.

5.3.2. Multi-Element Variation Diagram

Primitive mantle normalized trace element diagram for Ashenge and Aiba basalts is presented in Fig.5.9. On this normalized diagram samples of Ashenge and Aiba basalts are homogeneous overall: where the investigated samples are characterized by enrichment in incompatible trace elements, notably a strong enrichment in high field strength elements (HFSE).However, it is clearly visible that samples of Ashenge basalts are highly incompatible element enriched than samples of Aiba basalts. Moreover, primitive-mantle-normalized trace element diagram displays considerable trough at K and P. Additionally, on this diagram, there is positive Nb anomaly in the samples of Ashenge basalts whereas samples of Aiba basalts exhibit generally negative or no Nb anomaly. The pronounced positive anomaly of Pb could be linked to the mobility because this element is highly mobile under secondary processes such as hydrothermal activities, alterations and metamorphic processes (Rollison, 1993).

Further, OIB normalized multi element variation diagram is presented in appendix V and in this diagram the negative and slightly positive Nb anomaly of Aiba and Ashenge basalts is clearly observed respectively. In addition, the studied samples of Ashenge and Aiba basalts have generally similar pattern to that of OIB.

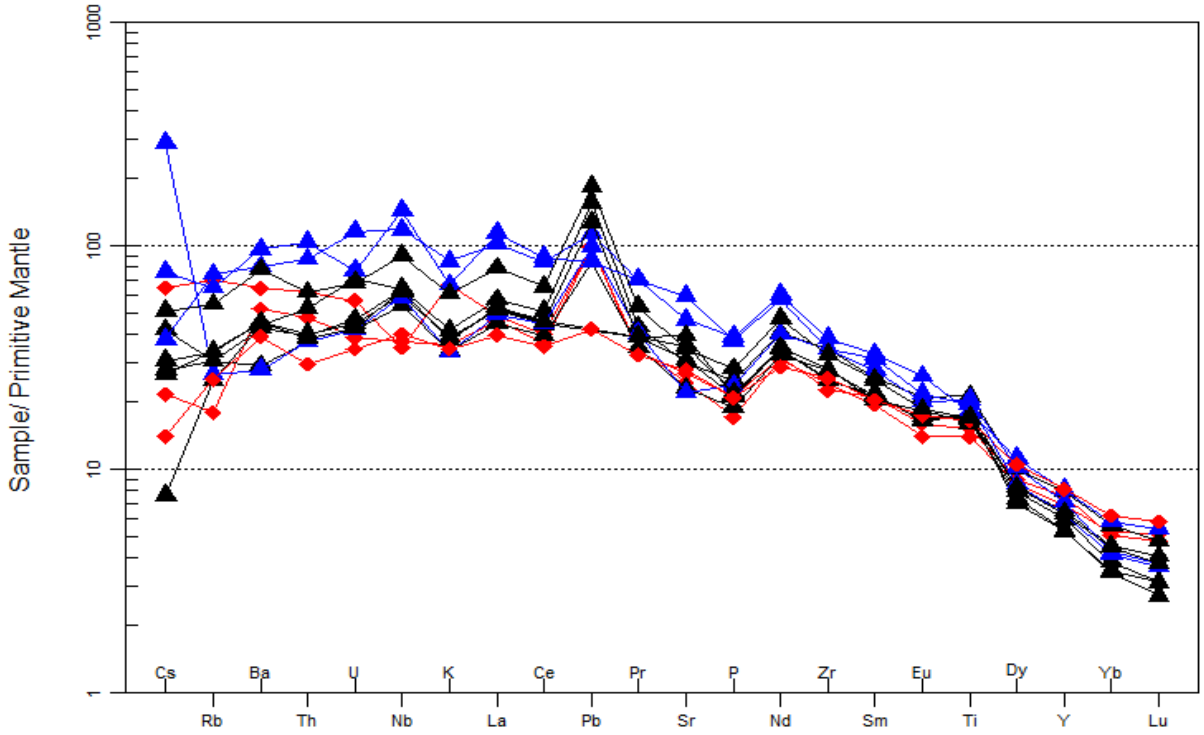

Fig.5.9: Primitive mantle-normalized multi-element variation diagram for Aiba and Ashenge basalts. The normalization values are from Sun and McDonough (1989).Symbols are as in Fig. 5. 1.

5.3.3. Rare Earth Element (REE) variation diagram

The chondrite normalized REE patterns of Ashenge and Aiba basalts is shown in Fig.6. The analyzed samples show strong REE enrichment, especially in the LREE with a (La/Yb)N value of 5.59-25.52. Further, the studied samples have relatively flat HREE pattern (Gd/YbN:2.31-4.02).Particularly, samples of Aiba basalts are characterized by their (La/Yb)N and (Gd/Yb) N of 5.99-8.61 and 2.31-2.65 respectively. In contrast, samples of Ashenge basalts have a (La/Yb) N and (Gd/Yb)N of 9.22-25.52 and 2.89-4.02 respectively. None of the lavas show significant anomalies in Eu (Eu/ Eu*= 0.93-l, 071), which can be linked to the lack of plagioclase fractionation on the early fractionating phases. Furthermore, on this chondrite normalized REE diagram, the studied samples have parallel to sub parallel patterns within each basaltic groups but the two basaltic groups (Ashenge and Aiba basalts) show cross cutting pattern.

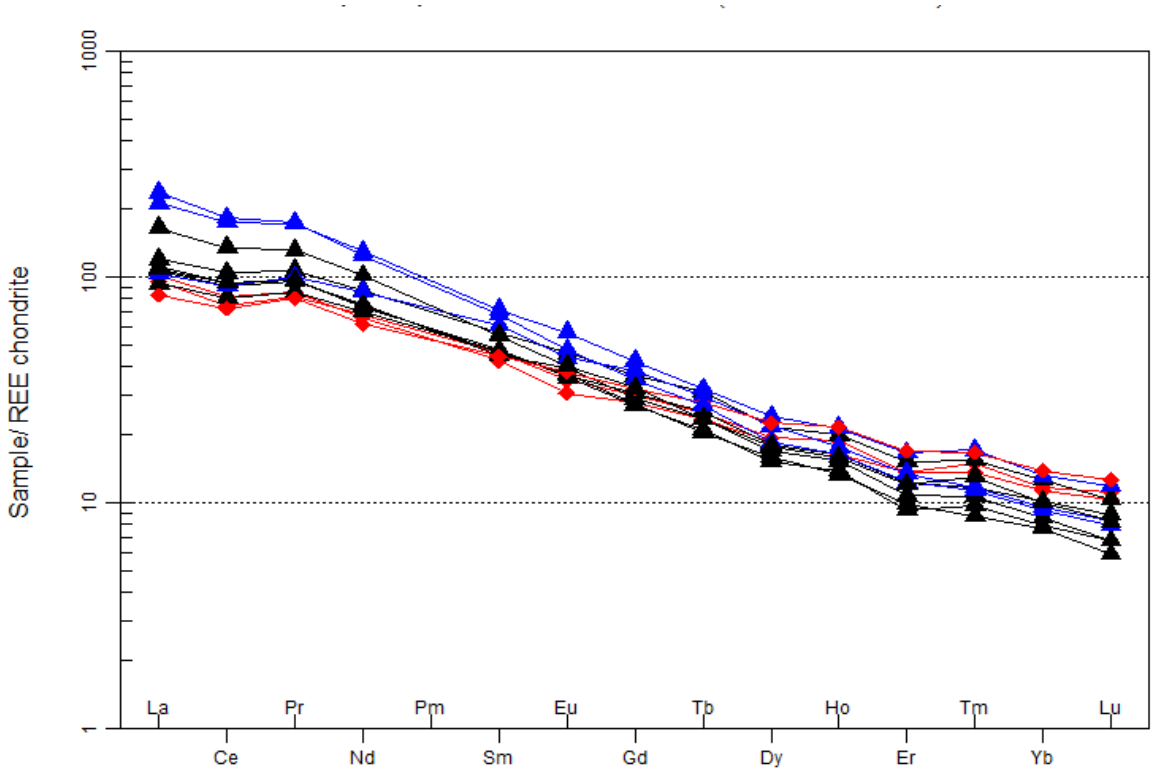

Fig.5.10: Chondrite -normalized REE pattern for Aiba and Ashenge basalts. The normalization values are from Nakamura (1974).Symbols are as in Fig. 5. 1.

CHAPTER SIX

DISCUSSION

6.1. Introduction

Several studies have been carried out on both the rift and plateau volcanic of Ethiopia (e.g. Pik et al.,1998;1999;2006;Tadiwos Chernet et al.,1998;Natali et al.,2011,2013;Gidey Weldegebriel et al.,1990;Peccerillo et al.,2003,2007;Dereje Ayalew et al.,2006; Chorowicz et al.,1998; Bonini et al.,2005).The results of these works was majorly dependent on geochemical data (major element, trace element and isotopic data), to constrain the petrogenetic evolution of Ethiopian volcanic rocks. In the present study, which focuses on Maychew flood basalts (Ashenge and Aiba), is also largely dependent on geochemical data particularly on major and trace elements to understand the petrogenetic evolution of Ashenge and Aiba flood basalts. As discussed in the previous sections, the evolution of Ethiopian flood basalts has been related to fractional crystallization with or without concomitant crustal contamination.

6.2. Fractional Crystallization

Primary magma in equilibrium with a typical upper mantle mineral assemblage (Willson,1989;Frey et al., 1978; Hess, 1992 as cited in Dereje Ayalew et al., 2016) are characterized by their higher compatible trace element contents such as Ni (>400–500 ppm), Cr(>1000 ppm) and MgO content (10–15 wt.%). However, the investigated samples, excluding the two high-MgO samples, are characterized by compatible trace element content such as Ni (5-153ppm), Cr (<10-600ppm) and 3.82 to 9.86 wt.% MgO. Therefore, such low values compared to the chemical characteristics of primary magma suggests that these rocks do not represent primary magmas but rather underwent olivine and/or clinopyroxene fractionation, consistent with the observed phenocrysts assemblage. Furthermore, the basaltic lavas have high concentrations of Sr (484-1250 ppm) and V (324–512 ppm) which reflect the lack of significant plagioclase and Fe–Ti oxides fractionation in the early stages of differentiation (Dereje Ayalew and Gibson, 2009), which is also evidenced by the lack of negative anomaly of Eu, Sr and Ti in REE plot and primitive mantle diagram (Fig.5.9 and Fig.5.10).

In particular, Aiba basalts have a compatible element contents of Ni (6-33 ppm), Co (25-41 ppm) and Cr (30-80 ppm) whereas Ashenge basalts, excluding the two high-MgO samples (T2S8 and T4O18), have compatible trace element content of Ni (5-130 ppm),Co (34-57 ppm) and Cr(<10-600 ppm). Hence, these high compatible trace element contents (Cr, Co, Ni) coupled with their relatively higher MgO value of Ashenge basalts indicates that they are less evolved and very limited extent of fractionation i.e. Aiba basalts are more fractionated than Ashenge basalts. The two anomalously high MgO samples (T2S8 and T4O18) have a compatible element concentration of Ni (446-542 ppm), Cr (780-1110 ppm) and Co (65-67 ppm), which is generally higher than the rest of Ashenge samples. However, the other compatible (excluding Ni, Cr, Co), and incompatible trace element concentration of these two anomalous samples is generally consistent with the rest of Ashenge samples (Table 5.1). Hence, the two samples (T2S8 and T4O18) with high MgO and Mg # must reflect olivine plus clinopyroxene accumulation rather than primitive characteristics of the magmas, as suggested in the petrographic section.

Furthermore, major element and selected compatible trace element variation diagram of Maychew flood basalts against MgO are presented in Fig.5.3 and Fig.5.5 respectively. The major element plot defines more or less continuous trends and/or coherent segmented trends marking the liquid line of descent, which represents the changing magma composition during fractional crystallization (Dereje Ayalew al., 2016).However, few major elements show distinct trends for each basaltic group, which could be due to accumulation and/or fractionation of heterogeneous phenocrysts or source heterogeneity (Dereje Ayalew et al., 1999). Accordingly, from major element variation diagram (Fig.5.3), CaO show negative correlation trend up to 9.86 Wt.% of MgO which is interpreted to be controlled by the removal of olivine, and after wards they show positive trend on the liquid line of descent, which is a suggestive of crystal liquid control by the fractionation of clinopyroxene from the melt. The inflection in the crystallization trend on 9.86 Wt. % of MgO value on MgO versus CaO plot could be related to the onset of fractionation of clinopyroxene. Further, the increasing trend of major elements like K_2O, Al_2O_3 and Na_2O against decreasing MgO could suggest that the differentiation of the melt is controlled by the fractionation of olivine from the system rather than feldspars; K- feldspar or plagioclase. On the TiO_2 vs. MgO variation diagram the relatively strong decreasing trend of TiO_2 against decreasing MgO (for Aiba basalts), and it's slight positive correlation (for Ashenge basalts) indicates that Fe-Ti oxides

were involved in the fractionating assemblage, which is consistent with the presence of subhedral to euhedral phenocrysts of opaque minerals in the phenocrysts assemblage, as suggested in the petrographic section.

Further, on the P_2O_5 vs. MgO variation, the positive trend observed among samples of Aiba basalts can be interpreted to the fractionation of P_2O_5 bearing mineral (possibly apatite) whereas the negative correlation among samples of Ashenge basalts can indicate that apatite was not prominently involved in the fractionating assemblage, which is consistent with the absence of apatite in the phenocrysts assemblage of Ashenge basalts, as suggested in petrographic section. Moreover, the flat to decreasing concentration of Fe_2O_3 with decreasing MgO can also be related to the fractionation of olivine from the system. Besides the trough at K and P on primitive-mantle-normalized trace element plots could be as consequence of k-feldspar and apatite fractionation, respectively.

Moreover, from trace element variation diagram (Fig.5.5), the decreasing trend of Ni, Co and Cr against decreasing MgO also supports fractionation of olivine and clinopyroxene $\pm$ spinel. In similar fashion to some of major element variation diagrams (e.g.K_2O, P_2O_5), the incompatible trace element variation diagrams do not indicate simple suit-wide differentiation trends. Instead, these plots show distinct trends between Ashenge and Aiba basalts.

As it is shown in Fig.5.6, couple of plots of incompatible trace elements (e.g. Th, U, Ba, and La) against MgO shows that these elements (Th, U, Ba and La) behave as incompatible element which confirms that fractionation played a major role in the evolution of these rocks (Dereje Ayalew et al., 2006). Moreover, from petrographic description, the presence of zoning (concentric compositional variation) in the phenocrysts of principally clinopyroxene and plagioclase may also indicate the involvement of fractional crystallization in the evolution of these basaltic rocks. Moreover, Rollinson (1993) have stated that the fractionating mineral assemblage is normally indicated by the phenocrysts present. Thus, olivine, clinopyroxene, and plagioclase ± Fe-Ti oxides were major fractionating phases in the petrogenetic history of these rocks.

Collectively, few major and all selected trace element plots of the studied samples do not illustrate simple suite-wide differentiation trends. Instead, these plots shows distinctions between the two basalt groups which can be indicative of group specific petrogenetic

histories (Mulugeta Alene et al., 2017).Further, from petrographic description, samples of Aiba basalt are dominated by plagioclase with some clinopyroxene and olivine, consistent with shallow level fractionation whereas samples of Ashenge basalts are dominated by clinopyroxene and olivine, compatible with deeper level fractionation(Pik et al.,1998).Thus, Aiba basalts and Ashenge basalts have undergone shallow level fractionation and deeper level fractionation respectively.

6.3. Crustal Contamination

The studied samples are characterized by strong enrichment in LREE and in highly incompatible trace elements (Table 5.1 and Fig.6). The enrichment in LREE and in highly incompatible elements may either be a consequence of crustal contamination or derivation from enriched mantle source (Dereje Ayalew et al., 2016). According to Peng et al. (1994, as cited in Dereje Ayalew et al., 1999) negative Nb and Ta spikes in the spider diagram and high trace element ratios such as Rb/Nb and Th/Ta are good indicators of crustal contamination. Moreover, Ce/Pb, Nb/U, La/Nb, and La/Ta ratios of mafic lavas are sensitive to contamination and well-defined for primary mantle-derived liquids (Ce/Pb ratio:25 ± 5, Nb/U:47±10, Hofmann et al., 1986 as cited in Dereje Ayalew et al., 2016; La/Nb ratio < 1.5, and La/Ta ratio <22, Hart et al., 1989 as cited in Miruts Hagos et al., 2016), making it useful indicators of crustal assimilation (Furman, 2007).

Accordingly, the studied samples of Ashenge basalts, in addition to their marked peak at Nb on the primitive mantle and OIB normalized multi-element variation diagrams(Fig.5.9, and Appendix IV), have relatively high Ta and Nb abundances and low trace element ratios (Rb/Nb: 0.34-0.56 and Th/Ta: 0.31-l.94,Table 5.2). In contrast, samples of Aiba basalt have low Ta and Nb abundances and high trace element ratios (Rb/Nb: 0.43-1.77 and Th/Ta: 1.92-4.01).In addition, samples of Aiba basalt shows generally negative Nb anomaly on both primitive mantle and OIB normalized multi-element variation diagram. Moreover, the samples of Aiba basalt have Ce/Pb and Nb/U ratios of 9.24 - 20.83 and 20.92 -39.72 respectively, whereas samples of Ashenge basalts have relatively higher Ce/Pb and Nb/U ratios of 8.17- 40.65 and 34.77-62.96 respectively. Further, Aiba basalts have relatively higher values of La/Nb and La/Ta elemental ratios (La/Nb: 0.96-1.89; La/Ta: 21-25.54) in contrast to the lower values of Ashenge basalts (La/Nb:0.76-0.86; La/Ta:3.31-21.41).Collectively these trace element characteristics illustrate the fact that Aiba and Ashenge basalts experienced different degrees of crustal contamination, being higher degree

of crustal contamination for Aiba basalts than Ashenge basalts. Thus the trace element characteristics of the studied samples, strong enrichment in LREE and in highly incompatible trace elements, can be attributed to an enriched mantle source and/or crustal contamination.

6.4. Magma Generation and Source Rock Characteristics

The samples of Ashenge and Aiba basalts (including T4O18 and T2S8) show a wide compositional variation in terms of their major and trace element concentrations (Table 5.1). In support of this, as it is shown in Table 5.2 ,the ratios of highly incompatible trace elements such as Zr/Nb (3.77-10.88), Hf/ La (0.12-0.28), Zr/Ce (2.44-4.87), La/Nb (0.76-1.89), Th/Nb (0.07-0.21) vary within the given suite, although they show a limited or uniform variation within each basalt groups. Normally, these ratios will not vary in the course of fractional crystallization and the variation observed may reflect either source heterogeneity or variation in petrogenetic processes (Dereje Ayalew et al., 1999; Rollison, 1993; Wilson, 1989; Miruts Hagos et al., 2016).

As suggested in the previous section (5.3.1), abundance-abundance and ratio –ratio plots of highly incompatible trace elements are presented in Fig.5.7 and 5.8 respectively. Accordingly, plots such as Yb vs.Tm, and Yb vs.Y, thought to be relatively insensitive to crustal contamination (Wilson, 1989), indicate simple correlation line for both samples of Ashenge and Aiba basalts, and this indicates their origin from common mantle source (Rollison, 1993).Further, the intersecting pattern of the two trends at about the same point also supports their origination from a common mantle source. However, the distinct trends observed on some of abundance – abundance and ratio-ratio plots of highly incompatible trace elements(Fig.5.7 and 5.8), which are highly sensitive to crustal contamination(Hart et al., 1989; Kent et al., 2002;Dereje Ayalew et al.,1999), could be related to variation of degree of crustal contamination between Ashenge and Aiba basalts. Thus, at least based on the existing trace element concentration and plots, the two basaltic groups; Ashenge and Aiba basalts, are originated from a common mantle source but have experienced different degree of crustal contamination, as suggested in section 6.3.

The investigated samples from study area exhibit trace element ratios such as Zr/Nb (3.77-10.88), Ba/La (5.75-13.55), La/Nb (0.76-1.89) and Ba/Nb (4.65-18.07), which overlap substantially the field of OIB (Sun and McDonough, 1989). This suggests that these lavas are derived from mantle sources that are similar to OIB-type sources or contain high proportion

of OIB-type sources at least on the basis of trace element ratios. Furthermore, the OIB normalized multi element variation diagram (Appendix IV) indicates that the analyzed samples have generally similar pattern to that of OIB, and thus Ashenge and Aiba flood basalts have OIB type mantle sources. However, the studied samples don't display trace element ratios typical of a MORB signature, implying that this component plays little or no role in the genesis of these lavas. As discussed in Section 5.2 and 5.3.1, Ashenge basalts have geochemical characteristics similar to HT2 basalts whereas Aiba basalts have a geochemical affinity similar to HT1. Pik et al. (1999) have described that both HT1 and HT2 basalts exhibit trace element ratios that completely overlap the field of OIBs. Further, both HT1 and HT2 have been interpreted to have a deep mantle origin (Pik et al., 1998; Lightfoot et al., 1990, as cited in Pik et al., 1998).Therefore, at least based on the present trace element concentration and ratios, and previous work comparison (Pik et al., 1998; 1998), Ashenge and Aiba basalts have deep mantle origin or, are formed from plume derived magmas, possibly Afar mantle plume.

Moreover, from chondrite-normalized rare earth element (REE) diagram(Fig.5.10), the fairly flat heavy Rare earth element (REE) pattern (Gd_N/Yb_N:2.31-4.02) along with the generally low CaO/Al_2O_3 ratios(0.5-1.34) of the studied samples most likely suggest a mantle source containing spinel rather than garnet(Dereje Ayalew et al., 2016). Thus, Ashenge and Aiba basalts are originated generally from, at least based on the existing major and trace element data, spinel bearing peridotite rather than garnet.

In general, from the previous sections the basaltic rocks of the study area have been treated if they have undergone contamination with the crustal materials and thus the ratios of the most susceptible incompatible trace elements (e.g. Ce/Pb, La/Nb, see section 6.3 for references) to contamination/assimilation indicates that crustal contamination process to have occurred, majorly for Aiba basalts .Additionally, it has been discussed that fractional crystallization have played a major role in the petrogenetic evolution of these basaltic rocks. Hence, the compositional variations observed among samples of Ashenge and Aiba basalts are related to variation in the crystal fractionation histories and/or crustal contamination, rather than source heterogeneity.

CHAPTER SEVEN

CONCLUSION AND RECOMMENDATION

7.1. Conclusion

Based on field observations, petrographic and geochemical data (major and trace elements) obtained in the present study; the following points have been drawn:

- ✓ The observed tectonic difference between the tilted Ashenge basalts and horizontal to sub horizontal Aiba basalts is also manifested on their petrology, petrography, and geochemistry (major and trace element concentrations and ratios).
- ✓ Petrographically, the lavas have generally aphyric to variably porphyritic texture with phenocrysts of clinopyroxene, olivine, plagioclase and very few Fe-Ti oxides set in a plagioclase dominated intersertal and intergranular textured microcrystalline matrix.
- ✓ Major and trace element data of the current study confirms that Ashenge flood basalts have a very similar geochemical pattern with High Titanium two basalt (HT2) of Northwestern Ethiopia continental flood basalt, whereas Aiba basalts have a geochemical affinity similar to High Titanium one (HT1).
- ✓ Both basaltic groups were evolved following different paths of petrogenetic processes such as fractional crystallization and/or crustal contamination. Aiba basalts have undergone shallow level fractionation, whereas Ashenge basalts have undergone deeper level fractionation. Further, Aiba basalts are much more differentiated and contaminated than Ashenge basalts.
- ✓ The distinct trends observed on selected major and trace variation diagrams, and the intersecting pattern on chondrite normalized REE diagram among samples of Ashenge and Aiba basalts is attributed to either variation in degree of crustal contamination and/or depth of fractionation.
- ✓ Ratios and plots of highly incompatible trace elements suggested that both basaltic groups were originated from a common OIB like mantle source. Thus the observed compositional variation between Ashenge and Aiba basalt is as a result of variation in crystallization histories and/or crustal contamination, instead of source heterogeneity.

7.2. Recommendation

- ✓ From field observation it is clearly shown that Ashenge basalts are tilted whereas Aiba basalts are Horizontal to sub horizontal. Thus to understand and determine the reason behind this tectonic difference between the two basaltic groups further structural and geodynamic considerations are strongly recommended.
- ✓ Large numbers of samples along with their isotopic results to further characterize the source region and the petrogenetic processes involved in the evolution of these basaltic units are also strongly recommended.

REFERENCES

Baker, J., Snee, L. and Menzies, M. (1996). A brief Oligocene period of flood volcanism in Yemen. *Earth and Planetary Science Letters,* **138**: 39–55.

Bastow, I., Stuart, G., Kendall, J. and Ebinger, C. (2005). Upper-mantle seismic structure in a region of incipient continental breakup: northern Ethiopian rift. *Geophysical Journal International*, **162**:479–493.

Beccaluva, L., Bianchini, G., Natali, C. and Siena, F. (2009). Continental flood basalts and mantle plumes: a case study of the northern Ethiopian plateau. *Journal of Petrology*, **50**: 1377– 1403.

Blanford, W.T. (1869). On the geology of a portion of Abyssinia. *l. Geol. Soc. London* 25, 401-406.

Blanford, W.T. (1870). Observations on the geology and zoology of Abyssinia. Made during the progress of the British Expedition to that country in1867-8. Macmillan. 487p.

Bonini, M., Corti, G., Innocenti, F., Manetti, P., Mazzarini, F., Tsegaye Abebe and Pecskay, Z. (2005). Evolution of the Main Ethiopian Rift in the frame of Afar and Kenya rifts propagation. *Tectonics,* **24**: TC1007. Doi: 10.1029/2004TC001680.

Bosworth, W. and Daniel F. Stockli, D.F. (2016). Early magmatism in the greater Red Sea rift: Timing and significance. *Canadian Journal of Earth Sciences***, 53**: 1158–1176.DOI: 10.1139/cjes-2016-0019.

Chorowicz, J., Collet, B., Bonavia, F., Mohr, P., Parrot, J.F. and Tesfaye Korme (1998). The Tana basin, Ethiopia: intra-plateau uplift, rifting and subsidence. *Tectonophysics* **295**:351–367.

Coulié, E., Quidelleur, X., Gillot, P.Y., Courtillot, V., Lefivre, J.C.and Chiesa, S. (2003). Comparative K-Ar and Ar-Ar dating of Ethiopian and Yemenite Oligocene volcanism: implications for timing and duration of the Ethiopian traps. *Earth and Planetary Science Letters,***206**: 477-492.

Courtillot, V., Jaupart, C., Manighetti, I., Tapponnier, P. and Besse, J. (1999).On causal links between flood basalts and continental breakup. *Earth and Planetary Science Letters*, **166**: 177-195.

Corti, G. (2009). Continental rift evolution: From rift initiation to incipient break-up in the Main Ethiopian Rift. East Africa. *Earth-Science Reviews*, **96**: 1–53.

Cox, K.G., J.D. Bell and R.J. Pankhurst (1979). The Interpretation of Igneous Rocks. Allen and Unwin.

Cox, K.G. (1980).A model for flood basalt volcanism.*J.Petrol*.**21**: 629-650.

Cox.K.G. and C.J. Hawkesworth (1985).Geochemical stratigraphy of the Deccan Traps at Mahabaleshwar, Western Ghats, India, with implications for open system magmatic processes.*J. Petrol.* **26**: 355-377.

Davidson, A. and Rex, D.C. (1980).Age of volcanism and rifting in south-western Ethiopia. *Nature*, **283**: 654–658.

Dereje Ayalew, Gezahegne Yirgu and Pik, R. (1999).Geochemical and isotopic (Sr, Nd and Pb) characteristics of volcanic rocks from southwestern Ethiopia. *Journal of African Earth Sciences*, **29**: 381-391.

Dereje Ayalew, Barbey, P., Marty, B., Reisberg, L., Gezahegn Yirgu and Pik, R. (2002). Source, genesis, and timing of giant ignimbrite deposits associated with Ethiopian continental flood basalts. *Geochimica et Cosmochimica Acta*, **66**(8): 1429–144.

Dereje Ayalew and Gezahegn Yirgu (2003). Crustal contribution to the genesis of Ethiopian plateau rhyolitic ignimbrites: Basalt and rhyolite geochemical provinciality. *Journal of the Geological Society*, **160**: 47-56. Doi: 10.1144/0016-764901-169.

Dereje Ayalew, Marty, B., Barbey, P., Gezahegn Yirgu and Endale Ketefo (2006).Sub-lithospheric source for quaternary alkaline Tepi shield, southwest Ethiopia. *Geochemical Journal***40**: 47–56.

Dereje Ayalew & Gibson, I.S. (2009). Head-to-tail transition of the Afar mantle plume: geochemical evidence from a Miocene bimodal basalt–rhyolite succession in the Ethiopian large igneous province. *Lithos*,**112**: 461–476.

Dereje Ayalew (2011).The relations between felsic and mafic volcanic rocks in continental flood basalts of Ethiopia: implication for the thermal weakening of the crust. *Geological Society, London, Special Publications*, **357**: 253-264.doi:10.1144/SP357.13.8.

Ebinger, C.J. and Sleep, N.H. (1988).Cenozoic magmatism throughout east Africa resulting from impact of a single plume. *Nature*, **395**: 788–791.

Ebinger, C.J., Tesfaye Yemane, Gidey WoldeGabriel, Aronson, J.L. and Walter, R.C. (1993).Late Eocene Recent volcanism and faulting in the southern Main Ethiopian Rift. *Journal of the Geological Society of London*, **150**: 99–108.

Ewart, A., Milner, S. C., Armstrong, R. A. and Ducan, A. R. (1998).Etendeka volcanism of the Goboboseb Mountains and Messum igneous complex, Namibia. Part 1: geochemical evidence of early Cretaceous Tristan plume melts and the role of crustal contamination in the Paraná- Etendeka CFB. *J. Petrol*. **39**:191–225.

Farnetani, C.G., Richards, M.A. and Ghiorso, M.S.(1996).Petrological models of magma evolution and deep crustal structure beneath. Earth Planeat.Sci.Lett.**143**: 81-94.

Frey, F., Green, D. and Roy, S.(1978). Integrated models of basalt petrogenesis: a study of quartz tholeiites to olivine melilites from South Eastern Australia utilizing geochemical and experimental petrological data. *Journal of Petrology*,**19:** 463–513.

Frost, B.R. and Frost, C.D. (2014).*Essentials of Igneous and Metamorphic Petrology*. Cambridge University Press, 304pp.

Furman, T., Bryce, J.G., Karson, J. and Iotti, A. (2004). East African rift system (EARS) plume structure: insight from Quaternary mafic lavas of Turkana, Kenya. *Journal of Petrology*, **45**: 1069–1088.

Furman, T. (2007). Geochemistry of East African Rift basalts: an overview. *Journal of African Earth Sciences*, **48**:157–160.

Gani, N.DS. Gani, M.R. and Abdelsalam, M.G. (2007).Blue Nile incision on the Ethiopian Plateau: Pulsed plateau growth, Pliocene uplift, and hominin evolution.*GSA Today*, **17**(9):4-11. Doi: 10.1130/GSAT01709A.1.

Gass, I.G. (1970). The evolution of volcanism in the junction area of the Red Sea, Gulf of Aden and Ethiopian rifts. *Phil. Trans. Roy. Soc. London* A.**267**: 369-381.

George, R., Rogers, N. and Kelly, S. (1998). Earliest magmatism in Ethiopia: evidence for two mantle plumes in one flood basalt province. *Geology*, **26**: 923-926.

Gidey WoldeGabriel, G., Aronson, J.L. and Walter, R.C. (1990).Geology, geochronology, and rift basin development in the central sector of the Main Ethiopia Rift. *Geological Society of America Bulletin*, **102**: 439–458.

Giday WoldeGabriel, Heiken, G., White, T D., Berhane Asfaw, Hart, W K. and Renne, P. R. (2000).Volcanism, tectonism, sedimentation, and the paleoanthropological record in the Ethiopian Rift System. *Geological Society of America*, Special Paper, **345**: 83-98.

Hart, W.K., Giday WoldeGabriel, Walter, R.C. and Mertzman, S.A. (1989). Basaltic volcanism in Ethiopia: constraints on continental rifting and mantle interactions. *Journal of Geophysical Research*,**94**: 7731–7748.

Hawkesworth, C., Kelley, S., Turner, S., Le Roex, A. and Storey, B. (1999). Mantle processes during Gondwana break-up and dispersal. *Journal of African Earth Sciences*, **28**: 239-261.

Hess, P. (1992). Phase equilibria constraints on the origin of ocean floor basalts. *Geophysical Monograph*, **71**: 67–102.

Hofmann, A.W., Jochum, K.P., Seufert, M. and White, W.M. (1986). Nb and Pb in oceanic basalts: new constraints on mantle evolution. *Earth and Planetary Science Letters*, **79**: 33–45.

Hofmann, C., Courtillot, V., Féraud, G., Rochette, P., Gezahegn Yirgu, Endale Ketefo, and Pik, R. (1997). Timing of the Ethiopian flood basalt event and implications for plume birth and global change: *Nature*, **389**: 838–841.

Hooper, P.R. (1982).The Columbia River basalts.*Science*,**215**:1463-1468.

http://en.climate-org/region/1505/?page=2accesedon 5/16/2018

https://www.climate-policy-watcher.org/plate-tectonics/large-igneous-province-flood-basalt a.html accessed on 5/24/2018

Kent, A.J.R., Baker, J.A., Wiedenbeck, M.(2002).Contamination and melt aggregation processes in continental flood basalts: constraints from melt inclusions in Oligocene basalts from Yemen. *Earth and planetary Science Letters*, **202:**577-594.

Kieffer, B., Arndt, N., LaPierre, H., Bastien, F., Bosch, D., Pecher, A., Gezahegn Yirgu, Dereje Ayalew, Weis, D., Jerram, D., Keller F. and Meugniot, C. (2004). Flood and shield basalts from Ethiopia: magmas from the African Super swell. *Journal of Petrology*, **45**: 793–834.

Kurkura Kabeto (2010). Geological and geochemical variations in Mid-Tertiary Ethiopian Flood Basalt Province, Maychew, Tigray Region, and Ethiopia.MEJS, **2** (1): *4-25.*

Kuster, D., Dwivedi, S. B., Kabeto, K., Mehary, K and Matheis, G. (2005). Petrogenetic reconnaissance investigation of mafic sills associated with flood basalts, Mekelle basin, northern Ethiopia: implication for Ni-Cu exploration. *J. Geochemical Exploration*,**85**: 63 – 79.

Lightfoot, P.C., Hawkesworth, C.J., Devey, C.W., Rogers, N.W. and Van Calsteren, P.W.C.(1990). Source and differentiation of Deccan trap lavas, implications of geochemical and mineral chemical variations. *J. Petrol*.**31**:1165–1200.

MacDonald, G.A. and Katsura, T. (1964).Chemical composition of Hawaiian lavas.*J.Petrol*.**5**: 82-133.

Marty, B., Pik, R., and Gezahegne Yirgu (1996).Helium isotopic variations in Ethiopian plume lavas; nature of magmatic sources and limit on lower mantle contribution. *Earth and Planetary Science Letters*, **144**: 223–237.

Melese Tadesse, Henok Bekele, Bezayit Mitiku, Meskerem Teshome, Asamenew Besufekade, Muhammed Edris, Getachew Burussa, Ezra Yehualaeshet, Shimeles Ashenafi and Tadesse Alemu (2011).Geology, Geochemistry and gravity survey of the Maychew area. Geological survey of Ethiopia, basic geoscience mapping core process. Unpublished technical report, Memoir, **31**: 61pp.

Mengesha Tefera, Tadiwos Chernet and Workineh Haro (1990).Geological map of Ethiopia. Ethiopian institutes of geological surveys, Regional Geology Department.

Mengesha Tefera, Tadiwos Chernet and Workineh Haro (1996).Exploration of the geological map of Ethiopia (1:20,000,000). Ethiopian institutes of geological surveys. Unpublished technical report, Addis Ababa, Ethiopia, 83pp.

Merla, G. and E. Minucci (1938).*Missione Geologica nel Tigrai*.- 1 *La serie dei terreni. R. Acad. Ital*. 363 p.

Merla, G., Abbate, E., Azzaroli, A., Bruni, P., Caunti, P., Fazzuoli, M., Sagri, M. and Tacconi, P. (1979). Geological map of Ethiopia and Somalia (1973):1:2,000,000 and comment with major land forms, 2-98.

Miruts Hagos, Koeberl, C., and Vries, B.V.W.D. (2016). The Quaternary volcanic rocks of the northern Afar Depression (northern Ethiopia): Perspectives on petrology, geochemistry, and tectonics. *Journal of African Earth Sciences,* **117:29**-47pp

Mohr, P. (1963). The Geology of Ethiopia, University college of Addis Ababa Press.

Mohr, P.A. (1983). Ethiopian Flood basalt provinces. *Nature*, **303**: 577-583.

Mohr, P. and C.A. Wood (1976).Volcano spacings and lithospheric attenuation in the Eastern Rift of Africa. *Earth planet sci. Lett*. **33**: 126-144.

Mohr, P. and Zanettin, B. (1988).The Ethiopian food basalt province. **In**: Macdougall, J.D. (Ed.), Continental flood basalts. *Kluwer Academic Publishers*, 63–110.

Molla Mekonnen Alemu (2016). Climatic Data and Rainfed Land Evaluation, the Case of Maichew, Northern Ethiopia, *International Journal of Agriculture and Forestry*, **6**(2):pp. 80-85. Doi: 10.5923/j.ijaf.20160602.04.

Mulugeta Alene, Hart, W.K., Saylor, B.Z., Deino, A., Mertzman, S., Yohannes Haile-Selassie and Gibert, L.B. (2017). Geochemistry of Woranso–Mille Pliocene basalts from west-central Afar, Ethiopia: Implications for mantle source characteristics and rift evolution. *Lithos*, **282-283**:187-200.

Nakamura, N. (1974). Determination of REE, Ba, Fe, Mg, Na and K in carbonaceous and ordinary chondrite. *Geochimica Cosmochimica Acta*, **38:** 757-775.

Natali, C., Beccaluva, L., Bianchini, G. and Siena, F. (2011). Rhyolites associated to Ethiopian CFB: Clues for initial rifting at Afar plume axis. *Earth and Planetary Science Letters*, **312**: 59-68.

Natali C, Beccaluva L, Bianchini G. and Siena F. (2013).The Axum–Adwa basalt–trachyte complex: a late magmatic activity at the periphery of the Afar plume. *Contrib Mineral Petrol*, **166**, 351–370.

Peccirillo, E.M., E. Justin-Visentin, B. Zanettin, J.-L.Joron and M. Treuil (1979). Geodynamic evolution from plateau to rift: major and trace element geochemistry of the central eastern Ethiopian Plateau volcanics. *Neues Jb. Geol. Palaont. Abh.***158**:139-179.

Peccerillo, A., Barberio, M.R., Gezahegn Yirgu, Dereje Ayalew, Barberi, M. and Wu, T.W. (2003). Relationships between mafic and acid peralkaline magmatism in continental rift settings: a petrological, geochemical and isotopic study of the Gedemsa volcano, central Ethiopian Rift. *Journal of Petrology*, **44**(11): 2003-2032. Doi: 10.1093/petrology/egg068.

Peccerillo, A., Donati, C., Santo, A.P., Orlando, A., Gezahegn Yirgu and Dereje Ayalew (2007). Petrogenesis of silicic peralkaline rocks in the Ethiopian rift: geochemical evidence and volcanological implications. *Journal of African Earth Sciences*, **48**: 161–173.

Pik, R., Deniel, C., Coulon, C., Gezahegn Yirgu, Hofmann, C. and Dereje Ayalew (1998). The Northwest Ethiopian plateau flood basalts: classification and spatial distribution of magma types. *Journal of Volcanology and Geothermal Research*, **81**: 91–111.

Pik, R., Deniel, C., Coulon, C., Gezahegn Yirgu and Marty B. (1999). Isotopic and trace element signatures of Ethiopian flood basalts: Evidence for plume–lithosphere interactions. *Geochimica et Cosmochimica Acta*, **63**(15): 2263–2279.

Pik, R., Marty, B. and Hilton, D.R. (2006). How many mantle plumes in Africa? The Geochemical point of view. *Chemical Geology*, **226**:100-114.

Pik, R., Marty, B., Carignan,J. and Lave,J.(2003). Stability of the Upper Nile drainage network (Ethiopia) deduced from (U-Th)/He thermochronometry: implications for uplift and erosion of the Afar plume dome.

Peng, Z.X., Mahoney, J., Hooper, P., Harris, C. and Beane, J. (1994).A role of lower continental crust in the flood basalt genesis? Isotopic and incompatible element study of the lower six formations of the western Deccan Traps. *Geochimica Cosmochimica Acta*, **58**: 267-288.

Rochette P., Tamrat E., Féraud G., Pik R., Courtillot V., Endale Ketefo, Coulon C., Hofmann C., Vandamme D. and Gezahegne Yirgu (1998) . Magnetostratigraphy and timing of the Oligocene Ethiopian raps. *Earth planet.Sci.Lett*, **164**:497-510.

Rogers, N., Macdonald, R., Fitton, J.G., George, R., Smith, M. and Barreiro, B. (2000). Two mantle plumes beneath the East African Rift System: Sr, Nd and Pb isotope evidence from Kenya Rift basalts. *Earth and Planeta~ Science Letters,* **176**: 387-400.

Rollinson, H. R. (1993). Using geochemical data: Evaluation, presentation, interpretation: Longman Group UK Ltd., 352 pp.

Rooney, T., Furman, T., Gezahegn Yirgu and Dereje Ayalew (2005).Structure of the Ethiopian lithosphere; xenolith evidence in the Main Ethiopian Rift. *Geochimica et Cosmochimica Acta, 69***:** 3889–3910.

Rooney, T., Furman, T., Bastow, I., Dereje Ayalew and Gezahegn Yirgu (2007).Lithospheric modification during crustal extension in the Main Ethiopian Rift. *Journal of Geophysical Research,* **112**: 1-21. B10201. Doi: 10.1029/2006JB004916.

Rooney, O.T., Hart, K.W., Hall, M.C., Dereje Ayalew, Ghiorso, S.M., Hidalgo, P. and Gezahegn Yirgu (2012). Peralkaline magma evolution and tephra record in the Ethiopian Rift. *Contrib Mineral Petrol*, **164**: 407-426. DOI 10.1007/s00410-012-0744-6.

Seife Michael Berhe, Berhe Desta, Nicoletti, M. and Mengesha Tefera (1987).Geology, geochronology and geodynamic implications of the Cenozoic magmatic province in W and SE Ethiopia. *Journal of the Geological Society, London,* **144**: 213- 226.

Storey, B.C. (1995). The role of mantle plumes in continental breakup: case histories from Gondwanaland. *Nature*, **377**: 301.

Stewart, K. and Rogers, N.(1996). Mantle plume and lithosphere contribution to basalts from southern Ethiopian. *Earth Planetary Science Letters*, **139**(2): 195-211.

Sun, S., and McDonough, W.F. (1989). Chemical and isotopic systematics of oceanic basalts: implications for mantle composition and processes: In Sunders, A.D., and Norry, M.J. (eds), Magmatism in ocean basins. *Geological Society Special,* **42:** 313-345.

Tadiwos Chernet, Hart, W.K., Aronson, J.L. and Walter, R.C. (1998). New age constraints on the timing of volcanism and tectonism in the northern Main Ethiopian Rift-southern Afar transition zone (Ethiopia). *Journal of Volcanology and Geothermal Research,* **80**: 267– 280.

Tommasini, S., Manetti, P., Innocenti, F., Tsegaye Abebe, Sintoni, M.F. and Conticelli, S. (2005).The Ethiopian subcontinental mantle domains: geochemical evidence from Cenozoic mafic lavas. *Mineralogy and Petrology,***84**: 259–281 DOI 10.1007/s00710-005-0081-9

Ukstins, I.A., Renne, P.R., Wolfeden, E., Baker, J., Dereje Ayalew and Menzies, M. (2002). Matching conjugate volcanic rifted margins: 40Ar/39Ar chronostratigraphy of pre- and syn-rift bimodal flood volcanism in Ethiopia and Yemen. *Earth and Planetary Science Letters*, **198**:289–306.

Wager, L., R., and Deer, W.A., 1939. Geological investigations in East Greenland, part III. The petrology of the Skaergaard intrusions. Kangerdlugessuaq, East Greenland, Medd. Om Gronland, **105**, no. 1-352.

Watchron,F.,Nicholas,G. and Bosence,D.(1998).Rift-related sedimentation and stratigraphy ,southern Yemen(Gulf of Aden).In:Purser,B.&Bosence,D.(eds) Sedimentary and Tectonic Evolution of Rift Basins.Chapman&Hall,pp.165-189.

Wilson, M. (1989).Igneous Petrogenesis a global tectonic approach, Unwin Hyman, London, 480pp.

Wolfenden, E., Ebinger, C., Gezahegne Yirgu, Deino, A. and Dereje Ayalew (2004). Evolution of the northern Main Ethiopian Rift: birth of a triple junction. *Earth and Planetary Science Letters,* **224**: 213–228.

Wolfenden, E., Ebinger, C., Gezahegne Yirgu, Renne, P. and Kelley, S.P. (2005). Evolution of the southern Red Sea rift: birth of a magmatic margin. *Geological Society of America Bulletin*, **117**: 846-864.

Zanettin, B., Justin Visentin, E. and Peccerillo, E. M. (1978).Volcanic succession, tectonics and magmatology in central Ethiopia. *Atti e Memorie dell'Accademia Patavina di Scienze Lettere ed Arti*, **90:** 5-19

Zanettin, B., Justin-Visentin, E., Nicoletti M. and Peccerillo E.M. (1980). Correlation among Ethiopian volcanic formations with special references to the chronological and stratigraphic Problems of the "Trap Series ".In: Geodynamic Evolution of the Afro – Arabian rift system. *Accademia Nazionale dei Lincei, Roma,* **47**: 231-52.

List of Appendices

Appendix I

Recalculated (volatile free basis) major element data for Ashenge and Aiba basalts.

Sample	SiO_2	TiO_2	Al_2O_3	Fe_2O_3	MnO	MgO	CaO	Na_2O	K_2O	P_2O_5	Sum
T1S2	54.76	3.02	14.9	10.5	0.15	3.84	7.44	3	2	0.37	99.97
T1S3	51.35	3.29	14.57	12.91	0.19	5.01	8.18	2.96	1.09	0.45	100
T2S8	46.31	3.85	9.4	14.35	0.18	13.38	9.25	1.85	1.02	0.41	100
T3S17	47.8	4.58	12.26	14.61	0.19	6.6	9.66	2.5	1.26	0.54	100
T3S6	48.54	3.47	11.12	13.87	0.19	8.32	10.45	2.4	1.17	0.47	100
T4S3	48.09	3.89	14.51	13.94	0.24	4.27	8.56	3.1	2.56	0.85	100.01
T4018	46.56	4.41	7.54	14.38	0.17	13.15	10.13	2.15	1	0.51	100
T4S13	46.67	3.61	10.86	13.98	0.2	10	10.91	2.2	1.14	0.46	100.03
TSS1	46.81	3.74	11.24	14.02	0.2	9.38	10.88	2.12	1.13	0.47	99.99
T6S3	49.47	3.56	14.48	13.12	0.19	5.27	9.48	3	1.04	0.45	100.06
T7	44.17	4.21	10.89	16.77	0.27	6.11	12.75	2.01	2	0.82	100
T7S9	48.99	3.68	12.38	13.72	0.17	6.59	9.01	3.04	1.82	0.61	100.01

Appendix II

CIPW Norm Calculation Results

	Normative Minerals											
Sample	Q	Or	Ab	An	Di	Hy	Ol	Il	Hm	Tn	Ap	Sum
T1S2	11.87	11.82	25.42	21.32	2.51	8.4	0	0.32	10.5	6.98	0.88	100.02
T1S3	9.33	6.41	25.08	23.24	2.87	11.16	0	0.41	12.91	7.54	1.07	100.02
T6S3	6	6.12	24.93	23.22	7.17	9.8	0	0.41	13.12	8.21	1.07	100.05
T3S17	5.02	7.43	21.18	18.5	8.35	12.57	0	0.42	14.61	10.7	1.28	100.06
T2S8	0	6.01	15.67	14.34	12.62	24.98	1.75	0.39	14.35	8.94	0.96	100.01
T3S6	3.67	6.91	20.32	16.13	16.61	13.02	0	0.4	13.87	8	1.1	100.03
T5S1	1.3	6.7	17.97	17.78	16.2	15.86	0	0.42	14.02	8.65	1.12	100.02
T4S13	0.02	6.72	18.63	16.38	17.87	16.63	0	0.43	13.95	8.31	1.08	100.02
T7S9	2.56	10.77	25.68	14.77	10.73	11.43	0	0.36	13.72	8.57	1.45	100.04
T4S3	2.02	15.13	26.22	18.12	4.82	8.4	0	0.51	13.94	8.88	2.01	100.05
T4018	0	5.93	18.18	7.97	18.89	19.87	2.89	0.37	14.38	10.35	1.21	100.03
T7	0	11.83	17.03	14.76	22.99	4.56	0	0.57	16.77	9.6	1.93	100.05

Abbreviations for the normative minerals is as in the list of acronyms

Appendix III

Major element and selected trace element data of LT, HT1 and HT2 basaltic groups (From Pik et al., 1998).

	HT1 basalts				LT basalts				
Sample	E44	E228	E230	E24	E166	E168	E171	E178	E181
SiO_2	48.01	49	50.57	48.69	50.15	49.95	48.65	49.1	48.63
TiO_2	3.84	3.5	3.07	3.26	1.58	2.1	1.88	1.98	1.32
Al_2O_3	12.96	14.43	14.79	12.85	15.9	15.3	14.78	15.58	16.5
Fe_2O_3	14.98	12.47	11.28	15.14	11.9	12.03	13.26	13	10.45
MnO	0.21	0.18	0.16	0.22	0.19	0.3	0.21	0.18	0.17
MgO	5.35	5.42	4.48	4.91	6.42	5.62	5.65	6.41	7.76
CaO	9.38	9	9.28	9.6	11.53	11.1	11.07	10.7	11.26
Na_2O	2.83	3.21	2.88	2.95	2.61	2.82	2.71	2.34	2.91

K_2O	0.81	1.16	1.02	0.59	0.27	0.59	0.24	0.27	0.56
P_2O_5	0.53	0.55	0.37	0.46	0.17	0.26	0.23	0.25	0.2
CaO/Al_20_3	0.72	0.62	0.63	0.75	0.73	0.73	0.75	0.69	0.68
Y	33.9	40.8	36.7	55.6	28.7	39.9	36.1	32.1	26.1
Nb	17.7	30	23	34.4	6.3	7.7	4.5	6.3	9.5
La	18.9	28.53	26.2	25.7	7.9	11.95	7.76	13.37	9.38

HT2 basalts

Sample	E33	E35	E37	E38	E40	E225	E226	E232
SiO_2	46.8	46.92	46.69	47.49	45.95	48.27	44.99	46.15
TiO_2	4.28	4.62	4.99	3.79	3.92	2.62	3.77	4.39
Al_2O_3	9.95	11.49	10.9	9.38	7.67	9.57	8.11	9.78
Fe_2O_3	14.67	14.07	14.66	12.81	13.74	13.1	13.79	13.1
MnO	0.2	0.19	0.18	0.17	0.18	0.18	0.18	0.19
MgO	10.6	7.05	6.84	13.61	16.1	13.51	15.97	10
CaO	9.81	10.35	9.91	8.81	9.22	10.1	8.68	9.53
Na_2O	2.2	2.46	2.48	1.9	1.55	1.84	1.48	3.25
K2O	0.72	0.77	1.11	1.13	0.43	0.41	0.96	1.21
P_2O_5	0.43	0.51	0.59	0.45	0.4	0.28	0.44	0.57
CaO/Al_20_3	0.99	0.9	0.91	0.94	1.2	1.06	1.07	0.97

Appendix IV

OIB normalized multi element variation diagram of Ashenge and Aiba basalts (normalization value are from Sun and McDonough, 1989).Symbols are as in fig.5.1

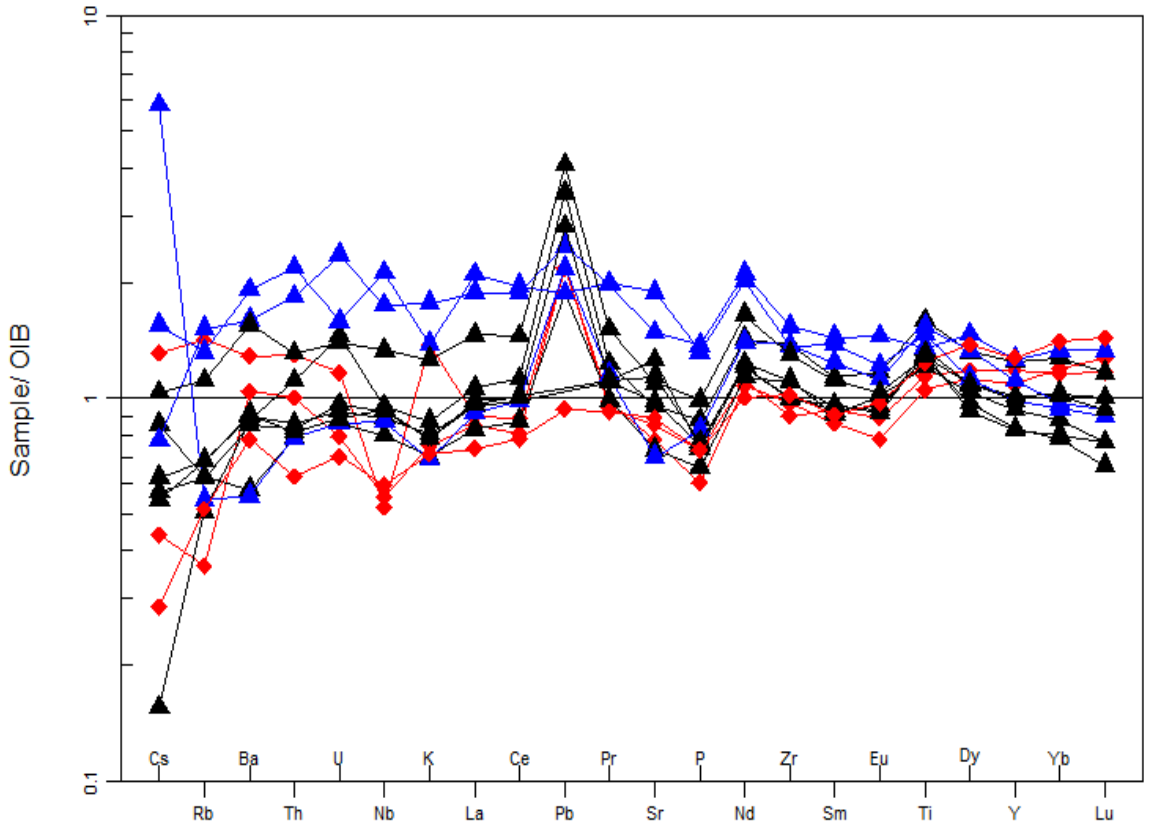

Appendix V

Structural data

№	structural element	Orientation (in degrees)			Location (UTM)	Associated Unit
	Inclined Beds					
		Strike	Dip	Dip direction	Easting: Northing	
1		75	10	SE	0555750:1414976	Pyroxene-olivine phyric basalt
2		266	15	SE	0555755:1414980	Pyroxene-olivine phyric basalt
3		85	10	SE	0555840: 1414080	Pyroxene-olivine phyric basalt
4		20	25	SE	0555820: 1414880	Pyroxene-olivine phyric basalt
5		80	24	SE	0556590: 1414201	Pyroxene-olivine phyric basalt
6		89	25	SE	0556550; 1414246	Pyroxene-olivine phyric basalt
7		265	25	SE	0556042: 1414200	Pyroxene-olivine phyric basalt
8		75	20	SE	0555587:1415425	Pyroxene-olivine phyric basalt
9		62	30	SE	0555221:1415129	Pyroxene-olivine phyric basalt
10		55	20	SE	0555348:1415424	Pyroxene-olivine phyric basalt
11		276	32	SW	0562892:1415674	Pyroxene-olivine phyric basalt
12		262	22	SE	0562411:1415464	Pyroxene-olivine phyric basalt
13		306	20	SW	0555557:1415639	Pyroxene-olivine phyric basalt
14		267	24	SE	0555762:1415618	Pyroxene-olivine phyric basalt
15		284	18	SW	0555557:1415639	Pyroxene-olivine phyric basalt
16		263	18	SE	0555523:1415361	Pyroxene-olivine phyric basalt
17		271	10	S	0556219:1414782	Pyroxene-olivine phyric basalt
18		248	46	SE	0556763:1414527	Pyroxene-olivine phyric basalt
19		287	15	SW	0555982:1414570	Pyroxene-olivine phyric basalt
20		251	25	SE	0556814:1413180	Pyroxene-olivine phyric basalt
21		255	24	SE	0562564:1417169	Pyroxene-olivine phyric basalt
22		257	20	SE	0561538:1416826	Pyroxene-olivine phyric basalt
23		239	30	SE	0557213:1416820	Pyroxene-olivine phyric basalt

24		262	34	SE	0557530:1416594	Pyroxene-olivine phyric basalt
25		250	45	SE	0557619:1416133	Pyroxene-olivine phyric basalt
26		245	25	SE	0558139:1417322	Pyroxene-olivine phyric basalt
27		256	22	SE	0558341:1416264	Pyroxene-olivine phyric basalt
28		260	23	SE	0558117:1411861	Pyroxene-olivine phyric basalt
29		257	20	SE	0558524:1411567	Pyroxene-olivine phyric basalt
30		260	24	SE	0558920:1411315	Pyroxene-olivine phyric basalt
31		246	20	SE	0561514:1416981	Pyroxene-olivine phyric basalt
32		207	45	SE	0555465: 1415902	Pyroxene-olivine phyric basalt
33		203	22	SE	0561321:1416524	Pyroxene-olivine phyric basalt
34		224	42	SE	0561245:1416469	Pyroxene-olivine phyric basalt
35		200	30	SE	0555465: 1415902	Pyroxene-olivine phyric basalt
36		221	33	SE	0561761:1416321	Pyroxene-olivine phyric basalt
37		210	46	SE	0555761:1416611	Pyroxene-olivine phyric basalt
38		49	23	SE	0558107: 1412036	Pyroxene-olivine phyric basalt
39		75	25	SE	0558225: 1411604	Pyroxene-olivine phyric basalt
40		64	30	SE	0559050: 1411093	Pyroxene-olivine phyric basalt
41		76	20	SE	0561288:1411010	Pyroxene-olivine phyric basalt
42		88	24	S	0558107: 1412036	Pyroxene-olivine phyric basalt
43		84	30	SE	0558225: 1411604	Pyroxene-olivine phyric basalt
44		112	40	SW	0559050: 1411093	Pyroxene-olivine phyric basalt
45		74	28	SE	0561288:1411010	Pyroxene-olivine phyric basalt
46		108	20	SW	0562054: 1411166	Pyroxene-olivine phyric basalt
47		110	20	SW	0560454: 1412764	Pyroxene-olivine phyric basalt
48		99	25	SW	0560598: 1413012	Pyroxene-olivine phyric basalt
49		73	25	SE	0561750:1412988	Pyroxene-olivine phyric basalt
50		86	30	SE	0562247:1413435	Pyroxene-olivine phyric basalt
51		79	25	SE	0556594:1414246	Pyroxene-olivine phyric basalt
52		262	27	SE	0555739:1414688	Pyroxene-olivine phyric basalt
53		264	22	SE	0555680:1414500	Pyroxene-olivine phyric basalt

54		263	20	SE	0555800:1414323	Pyroxene-olivine phyric basalt
55		70	25	SE	0556947:1413581	Pyroxene phyric basalt
56		71	20	SE	0562327:1412769	Pyroxene phyric basalt
57		67	32	SE	0562611:1412410	Pyroxene phyric basalt
58		74	28	SE	0562611:1412410	Pyroxene phyric basalt
59		70	24	SE	0562534:1412382	Pyroxene phyric basalt
60		64	20	SE	0556966:1411950	Pyroxene phyric basalt
61		71	26	SE	0556979:1411960	Pyroxene phyric basalt
62		70	35	SE	0556966:1411950	Pyroxene phyric basalt
63		57	25	SE	0556979:1411899	Pyroxene phyric basalt
64		51	30	SE	0562528:1412382	Pyroxene phyric basalt
65		56	23	SE	0562518:1412581	Pyroxene phyric basalt
66		53	28	SE	0562594:1412433	Pyroxene phyric basalt
67		60	34	SE	0562266:1412869	Pyroxene phyric basalt
68		57	27	SE	0562472:1412511	Pyroxene phyric basalt
69		48	25	SE	0562892:1414428	Pyroxene phyric basalt
70		51	29	SE	0562864:1414219	Pyroxene phyric basalt
71		51	31	SE	0562910:1414383	Pyroxene phyric basalt
72		54	30	SE	0562910:1414383	Pyroxene phyric basalt
73		59	23	SE	0556879:1413481	Pyroxene phyric basalt
74		49	25	SE	0556902:1412264	Pyroxene phyric basalt
75		43	30	SE	0556894:1412481	Pyroxene phyric basalt
76		50	18	SE	0556739:1412189	Pyroxene phyric basalt
77		49	22	SE	0556783:1411891	Pyroxene phyric basalt
78		46	26	SE	0556847:1413649	Pyroxene phyric basalt
79		63	25	SE	0556423:1412802	Pyroxene phyric basalt
80		55	23	SE	0556311:1412595	Pyroxene phyric basalt
81		65	31	SE	0556558:1412116	Pyroxene phyric basalt

82		49	34	SE	0556765:1413338	Pyroxene phyric basalt
83		54	31	SE	0556769:1413327	Pyroxene phyric basalt
84		53	28	SE	0556753:1412084	Pyroxene phyric basalt
85		49	20	SE	0556922:1412026	Pyroxene phyric basalt
86		86	18	SE	0556847:1413623	Pyroxene phyric basalt
	Joints					
1		0	75	E	0555750:1414976	Pyroxene-olivine phyric basalt
2		70	81	NW	0561964:1416723	Pyroxene-olivine phyric basalt
3		56	80	SE	0562918:1416511	Pyroxene-olivine phyric basalt
4		323	78	NE	0561720:1416192	Pyroxene-olivine phyric basalt
5		325	76	NE	0556763:1414527	Pyroxene-olivine phyric basalt
6		314	72	NE	0556882:1413921	Pyroxene-olivine phyric basalt
7		350	50	NE	0555569:1415337	Pyroxene-olivine phyric basalt
8		344	82	NE	0555762:1415618	Pyroxene-olivine phyric basalt
9		340	70	NE	0561411:1411924	Pyroxene-olivine phyric basalt
10		342	80	SE	0560459:1412310	Pyroxene-olivine phyric basalt
11		338	70	NE	0560230:1413510	Pyroxene-olivine phyric basalt
12		354	73	NE	0562161:1411491	Pyroxene-olivine phyric basalt
13		340	30	NE	0562724:1411819	Pyroxene-olivine phyric basalt
14		349	65	NE	0555620:1416211	Pyroxene-olivine phyric basalt
15		348	65	NE	0556881:1413927	Pyroxene-olivine phyric basalt
16		314	55	NE	0555498:1415850	Pyroxene-olivine phyric basalt
17		302	42	NE	0555450:1415800	Pyroxene-olivine phyric basalt
18		273	68	NE	0556566:1412127	Pyroxene-olivine phyric basalt
19		341	60	NE	0561714:1411110	Pyroxene-olivine phyric basalt
20		349	55	NE	0555465:1415902	Pyroxene-olivine phyric basalt
21		345	65	NE	0555569:1415337	Pyroxene-olivine phyric basalt
22		359	62	E	0562494:1413287	Pyroxene phyric basalt
23		293	60	NE	0562305:1413146	Pyroxene phyric basalt

24		268	53	NE	0562611:1412410	Pyroxene phyric basalt
25		312	68	NE	0556847:1413649	Pyroxene phyric basalt
26		352	55	NE	0556847:1413623	Pyroxene phyric basalt
27		346	61	NE	0556979:1411960	Pyroxene phyric basalt
28		326	64	NE	0556966:1411950	Pyroxene phyric basalt
29		15	65	SE	0556979:1411899	Pyroxene phyric basalt
30		15	58	SE	0558987:1417989	Aphyric basalt
31		20	68	SE	0559048:1417895	Aphyric basalt
32		18	70	SE	0562010:1417945	Aphyric basalt
33		30	61	SE	0557239:1417461	Aphyric basalt
34		0	70	E	0562354:1417563	Aphyric basalt
	Dikes					
No		Strike	Dip	Dip direction	Location	Associated unit
1		335	65	NE	0555466:1416236	Pyroxene- olivine phyric basalt
2		323	53	NE	0555460:1416200	Pyroxene- olivine phyric basalt
3		0	43	E	0555465:1415902	Pyroxene- olivine phyric basalt
4		340	61	NE	0555480:1416240	Pyroxene- olivine phyric basalt
5		345	64	SW	0555569:1415639	Pyroxene phyric basalt
6		353	56	NE	0556261:1412533	Pyroxene phyric basalt
7		328	52	NE	0559225:1411056	Pyroxene phyric basalt
8		5	63	SE	0562261:1412835	Pyroxene phyric basalt
9		330	38	SW	0555340:1416629	Pyroxene phyric basalt

Appendix VI

Detailed petrographic descriptions of Ashenge and Aiba basalts, Maychew, Northern Ethiopia.

Thin section code	Rock name	Location(UTM) and Elevation(m)	Formation	Description
T4S13	Pyroxene-Olivine phyric Basalt	0556558E 1412116N 2945m	Ashenge	Subhedral and Euhedral shaped micro-mega phenocrysts of clinopyroxene, olivine, and very few plagioclases are embedded in intergranular and intersertal textured pilotaxitic groundmass of predominantly plagioclase microlites. Further, the phenocrysts of clinopyroxene have glomerophyric nature, and shows concentric zoning. The proportion of phenocrysts is about 45 vol.%. The modal proportion indicates that it is composed of 76% clinopyroxene, 16% olivine, 5% plagioclase, and 3% opaque minerals.
T5S1	Pyroxene-Olivine phyric Basalt	0558107E 1412036N 2497m	Ashenge	It is highly porphyritic texture with phenocrysts of clinopyroxene, plagioclase, olivine, and very few scattered opaque minerals. The megacrysts of clinopyroxene crystals are generally euhedral and show zoning. The phenocrysts have about 40 vol. %. The modal composition indicates that it is composed of 54% clinopyroxene, 30% olivine, 13% plagioclase, and 3% opaque minerals.
Tb	Pyroxene-Olivine phyric Basalt	556982E 1411571N 2668m	Ashenge	Euhedral shaped megacrysts of clinopyroxene, and subhedral shaped and elongated micro-megacrysts of plagioclase with few olivine and opaque minerals are embedded in a plagioclase dominated groundmass. The volume % of the phenocrysts is about 40%.It shows intergranular texture where the interstices of plagioclase laths are filled by olivine and partly clinopyroxene. The modal proportion of this sample is 50% clinopyroxene, 37% plagioclase,

				11 %olivine, and 2% opaque minerals.
T2S8	Pyroxene-Olivine phyric Basalt	0557592E 1416336N 2652m	Ashenge	Phenocrysts of clinopyroxene, olivine, and microphenocrysts of very few plagioclases are set in a medium grained and elongated plagioclase rich groundmass. The crystals of clinopyroxene are mostly euhedral and can reach up to 5mm diameter. The phenocrysts are about 30% by volume. Modal composition of this sample is 64% clinopyroxene, 26% olivine, 3% plagioclase and 7 % opaque minerals.
T4S9	Pyroxene-Olivine phyric Basalt	0556311E 1412595N 3014m	Ashenge	It is dominated by megacrysts of clinopyroxene, plagioclase, and olivine. Opaque minerals are also present both in groundmass and phenocryst assemblage. The proportion of the phenocrysts is about 30% by volume Modal proportion indicates that 60% clinopyroxene, 33% olivine and 7% plagioclase.
T7S9	Pyroxene-Olivine phyric Basalt	0562247E 1413435N 2351m	Ashenge	Micro -mega phenocrysts of clinopyroxene, olivine and plagioclase are set in intergranular and intersertal textured groundmass of the same mineral assemblage as the phenocrysts. The proportion of phenocrysts is about 40 vol. %. The groundmass shows pilotaxic texture where the plagioclases are randomly oriented. The olivine phenocrysts are partly to wholly altered to iddingsite. It is composed of 42% clinopyroxene, 30% plagioclase, 25% olivine, and 3% opaque minerals.
T3S6	Pyroxene-Olivine phyric Basalt	0555750E 1414976N 2728m	Ashenge	It is also dominated by phenocrysts of clinopyroxene, plagioclase, olivine and very few opaque minerals. The phenocrysts have a volume percentage of about 30%. The groundmass is dominated by plagioclase. Modal proportion indicates that it is composed of 45% clinopyroxene, 38%plagioclase, 14% olivine, and 3%opaque

				minerals.
T3S17	Pyroxene-Olivine phyric Basalt	555284E 1417604N	Ashenge	Relative to other samples of Ashenge basalts this sample is moderately porphyritic with phenocrysts of dominantly clinopyroxene and some olivine and plagioclase. The phenocrysts are about 20% by volume. The groundmass is still plagioclase rich but with considerable amount of clinopyroxene. Mineral content indicates: 55% clinopyroxene, 33% olivine, 12 % plagioclase.
T4O18	Pyroxene phyric Basalt	0556966E 1411950N 2687m	Ashenge	This sample is characterized by its porphyritic texture with phenocrysts of clinopyroxene (the dominant), olivine and opaque minerals embedded in a microcrystalline matrix consisting of the same phase as the phenocryst assemblage. The proportion of the phenocrysts is about 25 vol.%. Plagioclase phenocrysts are not present but they present in the groundmass. Most of the clinopyroxene crystals are euhedral. In this thin section there is very small amount of orthopyroxene (5%) which occurs in cluster with clinopyroxene. Modal proportion indicates that it is composed of 61% clinopyroxene, 30% olivine, 7% orthopyroxene and 2 % opaque minerals.
T4S5	Pyroxene phyric Basalt	0556769 1413327 2721m	Ashenge	It has glomerophyric texture where clinopyroxene and olivine are clustered to one another. The groundmass has the same mineral assemblage as the phenocrysts (i.e. clinopyroxene, olivine and oxides).Phenocryst proportion is about 20 vol. %. Plagioclase is not present in the phenocryst. Euhedral to subhedral crystals of opaque minerals are found on both the phenocrysts and groundmass. Mineral content of this sample 71% clinopyroxene, 22% olivine and 7% oxides.
T4S3	Pyroxene	0556847E	Ashenge	It is dominated by fine grained plagioclase laths.

	phyric Basalt	1413649N 2594m		The interstices between these plagioclase lathes are filled by olivine and clinopyroxene. Partly it shows trachytic texture. Modal proportion indicates that it is composed of 32% clinopyroxene, 18% olivine, 45% plagioclase and 5 % oxides.
T7	Pyroxene phyric Basalt	0561982E 1413087N	Ashenge	It is porphyritic texture with phenocrysts of clinopyroxene (the dominant) and some olivine and opaque minerals. The opaque have sub to euhedral crystal shape. Further, glomerophyric and poiklitic texture are also common. Phenocrysts range from 25 vol. % to 30 vol. %. Modal proportion indicates that it is a composed of 60% of clinopyroxene, 15% olivine, 20% oxides and 5% plagioclase.
T1S2	Aphyric Basalt	0562114E 1417907N 2924m	Aiba	It is characterized by fine-grained plagioclase rich groundmass on which highly scattered euhedral shaped megaphenocrysts of plagioclase are distributed. Phenocrysts are less than 10 vol. %. The plagioclase shows oscillatory zoning. The modal proportion indicates that it is 70% plagioclase, 17%olivine, 3% clinopyroxene and 10% Fe-Ti oxides. Further, this sample shows poiklitic texture.
T6S3	Aphyric Basalt	0559087E 1417810N 2824m	Aiba	Microphenocrysts of plagioclase are set in fine grained plagioclase rich groundmass. These microphenocrysts of plagioclase are distributed randomly whereas the plagioclase laths in the groundmass show trachytic texture. The proportion of the phenocrysts is about <5 Vol. % .The modal proportions indicate that: 60%plagioclase, 17% olivine, 15% oxides, and 8% clinopyroxene.
T2S3	Aphyric Basalt	0557237E 1417635N	Aiba	Aphyric to slightly porphyritic texture with sparsly distributed micro-mega phenocrysts of plagioclase and clinopyroxene. The proportion of phenocrysts do not exceed 5 vol%. It shows partly trachytic

		2946m		texture where the lath shaped plagioclases in the groundmass are strongly aligned. The modal composition is: 54% plagioclase, 27% olivine, 11% clinopyroxene and 8%Fe-Ti oxides.
T3S18	Aphyric Basalt	555902E 1417436N 2753m	Aiba	It has generally phyric texture. But, in places, it shows slightly porphyritic texture where phenocrysts of plagioclase are sparsely distributed in plagioclase dominated groundmass. The proportion of phenocrysts is about 8 vol. %. The plagioclase phenocrysts are elongated and euhedral shaped. Its modal proportion is 65% plagioclase,20% olivine,10% clinopyroxene, and 5% opaque minerals(Possibly Fe-Ti oxides)